

5. RESEARCH ACTIVITIES

5.1 NUCLEAR PHYSICS

R.K. Bhowmik and S.K. Datta

The collaboration between GSI and IUAC has been strengthened this year by performing a joint experiment on neutron-rich nuclei at IUAC. Lifetimes of excited states of ^{52}Ti have been measured in the reaction $^{48}\text{Ca}(^7\text{Li},p2n)$ using RDM technique. Precise measurement of these lifetimes is needed to evaluate the $B(E2)$ values of heavier Ti isotopes by Coulomb excitation at GSI.

The Charged Particle Detector Array (CPDA) has been used to study the reaction dynamics for Incomplete Fusion (IF) reaction induced by ^{16}O at 6 MeV/A. The differences in side-feeding pattern for IF and complete fusion reaction (CF) confirms the l -localisation in the former reaction. A spectroscopic study of ^{126}I has been carried out using this facility. The Perturbed Angular Distribution (PAD) setup has been used to measure the g -factors for the isomer in ^{169}Ta and electric quadrupole moments for the isomeric states in $^{170,171,172}\text{Hf}$ and ^{175}Ta .

A series of experiments have been carried out to study the reaction dynamics with loosely bound projectiles near barrier energies. Fusion cross-sections for $^{6,7}\text{Li}$ on ^{28}Si have been measured. Elastic scattering and fusion measurements on $^7\text{Li} + ^9\text{Be}$ have been completed for comparison with similar measurements on $^7\text{Li} + ^9\text{Be}$ carried out earlier.

The Neutron Array facility (NAND) in Beam Hall II has been commissioned and tested with ^{16}O beam from the Pelletron. Fourteen 5" x 5" neutron detectors with a large area MWPC were used in the setup. The special purpose electronics developed for neutron TOF and PSD has been tested. An experiment on fusion-fission dynamics using the system $^{16}\text{O} + ^{181}\text{Ta}$ at 100 MeV was carried out at the GPSC in old beam hall. Fission hindrance in ^{200}Pb has been investigated by measuring the γ -multiplicity tagged by the evaporation residues near barrier energies.

For the INGA facility funded by DST, the ordering of the Clover detectors along with anti-Compton shields has been completed and delivery of the detectors has commenced from Feb, 2006. The complete beam line layout along with the design of the detector stands has been finalised and the commissioning work would start during the 2nd half of 2006. The first stage of the HYRA facility (gas-filled section) is currently undergoing commissioning.

5.1.1 New shell structure at $N \gg Z$ - Lifetime measurement of the first excited 2^+ state in ^{52}Ti

H.J. Wollersheim¹, P. Doornenbal¹, A. Dewald², K.O. Zell², R.P. Singh³, R. Kumar³, S. Muralithar³, R.K. Bhowmik³, S.C. Pancholi⁴, S.K. Mandal⁴, Ranjeet⁴

¹Gesellschaft für Schwerionenforschung, P.O. Box 110552, D-64291 Darmstadt, Germany

²Institut für Kernphysik, Universität zu Köln, Zùlpicherstrasse 77, D-50937 Köln, Germany

³Inter-University Accelerator Centre, Post Box-10502, New Delhi 110 067

⁴Department of Physics and Astrophysics, University of Delhi, Delhi 110007

At $N \gg Z$ the persistence of shell strength, melting of Woods-Saxon shell gaps and enforcement of harmonic oscillator (sub)shells are of prime interest. The predictive power of mean field calculations is hampered by the poor knowledge of the isovector part of the interaction, which can be determined only by data at extreme N/Z ratios. Experimental signature for shell structure are large two-nucleon separation energy differences δ_{2n}/δ_{2p} , high $I^\pi=2^+$ excitation energies $E(2^+)$ and small $B(E2;0^+ \rightarrow 2^+)$ values. The basic experimental features of shell structure at $N \gg Z$ for medium-heavy nuclei have been reviewed recently [1].

In the Ca isotopes beyond $N=28$ a possible (sub)shell closure at $N=32,34$ seems to develop in $E(2^+)$. It has been reported recently that the Ti and Cr isotopes show a maximum in $E(2^+)$ at $N=32$. On the other hand within the $N=34$ isotones $E(2^+)$ is increasing from Fe to Cr in contrast to the expected trend towards midshell, which supports a $N=34$ closure. Besides masses, which due to short half-lives are difficult to measure, obviously $E(2^+)$ and $B(E2)$ values for $^{50-54}\text{Ca}$ are missing for a proof of the concept. Similarly a study of the $N=30-34$ isotones of Cr and Ti would reveal such a change in shell structure.

The even $^{52-56}\text{Ti}$ isotopes have been studied with intermediate-energy Coulomb excitation and absolute $B(E2;0^+ \rightarrow 2^+)$ transition rates have been obtained [2]. These data confirm the presence of a subshell closure at neutron number $N=32$ in neutron-rich nuclei above the doubly magic nucleus ^{48}Ca . The $B(E2;0^+ \rightarrow 2^+)$ value for ^{52}Ti agrees with an earlier measurement [3], albeit the errors are large: $B(E2;0^+ \rightarrow 2^+) = 665 (+515, -415) \text{ e}^2\text{fm}^4$. The method of intermediate-energy Coulomb excitation has been used by laboratories with projectile fragmentation facilities to measure absolute $B(E2;0^+ \rightarrow 2^+)$ values. For the neutron-rich $^{30,32,34}\text{Mg}$ isotopes, for example, $B(E2;0^+ \rightarrow 2^+)$ values have been obtained by three groups working in RIKEN [4,5], MSU [6], and GANIL [7]; however, their results are neither conclusive nor consistent. Therefore,

one $B(E2;0^+ \rightarrow 2^+)$ value has to be measured with different techniques in the mass region of interest, which is the aim of the present experiment.

Previously γ -ray studies of ^{51}Ti , ^{52}Ti and ^{52}V have been performed using ^7Li bombardment of ^{48}Ca [3]. However, the lifetime of the lowest 2^+ state in ^{52}Ti could not be determined with a single Ge detector, because the 1050 keV transition turned out to be also present in ^{52}V . In the present experiment the same reaction was chosen, however, the γ -ray detection system was improved. The metallic targets of ^{48}Ca ~ 0.5 mg/cm 2 thick were evaporated onto a stretched 2 mg/cm 2 gold foil and covered with a 0.1 mg/cm 2 Au layer. The beam energy for the ^7Li ions of 28 MeV was chosen following an excitation measurement. It results in an average recoil velocity of $v/c=1\%$. For the γ spectroscopy the local Gamma Detection Array (GDA) at IUAC was used which consists of 12 Compton suppressed Ge-detectors positioned in three rings at 50° , 98° and 144° , respectively. It surrounded the plunger apparatus and had a photopeak efficiency of $\sim 0.5\%$ at 1 MeV of gamma energy. With the present set-up the different reaction channels following the bombardment of ^{48}Ca with ^7Li were studied using the RDM set-up at IUAC. Channel selection was possible through coincidences which will allow an accurate lifetime measurement of the first excited state in ^{52}Ti . Fig.1 shows coincidence γ -ray spectra for different target to stopper

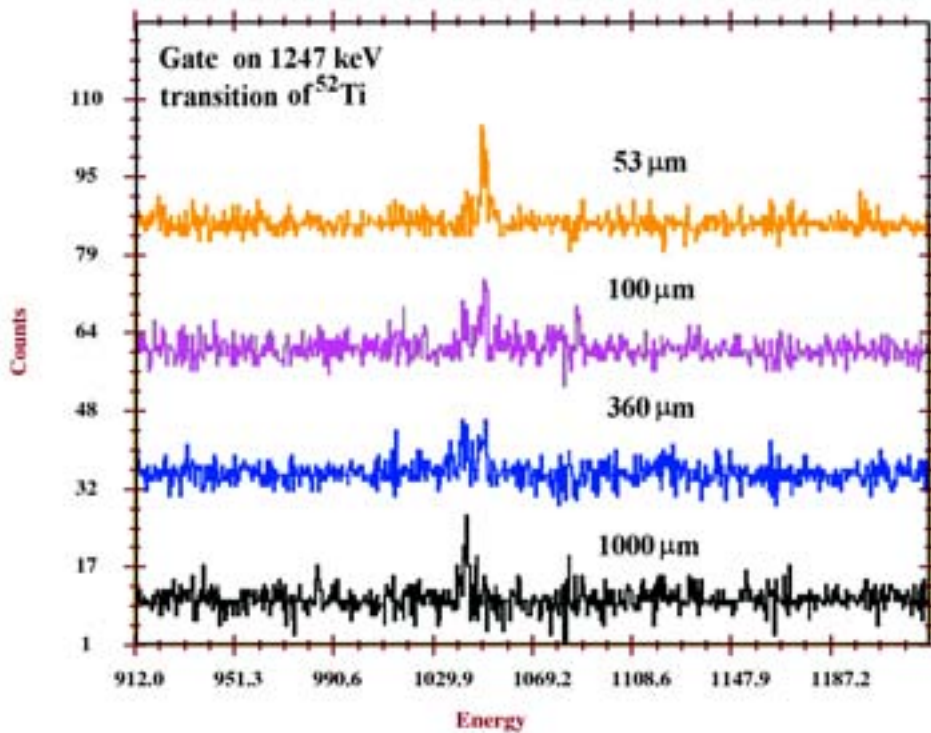


Fig. 1. Coincidence γ -spectra with a gate on the 1267 keV transition ($4^+ \rightarrow 2^+$ in ^{52}Ti) are shown for different target to stopper distances. The experimental decay curve will be extracted from the shifted and unshifted components of 1050 keV line ($2^+ \rightarrow 0^+$ transition) in ^{52}Ti .

distances. The gates were placed for the 98^0 Ge-detectors on the 1267 keV ($4^+ \rightarrow 2^+$) transition in ^{52}Ti in order to ensure a pure population of the 2^+ state in ^{52}Ti . The analysis of the 2^+ lifetime is in progress and will be determined from the decay curve which will be extracted from the shifted and unshifted components of the 1050 keV transition.

REFERENCES

- [1] H.Grawe, M. Lewitowicz, Nucl. Phys. A693 (2001) 116
- [2] D.-C. Dinca *et al.* Phys. Rev. C71 (2005) 041302
- [3] B.A. Brown *et al.* Phys. Rev. C14 (1976) 1016
- [4] T. Motobayashi *et al.* Phys. Lett. B346 (1995) 9
- [5] H. Iwasaki *et al.* Phys. Lett. B522 (2001) 227
- [6] B.Pritychenko *et al.* Phys. Lett. B461 (1999) 322
- [7] V. Chiste *et al.* Phys. Lett. B514 (2001) 233

5.1.2 High Spin States in ^{52}Cr

Rajesh Kumar¹, A. Kumar¹, S.K. Chamoli¹, L. Chaturvedi², S. Muralithar³, R.P. Singh³, N. Madhavan³, P. Sugathan³, J.J. Das³, R.K. Bhowmik³, Z. Naik⁴, C.R. Praharaj⁴, I.M. Govil¹

¹Department of Physics, Panjab University, Chandigarh 160014, INDIA

²Department of Physics, Banaras Hindu University, Banaras 221005, INDIA

³Inter-University Accelerator Centre, Post Box -10502, New Delhi 110 067

⁴Institute of Physics, Bhubaneswar 751005, INDIA

Most of the nuclei from ^{40}Ca to ^{56}Ni are well described by a shell model in which the most important configurations are $(f_{7/2})n$ and $(f_{7/2})n-r$ ($f_{5/2}$ $p_{3/2}$ $p_{1/2}$) r , where n is the number of particles outside the closed shell and $r = 1, 2, \dots$ [1-3]. In addition, states of opposite parity arise due to the excitations from the sd shell. Yrast spectroscopy of the majority of f-p shell nuclei follows the shell model expectation, exhibited somewhat irregular level spacing, often with a marked discontinuity at the termination of the $f_{7/2}$ band. This is particular apparent in the nuclei near N or $Z=20, 28$ where $J_{\text{max}} = 16$. Low-spin states roughly follow a $J(J+1)$ energy rule and a large $B(E2)$ values occur, the two features together suggests a collective rotation. At higher spin, but well below J_{max} , irregularities in the level spacing occur. These may be taken as evidence of either a level crossing with consequent back-bending, or alternatively as breakdown of collectivity and reappearance of the shell model behaviour.

The study of high spin states in $N \sim Z$, $f_{7/2}$ nuclei is of current interest. The nucleus ^{52}Cr has been studied earlier [4, 5] but the band structure has not been properly identified. The purpose of the present in-beam gamma spectroscopic investigation is to explore structural features of the ^{52}Cr nucleus and to resolve the ambiguities regarding the spin and parity assignment for the high spin states. In the present experiment the ^{52}Cr nucleus was populated using the $^{27}\text{Al}(^{28}\text{Si}, 3p)^{52}\text{Cr}$ fusion evaporation reaction at beam energy of 70 MeV. The beam was provided by the 15UD Pelletron facility at Nuclear Science Centre, New Delhi India. An isotopically enriched $500 \mu\text{g}/\text{cm}^2$ thick ^{27}Al target was used. The de-exciting gamma rays were detected using the Indian National Gamma Array (INGA) facility consisting of eight clover detectors combined with heavy Ion Reaction Analyzer (HIRA) at Nuclear Science Centre, New Delhi. Fig.1. shows the proposed level scheme of ^{52}Cr from the present work, where the ordering of transitions are based on relative γ -ray intensities and γ - γ coincidence relationship. The widths of the arrows are approximately equal to the intensities as obtained from the coincident spectra of the lowest transition, 1434 keV ($2^+ \rightarrow 0^+$). The level structure of ^{52}Cr has been established up to $E_x \sim 10$ MeV and tentative spin of $J \sim 13\hbar$. In addition to the transitions reported earlier [5], about ten new transitions have been identified in the present work. These transitions are marked by asterisk in the level scheme. We are able to interpret these states of ^{52}Cr by shell model configuration mixing using residual two-body interaction. Apart

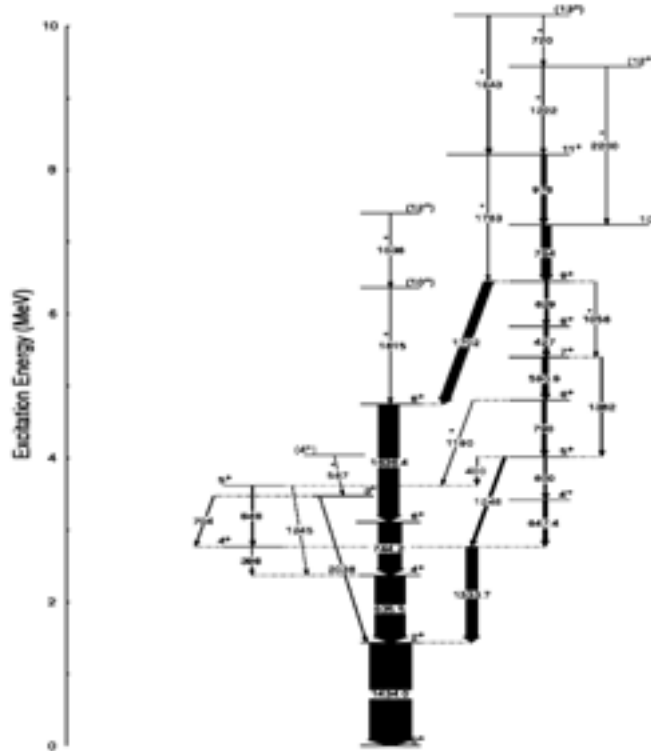


Fig.1. Level scheme for ^{52}Cr populated in $^{27}\text{Al}(^{28}\text{Si}, 3p)^{52}\text{Cr}$ reaction. Newly observed transitions are marked with an asterisk.

from the active protons in $f_{7/2}$ orbit, neutron excitation from $f_{7/2}$ to $p_{3/2}$ orbit is also considered. The representative gated spectrum is shown in Fig.2.

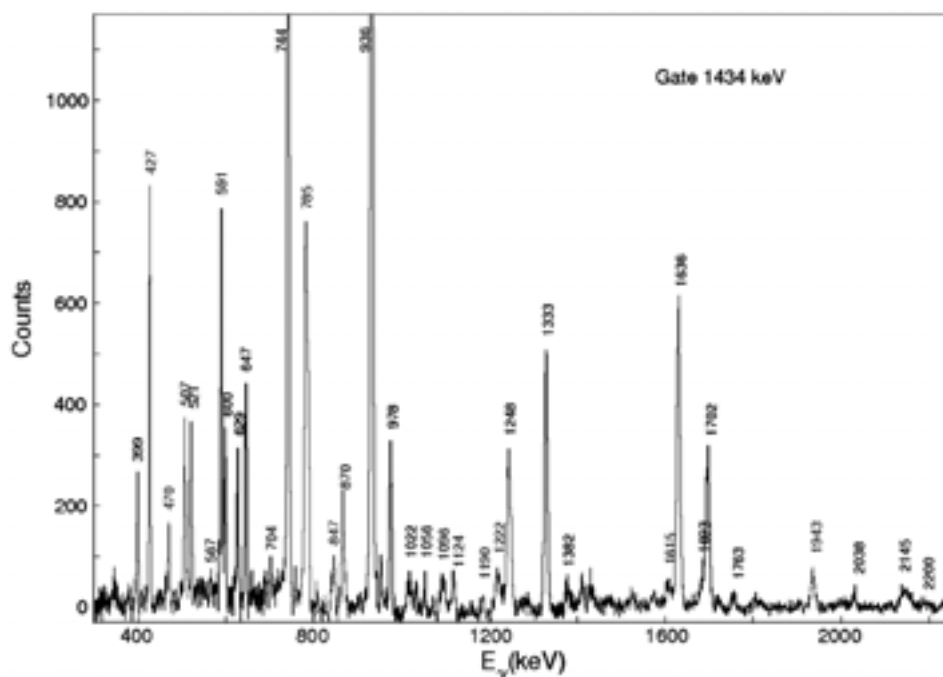


Fig.2. γ - γ coincidence spectrum with gate on 1434 keV transition. The transitions marked with asterisk belong to the neighbouring nuclei and the background.

REFERENCES

- [1] W. Kutschera et al. , Riv. Nuovo Cimento 1, 12 (1978)
- [2] A. Poves and A. Zuker, Phys. Rep. 70, 235 (1981)
- [3] R. B. Mooy et al. , Z. Phys. 312, 59 (1983)
- [4] I. P. Johnstone, Phys. Rev. C17, 1428 (1978)
- [5] P. Banerjee et al. , Phys. Rev C36, 2274 (1987)

5.1.3 Study of High Spin States in ^{85}Sr

Suresh Kumar¹, Sukhjeet Singh², Rishi Kumar Sinha³, Anukul Dhal³, S. Muralithar⁴, R.P. Singh⁴, Rakesh Kumar⁴, R.K. Bhowmik⁴, Paresh K. Joshi^{3,6}, L. Chaturvedi^{3,7}, S. Mandal⁴, S.C. Pancholi^{4,5} and A.K. Jain¹

¹Department of Physics, I .I .T. Roorkee, Roorkee-247667

²Department of Physics, G. N.D.U, Amritsar-143005

³Department of Physics, B. H.U, Varanasi-221005

⁴Inter-University Accelerator Centre, Post Box -10502, New Delhi 110 067

⁵Department of Physics, Delhi University, Delhi-110007

⁶Tata Institute of Fundamental Research, Mumbai-400005

⁷Pandit Ravishankar Shukla University, Chhatisgarh-492010

It is experimentally [1] known that as neutrons are removed from the closed neutron shell at $N = 50$, the population of the $p_{1/2}$ and $f_{5/2}$ proton orbits is affected to some extent. The result of this effect on the level structure of the strontium isotopes is largely un-known; but it is expected to result in a perturbing influence on some of the low-lying $g_{9/2}$ and $p_{1/2}$ neutron configurations. Despite these influences and the inadequacies of an extremely restricted basis the calculations indicate that the $g_{9/2}$ and $p_{1/2}$ orbits are the dominant ones in the low-lying configurations of the strontium isotopes [2]. Coexistence of different shapes have been found for the nucleus depending on the qp (quasiparticles) being $f_{5/2}$, $p_{1/2}$ and $g_{9/2}$ protons or $g_{9/2}$ neutrons [3, 4, 5]. Such a behavior might be also expected for the Sr nuclei, which can be characterized by only few neutron holes in $g_{9/2}$ and proton particles in $f_{5/2}$, $p_{1/2}$ and $g_{9/2}$ in the $N = 50$ closed shell as similar to the other Br, Kr, Rb, Y and Zr nuclei.

Also, observation of Magnetic Rotation (MR) bands (^{82}Rb and ^{84}Rb) [6] and prediction of such structure in the mass $A=80$ region (Br, Kr and Rb isotopes) [7] based on 3, 4-qp configuration provides a new hope of study in Sr nuclei, close to neutron shell at $N = 50$. Another question could be addressed is, why the 3-qp configuration leads to different structure for negative parity band for ^{83}Kr [4] and ^{87}Zr [8] ($N=47$) isotones. In addition, one would like to know how the high spin structure of the odd-Sr isotopes behave.

Our main focus, therefore, lies on the study of high spin states in ^{85}Sr and ^{87}Sr based on 3qp configuration. In present experiment, our main interest was to look for the possible band structure in ^{85}Sr .

Previously, this nucleus has been investigated via (α, xn) reaction by Arnell et al [5] and via $(^{12}\text{C}, 3n)$ reaction by Ivascu et al [6]. The ^{85}Sr nucleus was populated using the reaction $^{76}\text{Ge} (^{13}\text{C}, 4n\gamma) ^{85}\text{Sr}$ at 53 MeV. The ^{13}C beam was delivered by 15-UD Pelletron accelerator at IUAC, New Delhi. The target of ^{76}Ge (isotopically Enriched~99.90 %) was prepared by Ultra High Vacuum Technique. The target of thickness $\sim 650 \mu\text{g}/\text{cm}^2$ with a backing of ^{181}Ta was used. The thickness of backing material was $9.04 \text{ mg}/\text{cm}^2$. The γ - γ coincidence data were collected using a detector array of twelve Compton suppressed HPGe detectors (GDA facility at IUAC, New Delhi) along with a multiplicity filter of fourteen BGO detector. The HPGe detectors, at approximately 18 cm from the target, were arranged in three groups, each consisting of four detectors, at angles of 50° , 98° , 143° with respect to beam direction. The energy calibrations were obtained from the energies of the known γ -ray lines in ^{152}Eu and ^{133}Ba in the spectrum. A total of 270 million γ - γ events were collected in the list

mode. The data has been sorted by using the INGASORT [11] program. In the offline analysis, the data was sorted into $E\gamma$ - $E\gamma$ ($4K \times 4K$) matrix after gain matching of the all spectra to a dispersion of 0.5 keV per channel. The analysis of level scheme is being done by using the RADWARE program [12].

A preliminary level scheme as deduced from the present experimental data is shown in Fig.1. All levels were established on the basis of γ - γ coincidence relations. Levels up to 7 MeV have been established in our recent in-beam γ -ray studies. The Fig. 2 shows the gamma rays of negative and positive parity bands gated on the pervious known transitions. The level scheme built by γ - γ coincidence able to solve pervious controversy and small indication of γ - γ coincidence [9].

- (1) In particular, there was a mismatch between the level schemes of Arnell et al [9] and Ivascu et al [10] which could be resolved as a consequence of coincidence gamma above the 369 KeV. The second branch (863 keV) of the 3397 keV level proposed by Arnell *et al* [9] on the basis of the coincidence of this line with the 265 keV ray and the fit with the energy difference between the 3397 and 2534 keV levels, is not confirmed. We observe an 861 keV γ - ray, but it definitely de-excites another state, as it does not show coincidence with the 965 keV gamma ray and above the 965 gamma ray. This γ -ray is placed in the scheme (level as A) as shown in fig.1, which agree with the measurements by Bucurescu et al [13].
- (2) The placing of 167 keV and 494 keV gamma rays is reversed in the present level scheme (Fig.1), as the intensity of 494 keV γ is weak in 369 KeV gate, while 167 keV γ is stronger. This placing has also resolved the 200 keV γ -ray placing (level as B), coincidences with 369 keV and 444 keV γ not 265 keV γ -ray as indicated in work of Arnell *et al* [9].
- (3) In the positive parity band, the 454 keV gamma ray placing (level as C) is changed and new placement is shown in Fig.1.

The gamma ray transitions marked by * (Fig 1) have been observed for first time. The part of level scheme shown in circle (Fig. 1) are strongly observed with 200 keV gamma transition, but not seen in other transition. To assign a spin, parity and multipolarity for new gamma ray transitions, the polarization measurement and angular correlation data are required which is possible with INGA facility. Further analysis is in progress for the relative intensity measurements.

Financial support from the Ministry of Human Resources and the Department of Science and Technology (Govt. of India) at Roorkee and the IUAC at Amritsar are gratefully acknowledged.

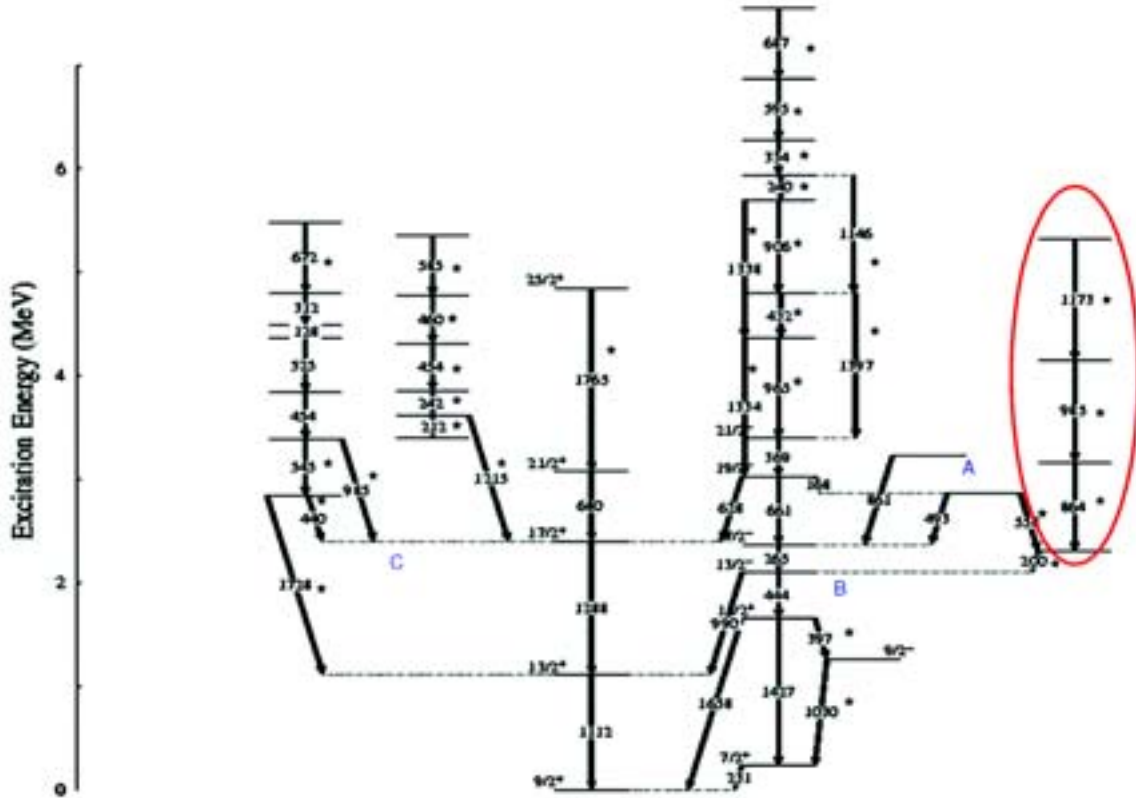


Fig 1. Tentative level scheme of ^{85}Sr

REFERENCES

- [1] J. V. Maher *et al.*, Phys. Rev. C3 (1971) 1162
- [2] J. E. Kitching *et al.*, Nucl. Phys. A177 (1971) 433
- [3] A. Petrovici *et al.*, Prog.Part.Nucl.Phys. 43 (1999) 485
- [4] P. Kemnitz *et al.*, Nucl. Phys. A456 (1986) 89
- [5] S. S. Malik , Priyanka Agarwal and A. K. Jain, Nucl. Phys. A732 (2004) 13
- [6] Amita, A. K. Jain and B. Singh, At .Data Nucl. Data Tables 74 (2000) 283
- [7] R. Schwengner *et al.*, Phys.Rev. C66 (2002) 024310
- [8] G. Y. Zhao *et al.*, Chin .Phys .Lett. 16 (1999) 345
- [9] S. E. Arnell *et al.*, Nucl. Phys. A280 (1977) 72
- [10] M. Ivaqu *et al.*, Rev. Roum. Phys. 23 (1978) 163
- [11] Ranjan Bhowmik, IUAC, private communication.
- [12] R. C. Radford, Nucl. Instr. Meth. A 361 (1995) 297
- [13] D. Bucurescu *et al.*, J. Phys. G: Nucl. Phys. 7 (1981) 399

5.1.4 Collective band structures of the ^{125}Cs nucleus

Kuljeet Singh¹, S. Sihotra¹, S.S. Malik², J. Goswamy³, D. Mehta¹, Nirmal Singh¹, Rakesh Kumar⁴, R.P. Singh⁴, S. Muralithar⁴, E.S. Paul⁵, Javid A. Sheikh⁶, and C.R. Praharaj⁷

¹Department of Physics, Panjab University, Chandigarh 160 014, India

²Department of Physics, Guru Nanak Dev University, Amritsar 143 005

³UIET, Panjab University, Chandigarh 160 014

⁴Inter-University Accelerator Centre, Post Box -10502, New Delhi 110 067

⁵Oliver Lodge Laboratory, University of Liverpool L69 7ZE, UK

⁶Department of Physics, Univ. of Kashmir, Hazrathbal, Srinagar, J & K 190006

⁷Institute of Physics, Bhubaneshwar 751 005

The ⁵⁵Cs isotopes lying in the transitional region above the Z=50 and below the N=82 shell closures are predicted to possess relatively flat potential-energy surfaces with respect to the quadrupole shape asymmetry parameter (γ). The triaxial deformation in this mass region has been evidenced by interpretation of observed crossing frequencies, staggering behaviour and $\Delta I=1$ doublet bands, which have been explained as the manifestation of chirality. Chiral bands have been observed in various odd-A and odd-odd nuclei with multiquasiparticle configurations that have substantial angular momentum components along the three principal axes. Another important feature is the magnetic dipole bands generated through the shears mechanism and have also been reported in the odd-A ¹³¹Cs and doubly-odd ¹³²Cs isotopes. Among the ⁵⁵Cs isotopes, band terminating states have been recently observed in ¹²³Cs at $I \sim 30\hbar$. The present in-beam gamma spectroscopic investigations are planned to probe for the above-mentioned structural features in the ¹²⁵Cs nucleus.

The excited states in the ¹²⁵Cs nucleus were populated using the ¹¹⁰Pd (¹⁹F, 4n) fusion-evaporation reaction at $E_{\text{lab}} = 75$ MeV. The ¹⁹F ion beam was delivered by the 15 UD Pelletron accelerator at Inter-University Accelerator Centre (IUAC), New Delhi. The target consisted of a self-supporting 1 mg/cm² thick ¹¹⁰Pd foil. The emitted γ -rays were detected using the Gamma Detector Array (GDA) comprising of 11 Compton-suppressed Ge detectors, one unsuppressed clover detector and a 14-element BGO multiplicity filter. The Ge detectors were mounted in three groups of four each making angles of 45°, 99° and 153° with the beam direction and having an inclination of $\pm 23^\circ$ with the horizontal plane. A total of 500 million coincidence events were collected in the experiment. Nuclides with major population in the reaction were ¹²⁴Cs (~25%), ¹²⁵Cs (~50%) and ¹²⁴Xe (~10%). In the off-line analysis, the recorded coincidence data were sorted into 4k \times 4k $E_\gamma - E_\gamma$ matrices. RADWARE graphical-analysis package was used to establish coincidence and intensity relationships for various gamma transitions. The level scheme of ¹²⁵Cs is shown in Fig. 1 with the band structures labeled 1-8.

The spin and parity of ground state ($t_{1/2} = 46.7$ m) has been assigned $I\pi = 1/2^+$ by Arlt et al. [1] from the EC decay of ¹²⁵Ba. The earlier known level schemes [2,3] established through in-beam spectroscopy following fusion-evaporation reactions have been substantially extended up to $I = 59/2 \hbar$ with the addition of about 40

transitions. The negative-parity band 1 built on an $\pi\tau = 11/2^-$ isomeric state ($t_{1/2} = 0.90$ (3) ms, excitation energy = 267 keV) is most intensely populated. Several new states de-exciting to both the signatures of the coupled band 3 form a new side band 7. This band is comprised of a regular sequence of low-energy transitions (likely to be M1) which are weak compared to the interband transitions to band 3. A newly observed sequence of transitions (likely to be E2) is shown as band 4 in Fig. 1 The decay of this band is fragmented, mostly connecting to the low-lying states with both the parities, and could not be established. On the basis of a partially identified decay pattern and the similarity to a band observed in ^{123}Cs , the lowest observed state of the band is expected to have an excitation energy of ~ 3 MeV and $\pi\tau = (23/2^+)$.

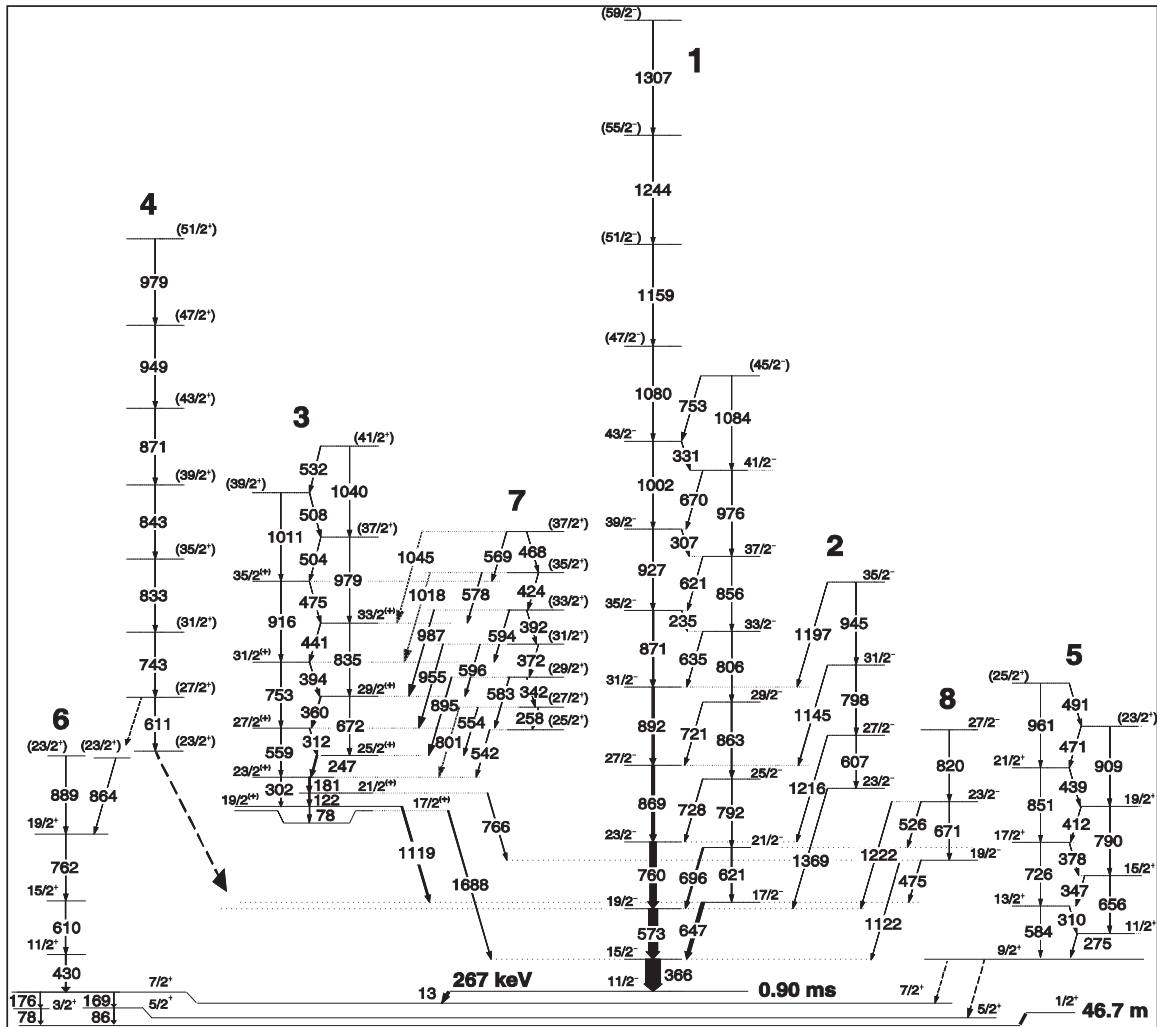


Fig.1. level scheme of ^{125}Cs

The present level scheme revealed rotational structures based on the $\pi h_{11/2}$ (band 1), the $\pi h_{11/2} \otimes \gamma$ -vibrational band (band 2), $\pi g_{9/2}$ (band 5) and $\pi g_{7/2}$ (band 6) orbitals. The rotational bands built on $\pi g_{7/2}$, $\pi g_{9/2}$ and $\pi h_{11/2}$ orbitals evolve into bands involving rotationally aligned $\nu(h_{11/2})^2$ and $\pi(h_{11/2})^2$ quasiparticles. A strongly

coupled band (Band 3) has been assigned a high-K $\pi h_{11/2} \otimes \nu g_{7/2} \otimes \nu h_{11/2}$ three-quasiparticle configuration and a new side band (Band 7) likely to be its chiral partner has been identified. Configurations assigned to various bands will be interpreted in the framework of Principal/Tilted Axis Cranking (PAC/TAC) model calculations. The authors are thankful to the Pelletron accelerator staff of the Inter-University Accelerator Centre, New Delhi, for their zealous support during the experiment. Financial support from UGC, New Delhi, under the Center of Advanced Study Funds, CSIR, New Delhi is duly acknowledged.

REFERENCES

- [1] P. Arlt *et al.*, Acta Phys. Pol. B 46, 433 (1975).
- [2] U. Garg *et al.*, Phys. Rev. C 19, 217 (1979).
- [3] J.R. Hughes *et al.*, Phys. Rev. C 44, 2390 (1991)

5.1.5 Study of high-spin structure of the nuclei around $A \sim 120$ near proton-drip line

I. Ray¹, U. Datta Pramanik¹, S.K. Basu², P. Banerjee¹, S. Bhattacharya¹, R.K. Bhowmik³, A. Goswami¹, R. Kshetri¹, Rakesh Kumar³, S. Mandal⁴, A. Mukherjee¹, B. Mukherjee¹, S. Muralithar³, Ranjeet⁴, M. Saha Sarkar¹, R.P. Singh³

¹Saha Institute Of Nuclear Physics, Kolkata

²Variable Energy Cyclotron centre, Kolkata

³Inter-University Accelerator Centre, Post Box -10502, New Delhi 110 067

⁴University of New Delhi, New Delhi

It has been already established that the shell structure changes in the nuclei near the neutron drip line. The properties of nuclei near the proton drip line are expected to be different than that for the neutron drip line due to large Coulomb barrier for protons. Our interest is to explore the structure of nuclei near proton-drip line. Nuclei around $A \sim 110-130$ region show a wide range of interesting features in high spin states which reflect different types of symmetry breaking mechanisms as well as maintaining symmetries. These are Chiral band, magnetic rotation band, anti magnetic rotation band, hyper deformed band etc. It is of special interest to look into the high spin states of the very neutron deficient nuclei to explore the features which have been observed in the neutron deficient nuclei close to the β -stable line.

High spin states of very neutron-deficient nuclei $^{118,120}\text{Xe}(S_p=4.6, 5.4 \text{ MeV})$, $^{120,121}\text{Cs}(S_p=2.5, 2.6 \text{ MeV})$, $^{120-122}\text{Ba}(S_p=3.9, 3.7, 4.4 \text{ MeV})$ (where valence protons

are loosely bound) were populated through fusion evaporation reaction $^{92}\text{Mo}(^{32}\text{S}, \text{x pyn})$. The ^{32}S beam at an energy of 140 MeV was obtained from 15UD Pelletron machine at NSC, New Delhi. The ^{92}Mo target with the thickness of $200 \mu\text{g}/\text{cm}^2$ was prepared by evaporation on a ^{197}Au backing. The thickness of gold backing was $13 \text{ mg}/\text{cm}^2$ to stop the recoils. The de-excited gamma-rays of the populated nuclei were detected in coincidence mode (γ - γ -t) with GDA (gamma detector array) consisting of 11 Compton suppressed HPGe detectors and one Clover detector without Compton shield. 14 BGO elements were used for multiplicity filter and gamma-sum energy. The data were acquired using CANDLE, an acquisition system developed at NSC.

The excitation function of the reaction $^{92}\text{Mo}(^{32}\text{S}, \text{x pyn})$ was studied with beam energies from 125 MeV to 145 MeV in step of 5 MeV. Preliminary data analysis showed that channels with major cross-sections are in agreement with PACE and CASCADE prediction with 5-10 MeV lower beam energy. CASCADE predictions for the cross-section of alpha emitting channels are underestimated. The compound nucleus ^{124}Ce is very neutron deficient. The main channels are 2p (Ba), 3p (Cs), 4p (Xe) and α 2p (Xe). The data were subsequently sorted offline using INGASORT program to produce a symmetrized 4k x 4k matrix of E_γ vs E_γ . ^{120}Cs can be a candidate for Chiral band. Fig.1 shows the sum of gated spectra of γ -ray transitions of the yrast band of ^{120}Cs . The low energy structure studied with different reaction [$^{107}\text{Ag}(^{16}\text{O}, 3\text{n})^{120}\text{Cs}$], has been confirmed by our data. The structure of yrast band is in agreement with previous reported work [1,2]. In addition to those we have observed some new γ -ray transitions (323, 335, 671, 770, 778, 901 KeV) in coincidence with γ -ray transitions of low-lying states. Further detail of the analysis is being continued.

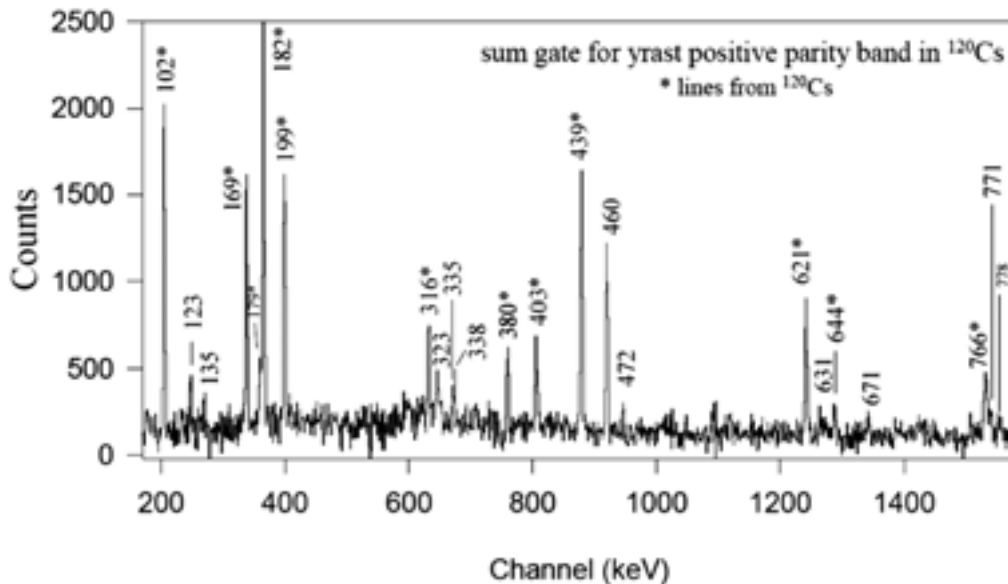


Fig.1. Sum of the gated spectra (102+169+182+199+440+621+766 KeV) of the Yrast band of ^{120}Cs .

High spin structure of ^{121}Cs is little known [3,4]. Our preliminary data analysis [Fig.2] is in agreement with earlier reported structure. More detailed analysis is going on to extend the information.

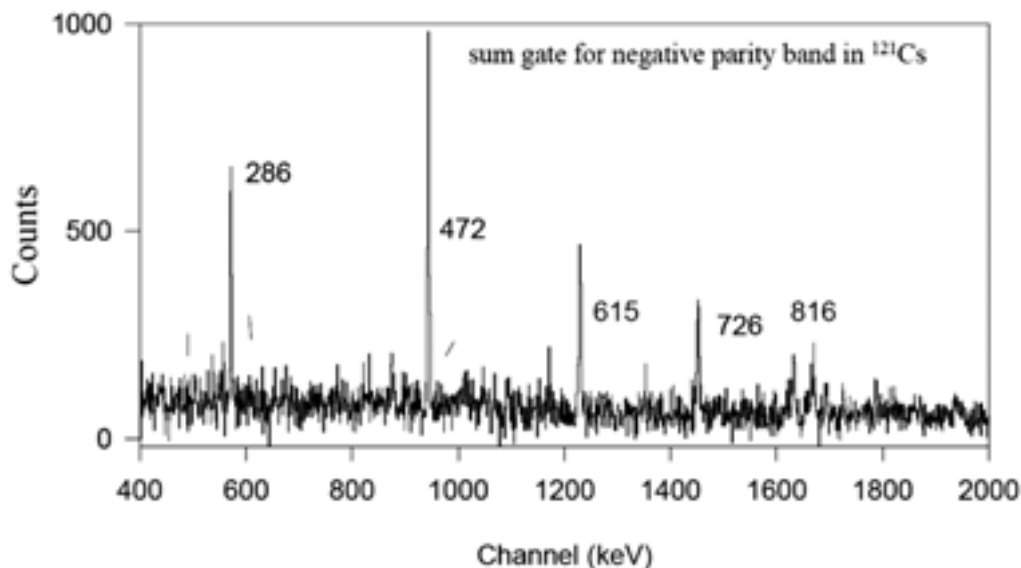


Fig 2. Sum-gated (286+615+816 KeV) spectra for negative parity band in ^{121}Cs

Most of the earlier experiments [1,2,3] were performed to study these isotopes using self-supporting target. Report on life time measurements are scarce. We will analysis the data using Doppler-shift attenuation technique for the lifetime of the high spin states of these isotopes.

Our main interest of this experimental project was to study $^{121,122}\text{La}$ study. Unfortunately, due to non-availability of thick target, our statistics of populating ^{121}La is very poor yet observable. So we would like to repeat the experiment with thick target.

We would like to gratefully acknowledge the support provided by the Pelletron stuff. The help from Mr. D. Kabiraj and Mr. S. R. Abhilash during target preparation is also appreciated.

REFERENCES

- [1] C.B. Moon et al. Nucl. Phys. A 696, 45 (2001)
- [2] B.Cederwall et al. Nucl. Phys A529, 410 (1991)
- [3] U.Garg et al. Phys. Rev. C19, 217 (1979)
- [4] F.Liden et al, Nucl. Phys. A 550, 365 (1992)

5.1.6 Lifetime Measurements in ^{81}Rb

Rishi Kumar Sinha¹, Anukul Dhal¹, Suresh Kumar², Rajesh Kumar³, R. Abhilash⁴, Dinesh Negi⁴, Rakesh Kumar⁴, R.P. Singh⁴, S. Muralithar⁴, R.K. Bhowmik⁴, I.M. Govil³, A.K. Jain², S.C. Pancholi^{4,5} and L. Chaturvedi^{1,*}.

¹Department of Physics, Banaras Hindu University, Varanasi- 221 005

²Department of Physics, IIT Roorkee, Roorkee- 247 667

³Department of Physics, Panjab University, Chandigarh- 160 014

⁴Inter-University Accelerator Centre, Post Box -10502, New Delhi 110 067

⁵Formerly at: Department of Physics, Delhi University, Delhi – 110 00

⁶Pandit Ravi Shankar Shukla University, Chattisgarh – 492 010

The region of nuclei with $A \sim 80$ is very rich in nuclear phenomena. It contains nuclei having large deformation with very interesting features. These nuclei have low density of single particle levels and large shell gaps of ~ 2 MeV at oblate ($\beta_2 \approx -0.3$, N or $Z = 34, 36$) and prolate ($\beta_2 \approx +0.4$, N or $Z = 38, 40$) shapes, exhibiting the dependence of nuclear shapes on proton number, neutron number and on their configuration as well as on spin and lead to shape-coexistence effects [1,2]. This has, therefore, generated a lot of interest to study nuclear shapes in nuclei in this mass region.

An experiment was performed to deduce the lifetimes of the high spin states of ^{81}Rb through Doppler Shift Attenuation Method (DSAM). ^{81}Rb is populated through the reaction $^{55}\text{Mn} (^{29}\text{Si}, 2\text{pn}) ^{81}\text{Rb}$ at 95 MeV of beam energy delivered by the 15 UD Pelletron facility at Inter University Accelerator Centre (IUAC), New Delhi. The target used was ^{55}Mn of thickness $690 \mu\text{g}/\text{cm}^2$ with a backing of Au of thickness $8.59 \text{ mg}/\text{cm}^2$. The γ -rays were detected using the Gamma Detector Array (GDA) setup in IUAC consisting of 10 Compton Suppressed HPGe detectors with relative efficiency of 25% with 14 BGO element multiplicity filter. The detectors were arranged in three different angles of 50° , 98° and 143° with the direction of beam. One clover detector was also used at the angle of 98° with respect to the beam direction. A total of 349 million γ - γ events were collected during the experiment.

The data was sorted out off-line using the INGASORT program. Fig 1 shows the sum spectra of the gates at 622, 875, 1024 and 1156 keV transitions.

For the lifetime measurements coincidence matrices were formed with all detectors versus the detectors at backward angle of 143° and forward angle of 50° . Fig 2 shows the Doppler broadened line shapes for the 1024 keV ($21/2^+ \rightarrow 17/2^+$) and 1156 keV ($25/2^+ \rightarrow 21/2^+$) gamma transitions for both the angles obtained by gating on the 622 keV ($13/2^+ \rightarrow 9/2^+$) transition which is below the transitions of interest. Analysis of the data is underway to determine the level lifetimes for investigating shape change at high spin.

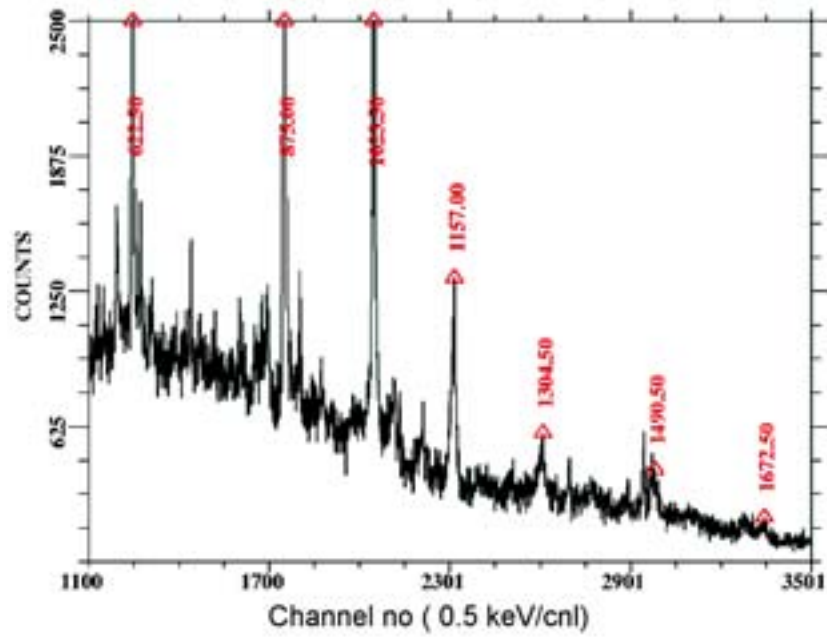


Fig.1 Sum gated spectra of 622, 875, 1024 and 1156 keV transitions of ^{81}Rb

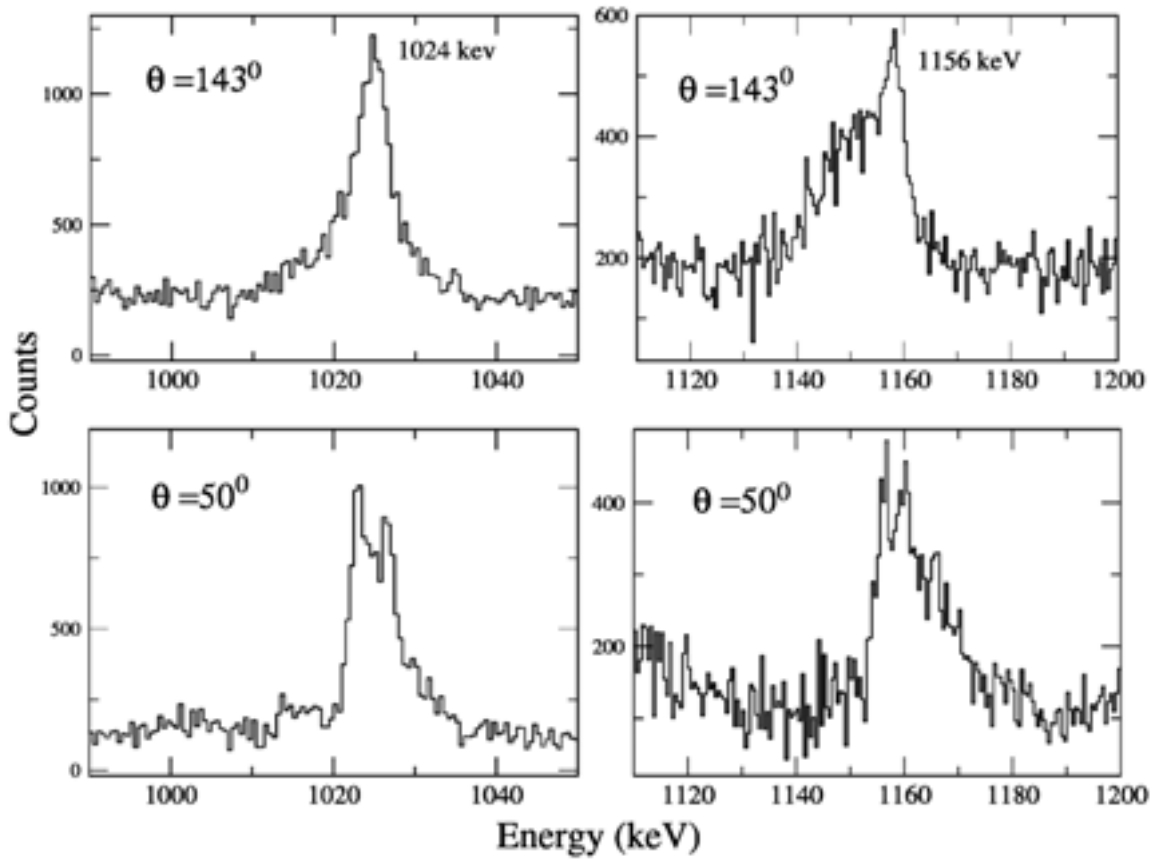


Fig. 2 Doppler broadened line shapes of 1024 and 1156 keV transition at backward and forward direction gated below the transition of interest.

REFERENCES

- [1] S. L. Tabor *et.al.*, Phys. Rev. C 39 (1989) 1359.
- [2] J. L. Doring *et.al.*, Phys. Rev. C 50 (1994) 1845.

5.1.7 Observation of anti-magnetic rotation in ^{108}Cd

P. Datta¹, S. Chattopadhyay², S. Bhattacharya², R.K. Bhowmik⁴, U. Datta Pramanik², T. Ghosh², A. Goswami², H.C. Jain³, P.K. Joshi³, N. Madhavan⁴, S. Muralithar⁴, S. Pal², R. Raut², P.V. Madhusudhana Rao⁴, R.P. Singh⁴, M. Saha-Sarkar²

¹Ananda Mohan College, Kolkata 700 009

²Saha Institute of Nuclear Physics, 1/AF Bidhan Nagar, Kolkata 700 064

³Tata Institute of Fundamental Research, Mumbai 400 005

⁴Inter-University Accelerator Centre, Post Box -10502, New Delhi 110 067

The Tilted Axis Cranking (TAC) model suggested by Frauendorf [1] has been remarkably successful in describing the rotation like band structure consisting magnetic dipole transitions (M1), found in nearly spherical nuclei. Similarly, though the presence of pure electric quadrupole band (E2) in nearly spherical nuclei may seem alien but it is possible within the frame work of TAC considering the double shear structure. The double shear structure in a nucleus is formed by the two high- j deformation aligned proton-holes (in time reverse orbit) are coupled with rotation aligned neutrons particles or vice versa. Since such geometry finally orient the resultant angular momentum along the principal axis, hence, it may gives rise to the rotational band structure. But these band will decays by weak E2 transitions with a falling $B(E2)$ rates with increasing spin indicating the underlying TAC mechanism. This phenomena has been termed as anti-magnetic rotation (AMR) [1,2] and first experimentally observed in ^{106}Cd .

In the previous work high spin structure of ^{108}Cd had been established by Thorslund et. al [3, 4] where the positive parity yrast band was extended up to $I^\pi=24^+$ and was identified as band 7. This band exhibits a sharp backbend at $I^\pi=10^+$ due to alignment of two $h_{11/2}$ neutrons followed by a slow alignment of $g_{7/2}$ neutrons. Thus, the high spin states of positive parity yrast bands in ^{108}Cd originate from the single particle configuration, namely, $\pi [g_{9/2}]^{-2} \otimes \nu [g_{7/2}^2 h_{11/2}^2]$. Thus, both from the single particle configuration and systematics of even-even Cd isotopes, it is quite expected that the positive parity band in ^{108}Cd may be originated due to anti-magnetic rotation. With this motivation the high spin states of ^{108}Cd were populated through $^{100}\text{Mo}(^{13}\text{C}, 5n)^{108}\text{Cd}$ reaction using 65 MeV ^{13}C beam from the 15-UD Pelletron at Nuclear Science Centre, New Delhi. The experiment was performed in an array consisting 8

Compton suppressed Clover detectors mounted on opposite sides at nominal angles 79° and 139° on either side with respect to the beam direction. The target was made of 1 mg/cm^2 of enriched ^{100}Mo backed with 9 mg/cm^2 natural Pb. A total list mode data of 800 million two fold γ - γ coincidences were collected. The data were sorted to form three matrices using the basic γ - γ sorting program INGASORT [5]. In order to understand the excitation mechanism of the positive parity yrast band in ^{108}Cd , the $B(E2)$ rates in this band has been calculated through the line shape analysis using the LINESHAPE analysis code of Wells and Johnson [6].

In the present work, the line shapes were observed above the $I^\pi=12^+$ level. Lifetime for each level were calculated for the two angles namely, 79° and 139° . The examples of the line shape fitting for three gamma-transitions 956.3, 1105.3 and 1260.3 keV deexciting the 16^+ , 18^+ and 20^+ levels, respectively, are presented in fig 1. In the present work, the level lifetime for 14^+ state was found to be $1.32(13)$ ps instead of $2.2(2)$ ps reported in the previous work [4].

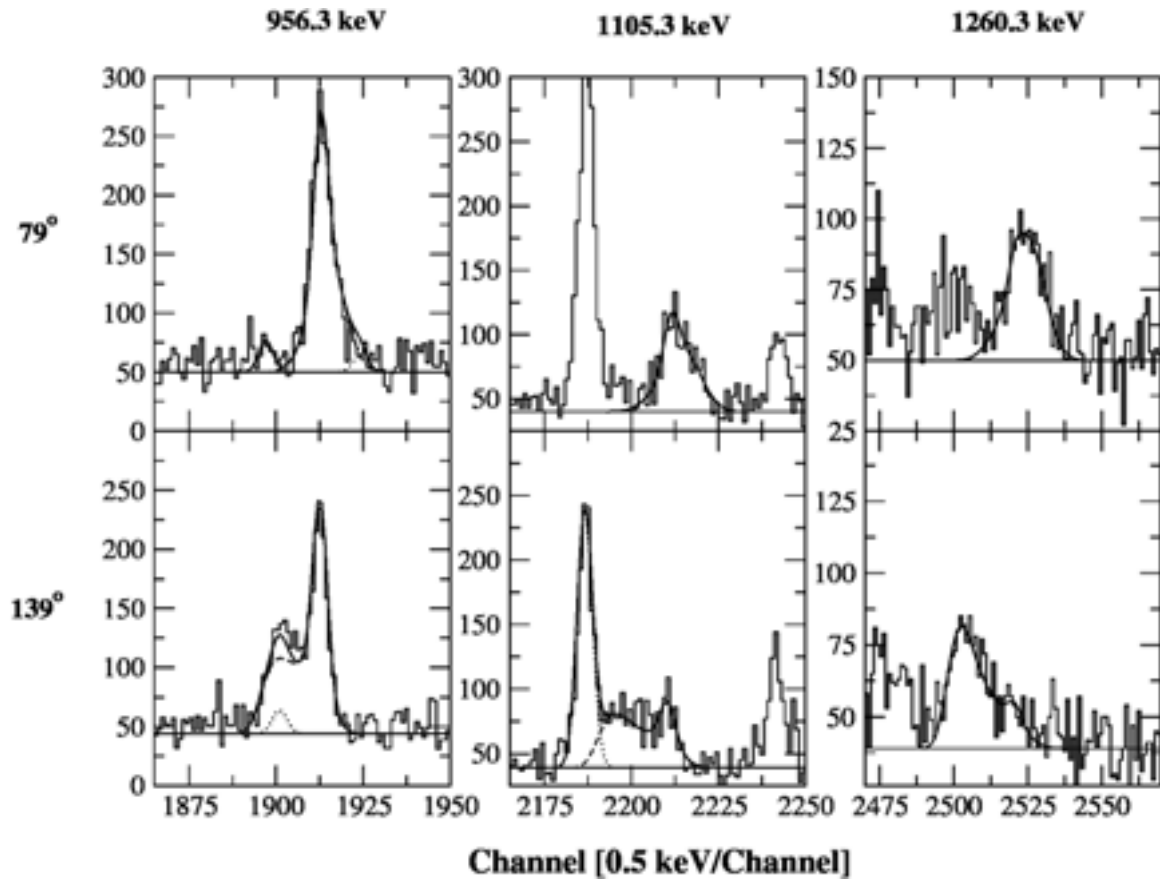


Fig. 1 Experimental and theoretical lineshapes for the 956.3, 1105.3 and 1260.3 keV gamma-rays of ^{108}Cd at the 79° and 139° angles with respect to the beam direction. The contaminant peaks are shown by dotted lines and theoretical line shapes are shown by solid lines.

The extracted $B(E2)$ values have been plotted in fig 2. It shows that the $B(E2)$ values decrease with the increasing spin. In order to investigate this behaviour, Total Routhian Surfaces (TRS) [7] calculations were performed at the frequencies $\hbar\omega = [E(I+1) - E(I-1)]/2$, where the level lifetimes have been measured. These calculations indicate that the quadrupole deformation β_2 remains constant at 0.17 up to $\hbar\omega = 0.50$ MeV. But, at higher frequencies, β_2 decreases. The corresponding $B(E2)$ values have been plotted in fig 2 by the dotted line and show good agreement with the measured values. It may be noted that TRS calculations assume rotation perpendicular to the symmetry axis and gives a good description of AMR because the resultant angular momentum of the double shears coincides with the rotational axis [8].

In an alternative effort a semi-classical model based upon the shears mechanism [2] based on the Tilted Axis Cranking mechanism has also been applied to calculate the $B(E2)$ values. These values have been calculated for two different values of eQ_{eff} . These values are $eQ_{\text{eff}}=1.1$ and 1.0 and plotted by the solid and dashed line, respectively. We have calculated [9] eQ_{eff} from the single particle quadrupole moments of the Nilsson states with Woods-Saxon potential at $\beta_2=0.17$.

It is clear from fig 2 that both TRS and TAC calculation reproduce the experimentally observed values. Since the rotational axis is along the one of the

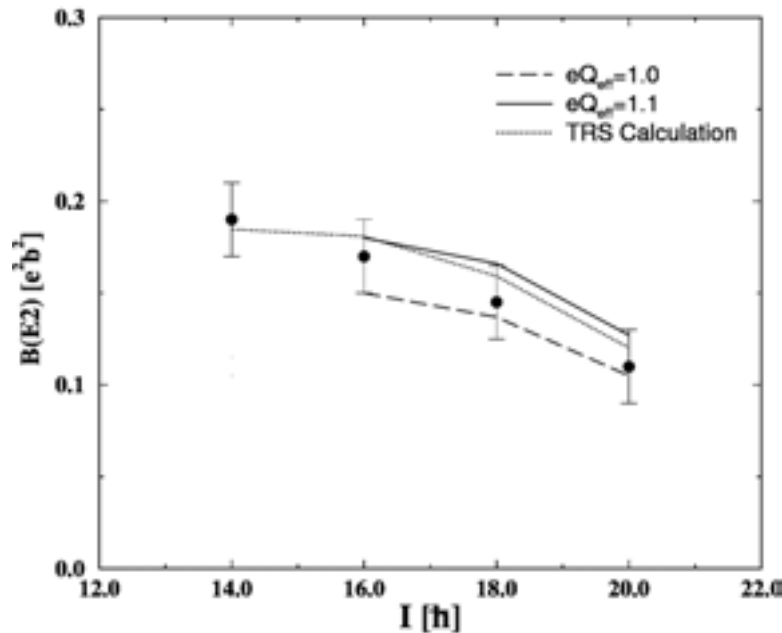


Fig 2 $B(E2)$ rates vs spin for positive parity yrast band of ^{108}Cd . The solid and dashed line indicate the $B(E2)$ values calculated using the semi-classical model with $eQ_{\text{eff}} = 1.1$ and 1.0 respectively while the dotted line indicates the $B(E2)$ values calculated by using the equilibrium deformations obtained from TRS calculation.

principal axis of the nucleus, it is expected that both the result will converge at the same point. This new evidence of AMR in ^{108}Cd in addition to that reported earlier in ^{106}Cd establishes AMR as a more general phenomenon.

REFERENCES

- [1] S. Frauendorf, Rev. of Mod. Phys.73 (2001) 463
- [2] R.M. Clark and A. O. Macchiavelli, Annu. Rev. Nucl. Part. Sci. 50 (2000) 1
- [3] I. Thorslund *et al.*, Nucl.Phys. A564 (1993) 285.
- [4] I. Thorslund *et al.*, Nucl.Phys. A568 (1994) 306.
- [5] R. K. Bhowmik, (private communication).
- [6] J. C. Wells and N. R. Johnson, (private communication).
- [7] R. A. Wyss *et al.*, Phys. Lett. B 215 (1988) 211.
- [8] A. J. Simons *et al.*, Phys. Rev. Lett. 91 (2003) 162501.
- [9] P. Datta *et al.*, Phys. Rev. C 71 (2005) 041305(R).

5.1.8 Spectroscopic Study of ^{126}I via Incomplete Fusion Reaction

S.R. Meher¹, Vinod Kumar¹, Pragma Das¹, R. Kumar², R.P. Singh², S. Muralithar² and R.K. Bhowmik²

¹Indian Institute of Technology-Bombay, Powai, Mumbai, 400076

²Inter-University Accelerator Centre, Post Box-10502, New Delhi 110067

Nuclei in the mass region 130 have been investigated extensively in the recent past. Special attention was given to odd-odd nuclei [1-3], particularly because of the possibility of their chiral behavior. However, the limited experimental data exist in the relatively neutron rich region close to β -stability line. These nuclei are either difficult to populate or not accessible via the much utilized heavy-ion reactions using the stable targets and projectiles. The incomplete fusion reactions (ICF) provide an attractive alternative, though such reactions are not well exploited for the spectroscopic studies. The main reason has been the existing knowledge of the reaction mechanism, offering very low production cross-section at the projectile energies above the Coulomb barrier. On the contrary, the high ICF cross-section values found for the neutron rich iodine isotopes, in our recent measurements [4], is a surprising and unexpected result. For example, the cross-section value as high as 170 mb for ^{126}I was obtained which motivated us to perform its spectroscopic study. The study so far done on ^{126}I was through (p, n) reaction [5]. Although many γ -lines were found but the yrast states were unidentified.

Our experiment at IUAC consisted of identifying the yrast high-spin states of ^{126}I using the ICF reaction $^{124}\text{Sn} (^{10}\text{B}, \alpha n) ^{126}\text{I}$ at beam energy of 70 MeV. The

charged particle detector array (CPDA) in conjunction with the GDA set-up was utilized. The CPDA was divided into three sections namely; detectors in the (i) forward cone ($\theta \sim 10^\circ - 60^\circ$), (ii) middle ring ($\theta \sim 60^\circ - 120^\circ$) and (iii) backward cone ($\sim 120^\circ - 170^\circ$). Here θ is the angle measured with respect to beam direction. The list mode data comprising of γ - γ coincidences, time spectra of charged particle detectors in three sections separately, were collected. Figure 1 shows the forward α -gated projected γ spectrum in comparison with total projected γ spectrum. The enhancement in the peak to background ratio for the γ -line belonging to α -channel is evident.

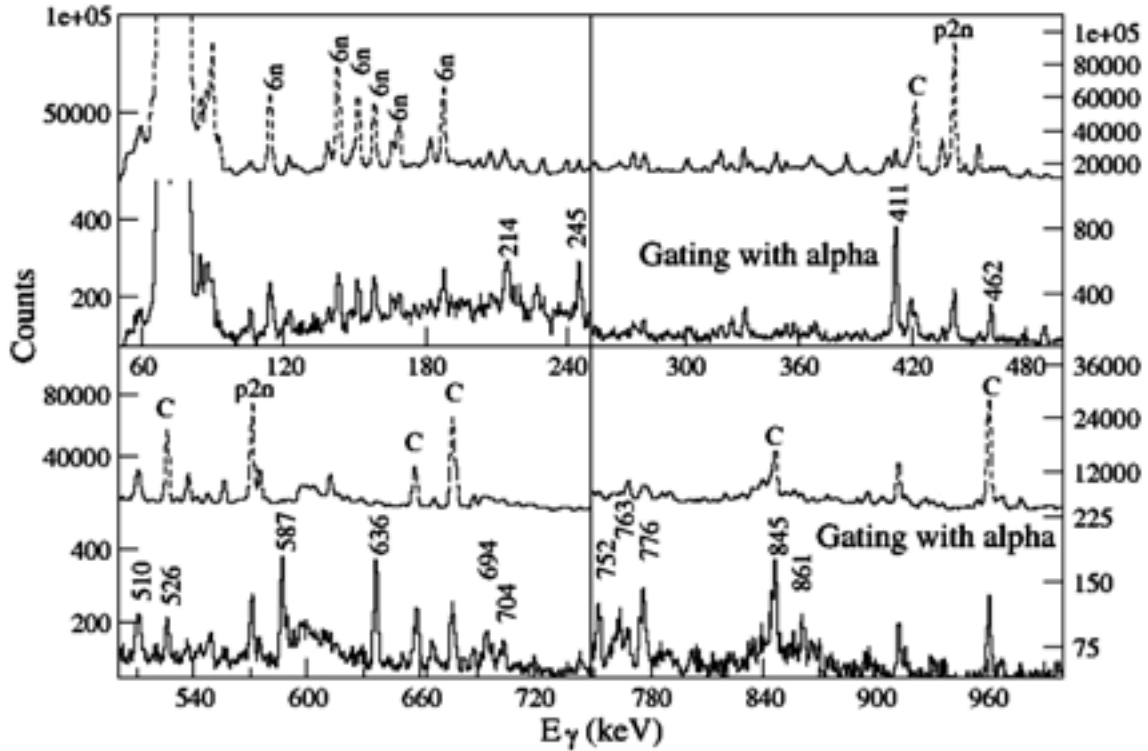


Fig. 1. The forward α -gated γ -spectrum (solid line) in comparison with the total projected γ -spectrum (dotted line). The peaks labeled with energy values correspond to residues formed after α -emission. 'C' identifies the peaks due to contamination.

REFERENCES

- [1] K.Starosta *et al.*, Phys. Rev. Lett. 86, 971 (2001).
- [2] Vinod Kumar *et al.*, Eur. Phys. J. A 17, 153 (2003).
- [3] C.Vaman *et al.*, Phys. Rev. Lett. 92, 032501 (2004).
- [4] S.R. Meher *et al.*, Proc. of DAE Nucl. Phys. Symp., 47 B, 282 (2004); Pragya Das, Proc. of DAE Nucl. Phys. Symp., 47 A, 177 (2004).
- [5] J. Burde *et al.*, Nucl. Phys. A 405, 205(1983).

5.1.9 Nuclear g-Factor Measurements of the $K^\pi = 5/2^-$ and $9/2^-$ Isomers in ^{169}Ta

V. Kumar¹, P. Thakur¹, A.K. Bhati¹, D. Negi², R.P. Singh², R.K. Bhowmik²

¹Centre for Advanced Study in Physics, Panjab University, Chandigarh-160014

²Inter-University Accelerator Centre, Post Box -10502, New Delhi-110067

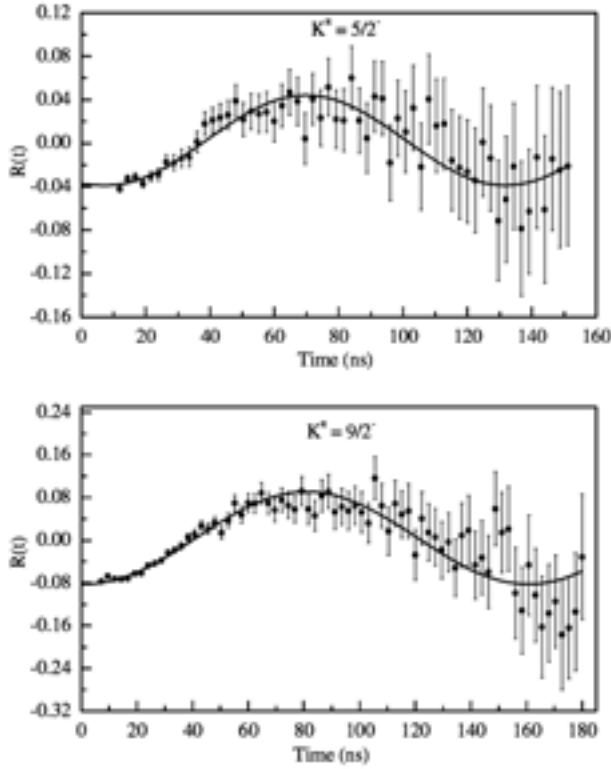


Fig 1. Spin rotation of $5/2^-$ and $9/2^-$ isomers in ^{169}Ta

The g-factors provide valuable information of the microscopic structure of the nuclei, as they are extremely sensitive to the single-particle components in the wave function and their intricate interplay with the collective degrees of freedom. Indirectly $B(M1)/B(E2)$ measurements provide information about g-factor of the state, but this usually involves the introduction of several assumptions. Therefore, direct measurement of g-factor provides critical test for the various theoretical models and their systematic behavior for the family of states of specific structure. The present measurement is a part of systematic studies of the nature of the low-energy high-K isomers occurring across the odd-Ta isotopic chain.

The excited states in ^{169}Ta have been populated through the nuclear reaction $^{159}\text{Tb}(^{16}\text{O}, 6n\gamma)^{169}\text{Ta}$ using 104 MeV ^{16}O pulsed beam with 1 μs repetition period. The target consisted of $750\mu\text{g}/\text{cm}^2$ natural Tb with Ta ($50\text{ mg}/\text{cm}^2$) backing to stop the recoiling nuclei. The time differential perturbed angular distribution (TDPAD) technique has been used for the magnetic moment measurements in the presence of 9.775(45) kG external magnetic field perpendicular to the plane of the detectors. The detectors were fixed at angles $\pm 45^\circ$. In order to investigate the delayed gamma rays produced in the reaction, energy spectra gated at different time intervals with respect to the beam pulses were created. The details of the data analysis have been given in the earlier reports [1].

The ratio function $R(t)$ was formed for the de-exciting γ -rays from the $5/2^-$ and the $9/2^-$ states. The $R(t)$ function was least squares fitted to the magnetic perturbation function for the two independent levels. The least squares fitted TDPAD spectra are shown in Fig. 1. The fitted values of Larmor frequencies ω_L for the $5/2^-$ and $9/2^-$ states are 25.32(61) Mrad/s and 19.74(37) Mrad/s, respectively. The extracted values of g-factors from the corresponding Larmor precession frequencies are $g(5/2^-) = +0.541(17)$ and $g(9/2^-) = +0.422(12)$ and the magnetic moments are $\mu(5/2^-) = +1.35(4) \mu_N$ and $\mu(9/2^-) = +1.90(5) \mu_N$. These results are shown in fig. 2 along with the previously reported experimental results.

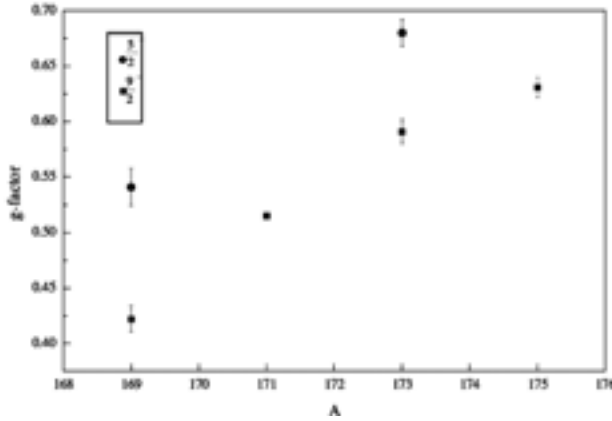


Fig. 2. Systematics of g-factors in odd-A Ta isotopes.

The g-factor measurements for the $\pi 5/2^- 1/2[541]$ ground state in ^{173}Ta were carried out using the nuclear magnetic resonance on oriented nuclei (NMR-ON) technique by König *et al.* [2]. The value of $\mu(5/2^-) = 1.703(34)$ in ^{173}Ta was observed slightly more than the theoretical calculated value 1.54 by Ekström *et al.* [3]. These calculations are not available for the ^{169}Ta isotope, but Ekström *et al.* have shown the reduction in the $g(5/2^-)$ - factor with increasing

deformation. The reduction of the g-value for the $5/2^-$ state as compared to that in ^{173}Ta can be due to the increase of deformation which we have also observed experimentally [4].

It is surprising to observe the smallest value of the g-factor for the $9/2^-$ state across the odd-A Ta isotopic chain. The theoretical calculations based on modified oscillator potential [3] have shown the magnetic moment of the $9/2^-$ isomer to be insensitive to the deformation parameter. The reduction of the $g(9/2^-)$ factor with decreasing neutron number has been considered due to particle octupole vibration coupling. The $9/2^-$ isomer is interpreted to be of mixed configuration $\pi 9/2^-[514]$ and $\pi 7/2^+[404] \otimes 3^-$.

REFERENCES

- [1] P.Thakur *et al.*, Hyperfine Interactions 136 (2001) 201.
- [2] C. König *et al.*, Nucl. Phys. A 534 (1991)344.
- [3] Ekström, H. Rubinsztein and P. Möller, Physica Scripta 14 (1976) 199.
- [4] V. Kumar *et al.*, Eur. Phys. J. A. 26 (2005) 311.

5.1.10 Electric Quadrupole Moment of the $K^\pi = 8^-$ and $23/2^-$ Isomeric States in $^{170,171,172}\text{Hf}$

V. Kumar¹, P. Thakur¹, A.K. Bhati¹, R.P. Singh², R.K. Bhowmik²

¹Centre for Advanced Study in Physics, Panjab University, Chandigarh-160014

²Inter-University Accelerator Centre, Post Box -10502, New Delhi-110067

The phenomenon of high-K isomerism is common in the $A \approx 170$ -190 mass region. Many high-K isomers are observed systematically across the hafnium isotopic chain [1]. There is renewed interest in the properties of these multi-qp states for understanding the structure of deformed nuclei [2].

The two-quasiparticle $K^\pi = 8^-$ isomers have been established to have $\pi(9/2^- [514] \otimes 7/2^+ [404])$ configuration in $^{170,172}\text{Hf}$ [3, 4] and have small additional mass-dependent admixture of $\nu(9/2^+ [624] \otimes 7/2^- [514])$ configuration. The odd neutron, $\nu 7/2^+ [633]$, coupled with the $K^\pi = 8^-$ configuration in even-even Hf isotopes was observed to give three-quasiparticle $K^\pi = 23/2^-$ isomer in ^{171}Hf [5]. The magnetic moment measurements have confirmed the configuration of the 8^- isomer in ^{172}Hf . The systematic comparison of the magnetic moments in $^{172,173,174,178}\text{Hf}$ [6] isotopes have been made with the predictions of the Nilsson quasiparticle model. The quadrupole moment measurements are still lacking in this region.

The electric quadrupole interaction of $K^\pi = 8^-$ and $K^\pi = 23/2^-$ isomers in $^{170,171,172}\text{Hf}$ isotopes has been measured at room temperature using the time differential perturbed angular distribution (TDPAD) technique. The aligned isomeric states were populated by the heavy-ion fusion evaporation reaction $^{160}\text{Gd}(^{16}\text{O}, xn\gamma)^{170,171,172}\text{Hf}$ with a pulsed ^{16}O ion beam (1.3 ns pulsed width) at beam energies 104, 92 and 78 MeV to populate the respective isomeric states. The repetition periods of 250 ns and 1 μs were used to excite the isomeric states in $^{170,171}\text{Hf}$ and ^{172}Hf , respectively. The target consisted of enriched 700 $\mu\text{g}/\text{cm}^2$ gadolinium (^{160}Gd) evaporated on 33 mg/cm^2 Hf foil serving as host medium to self implant recoiling nuclei.

The ratio function $G_{22}(t)$ was formed from the corresponding time spectra for each isotope and fitted to the theoretical quadrupole perturbation factor. The TDPAD spectra of the isomeric states in $^{170,171,172}\text{Hf}$ are shown Fig. 1. Using the measured value of the electric field gradient (efg) $900(3) \times 10^{15} \text{ V}/\text{cm}^2$ at 4.2 K in ^{178}Hf [7], the extracted values of the spectroscopic quadrupole moments Q_s and the intrinsic quadrupole moment Q_0 from the quadrupole interaction frequency ω_0 are listed in Table 1. The measured value of the efg in Hf at 4.2 K may be slightly higher than the value at room temperature.

Table 1: The quadrupole moments of $^{170,171,172}\text{Hf}$.

Isotope	I^π	Q_s	Q_0	$\beta_2^*(\text{exp.})$	$\beta_2^*(\text{th.})$ (g.s)
^{170}Hf	8^-	4.91(17)	7.00(24)	0.251(8)	0.260
^{171}Hf	$23/2^-$	4.92(17)	6.32(22)	0.225(8)	
^{172}Hf	8^-	5.40(19)	7.69(27)	0.273(9)	0.271

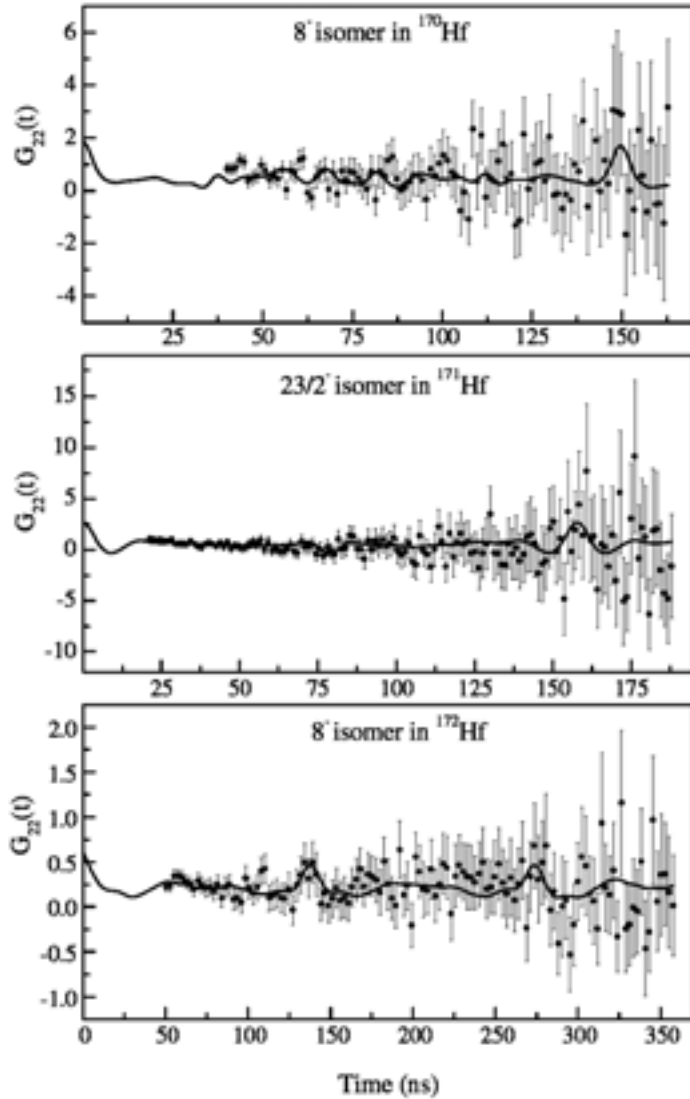


Fig. 1 : TDPAD spectra of the isomeric states in $^{170,171,172}\text{Hf}$

It has been observed that in most of the pure metallic systems the variation of the efg with temperature follows the well known $T^{3/2}$ law [8],

$$V_{zz}(T) = V_{zz}(T=0)(1 - BT^{3/2})$$

where B is the slope parameter. The parameter B which determines the temperature dependance of the efg has values ranging from $1 \times 10^{-5} \text{ K}^{-3/2}$ to $8 \times 10^{-5} \text{ K}^{-3/2}$ [8]. Considering the value of B as $1 \times 10^{-5} \text{ K}^{-3/2}$ (valid in the neighboring metallic systems), the value of Q_0 is affected within the quoted errors. The extracted values of the deformation parameter β_2 are divided by 1.1 to compare with the theoretical predictions by Nazarewicz *et al.* [9]. In the even-even Hf nuclei, the deformation value is approximately the same as that of the ground state and follows the predicted trend with neutron number. But the value of Q_0 for the 3-qp state $23/2^-$ in ^{171}Hf is $\sim 12\%$ less than the value assumed for the

extraction of $(g_K - g_R)/Q_0$ factor from the in-band analysis. In the present investigations, it was not possible to determine the sign of the quadrupole moment but the TRS calculations for the low-lying high-K states for the even-even hafnium isotopes [10] has shown that the multi-qp states have well-deformed prolate shapes. These measurements confirm the magnitude of the quadrupole deformation parameter considered at lower and intermediate spin states in Hf nuclei.

REFERENCES

- [1] P.M. Walker, Physica Scripta T5 (1983) 29.
- [2] P.M. Walker and G.D. Dracoulis, Nature 399 (1999) 35.
- [3] D.M. Cullen et al., Phys. Rev. C 60 (1999) 057303.
- [4] P.M. Walker et al., Nucl. Phys. A 293 (1977) 481.
- [5] G.D. Dracoulis and P.M. Walker, Nucl. Phys. A 330 (1979) 186.
- [6] P.M. Walker et al. Nucl. Phys. A 349 (1980) 1.
- [7] E.Gerdau et al., Hyperfine Structure and Nuclear Radiations, eds. E. Matthias and D.A. Shirley, North Holland, Amsterdam, (1968) p. 261.
- [8] J. Christiansen et al., Z. Phys. B 24 (1976) 177.
- [9] W. Nazarewicz et al. , Nucl. Phys. A 512 (1990) 61.
- [10] F.R. Xu et al., Phys. Rev. C 62 (2000) 014301.

5.1.11 Electric Quadrupole Moment of the $K^\pi = 9/2^-$ and $21/2^-$ isomeric States in ^{175}Ta

V. Kumar¹, P. Thakur¹, A.K. Bhati¹, R.P. Singh², R.K. Bhowmick²

¹Centre for Advanced Study in Physics, Panjab University, Chandigarh-160014

²Inter-University Accelerator Centre, Post Box -10502, New Delhi-110067

The odd tantalum nuclei belong to the mass region $A \sim 170-180$ characterised by well deformed symmetric shape. A large number of one- and multi-qp isomeric states with high-K were predicted [1] and have been observed at low energies in Hf [2], Ta [3], W [4] and Os [5]. The decay of K-isomers is hindered because of high K value and defines the isomeric level lifetime. Various K-mixing mechanisms, e.g. Coriolis mixing and tunneling through γ -degree of freedom etc., have been proposed to explain the violation of K-selection rule, but this complex process is still not properly understood [6]. A reliable information about the configuration and the shape of the nucleus in equilibrium is required to examine the K-mixing mechanisms involved.

The time differential perturbed angular distribution technique (TDPAD) has been employed for the quadrupole moment measurements of the isomeric states in

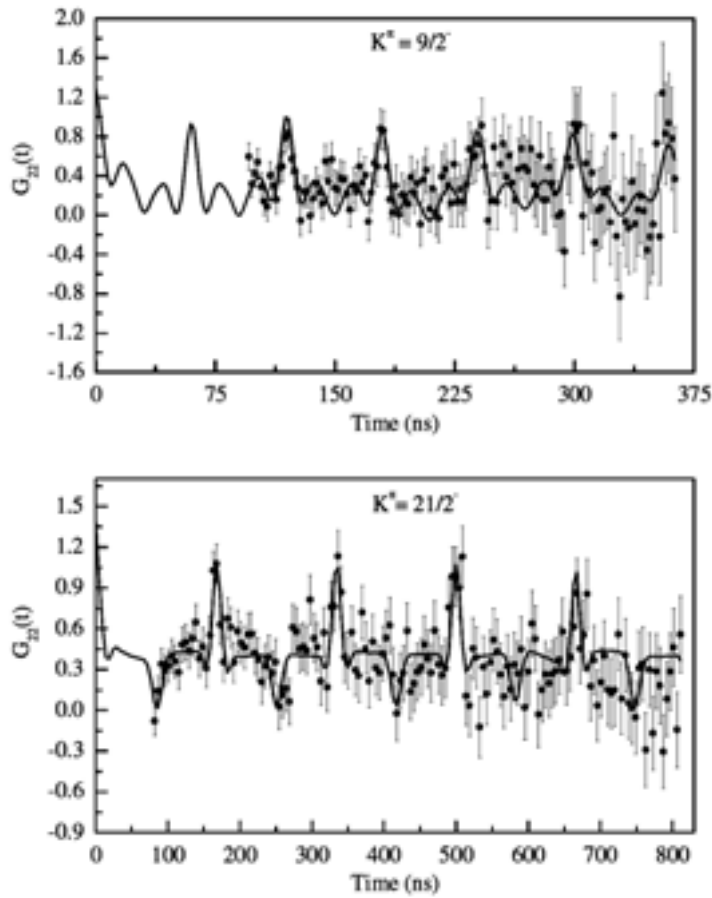


Fig. 1 : TDPAD spectra of 9/2⁻ and 21/2⁻ isomeric states in ¹⁷⁵Ta

fitted quadrupole interaction frequency ω_0 in ¹⁷⁵Ta along with the previously reported values in ^{169,171,173}Ta are listed in Table 1 and plotted in fig. 2.

Table 2 : The quadrupole moment s of the odd-Ta nuclei.

Isotope	I^π	Q_s	Q_0	$\beta_2(\text{exp.})$
¹⁶⁹ Ta	5/2 ⁻	2.23(13)	7.80(45)	0.303(17)
	9/2 ⁻	2.28(13)	4.18(13)	0.162(9)
¹⁷¹ Ta	9/2 ⁻	3.09(19)	5.66(34)	0.218(13)
¹⁷³ Ta	9/2 ⁻	2.66(6)	4.91(11)	0.188(4)
	21/2 ⁻	6.34(15)	8.33(22)	0.319(8)
¹⁷⁵ Ta	9/2 ⁻	2.80(16)	5.13(29)	0.195(11)
	21/2 ⁻	5.89(35)	7.74(46)	0.294(17)

¹⁷⁵Ta. An isotopically enriched target of ¹⁶⁰Gd with the thickness of 775 $\mu\text{g}/\text{cm}^2$ was evaporated on 13.6 mg/ cm^2 ¹⁵⁹Tb foil to self implant the recoiling nuclei. The detectors were fixed at angles, 0 $^\circ$ and 90 $^\circ$. In order to investigate the delayed gamma rays produced in the reaction, energy spectra gated at different time intervals with respect to the beam pulses were created.

The ratio function $G_{22}(t)$ was formed from the corresponding time spectra for each transition and fitted to the theoretical quadrupole perturbation factor for the respective isomeric states. The TDPAD spectra of the isomeric states in ¹⁷⁵Ta are shown Fig. 1. The extracted values of Q_s and Q_0 from the

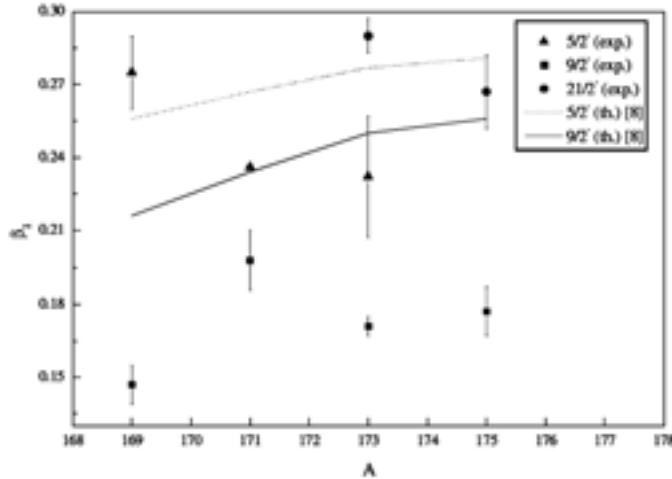


Fig. 2 : Systematics of the quadrupole moment in Ta isotopes

The variation in the magnitude and the direction of the quadrupole deformation of the one-qp state with the mass is at variance with the theoretical computed values. The variation in the induced deformation in the core is attributed to the different deformation driving forces of the one-quasiproton orbitals, $1/2^- [541]$ and $9/2^- [514]$ [7]. The occupation of the single-proton orbital influences the first crossing frequency of the band due to the alignment of the pair of $i_{13/2}$ neutrons also

through the configuration dependent deformation effects. The theoretical calculations of the deformation parameter [8] are based on the pure one-qp nature of the state. The deviation from the theoretical predictions is expected because of other microscopic details of the wave functions of the single particle states, e.g. K-mixing, coupling of octupole-vibrations etc., which have not been included here. The slight increase in the deformation for the 3-quasiparticle $21/2^-$ state in ^{173}Ta as compared to that in ^{175}Ta seems to be due to the enhancement of the π^3 fraction in the configuration. The sign of the quadrupole moment cannot be measured in the present experiment, which restricts the determination of the nature of the quadrupole deformation.

REFERENCES

- [1] O. Nathan and S.G. Nilsson, 'Alpha-, Beta- and Gamma-Ray Spectroscopy', ed. K. Siegbahn, North-Holland, Amsterdam, (1965), Chap. X.
- [2] N.L. Gjørup et al., Z. Phys. A 337 (1990) 353.
- [3] G.D. Dracoulis et al., Phys. Rev. C 53 (1996) 1205.
- [4] C.S. Purry et al., Phys. Rev. Lett. 75 (1995) 406.
- [5] J. Pedersen et al. Phys. Rev. Lett. 54 (1985) 306; Z. Phys. A 321 (1985) 217.
- [6] P.M. Walker and G.D. Dracoulis, Hyp. Int. 135 (2001) 83.
- [7] V. Kumar et al., Eur. Phys. J. A 26 (2005) 311.
- [8] W. Nazarewicz et al., Nucl. Phys. A 512 (1990) 61.

5.1.12 Investigation of scattering and reaction with loosely bound nuclei $^6,7\text{Li}$

Mandira Sinha¹, Mili Biswas², A.Mukherjee², Subinit Roy², P. Basu², H. Majumdar², R.Bhattacharya¹, B.R.Behera³, K.S.Golda⁴, S.K.Datta⁴, S.Kailas⁵

¹Gurudas College, Kolkata

²Saha Institute of Nuclear Physics, Kolkata-700 064

³Punjab University, Chandigarh, Panjub

⁴Inter-University Accelerator Centre, Post Box -10502, New Delhi 110067

⁵Nuclear Physics Division, BARC, Mumbai

Exploring the structure and reaction dynamics with loosely bound projectiles at near barrier energies is a challenging problem at present time. Simultaneous description of scattering, transfer/breakup and fusion with a consistent set of parameters for phenomenological or folding potentials is essential and necessary for proper understanding. Scattering measurements for weakly bound nuclei become important due to influence of break-up /transfer effects. In a recent work by Pakou et al [1] it has been conjectured that the polarization potential, which is produced by break-up, has an important role to play in the manifestation of contradictory behavior of real and imaginary parts of the optical model potential. In this background we measured angular distribution of elastic scattering for ${}^6,7\text{Li} + {}^{28}\text{Si}$ and thereby extract the optical model parameters and study their nature in the neighborhood of barrier.

Experiment was done using General Purpose Scattering Chamber of Pelletron Facility at IUAC, New Delhi with ${}^6,7\text{Li}$ beam (4-25 pna) with energies 16, 21 and 26 MeV. We used Si target sandwiched between two thin layers of Au (Au-Si-Au:95-143-30 $\mu\text{g}/\text{cm}^2$) to avoid oxidation. For energy calibration we used ${}^{160}\text{Er}$ beam at 20MeV. Four ($\Delta E-E$) telescope detectors and two monitor detectors (at $\pm 9.8^\circ$) were used. Two telescopes (25 μm , 300 μm) were for heavy ion (${}^6\text{Li}, {}^7\text{Li}, \alpha$) particle detection placed at Lower Arm, 12° apart, at a distance of 64, 60cm respectively subtending solid angles of $\Omega=1.18\times 10^{-4}$ and $\Omega=1.35\times 10^{-4}$ sr. The other two telescopes (150 μm , 5mm) were meant for light ion (p, d, t) particle detection placed at Upper Arm, 6° apart, at a distance of 56, 57 cm subtending $\Omega=1.51\times 10^{-4}$ and $\Omega=1.46\times 10^{-4}$ sr respectively at the target. Angular distributions were taken from 16° to 150° in steps of $4^\circ/10^\circ$.

We have measured target thickness of Au and Si from Rutherford scattering data and found these values to be 125 $\mu\text{g}/\text{cm}^2$ for Au and 143 $\mu\text{g}/\text{cm}^2$ for Si. Two typical 2D- spectra obtained from heavy ion particle telescope and light ion telescope are shown in figs.1 and 2. The elastic scattering data for ${}^6,7\text{Li} + {}^{28}\text{Si}$ were first analyzed. Optical model parameters were obtained from the fits to the experimental elastic scattering data (shown in fig.3 and fig.4) at three energies with coupled channel code ECIS94 using target deformation $\beta_2 = -0.47$ (g.s). All six parameters V, W_s, r, r_s, a, a_s were allowed to vary with constant volume imaginary potential W_v ($W_v = 60$ MeV, $R_v = 3.019$ fm, $a_v = 0.40$ fm) to achieve the best fit and the final values are shown in table 1 and table 2. Real and imaginary parts of potential for ${}^6\text{Li}+{}^{28}\text{Si}$ are almost constant with increasing energies. For ${}^7\text{Li}+{}^{28}\text{Si}$, real and imaginary strengths are almost similar for 16 & 21 MeV. Data for 26 MeV, showing oscillation beyond

$\theta_{cm} \sim 55.7^\circ$, need to be further extended. Theoretical analysis, with microscopic folding model calculation, is in progress. Simultaneous analysis of scattering, transfer/break-up and fusion will be done after extraction of evaporation α -, p- cross-sections (for fusion) and direct α & p component (for transfer) from our data to arrive at a consistent set of optical model parameters.

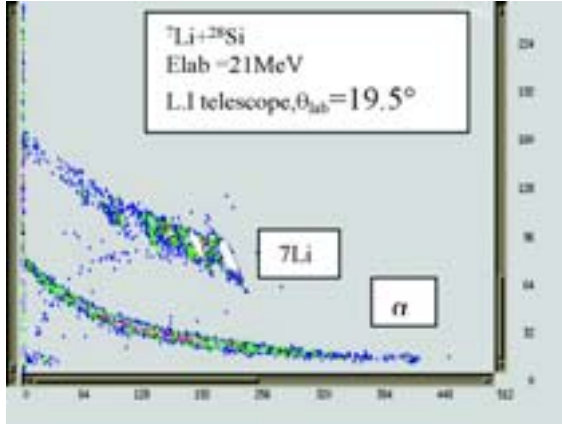


Fig 1: ΔE -E spectrum for HI telescope

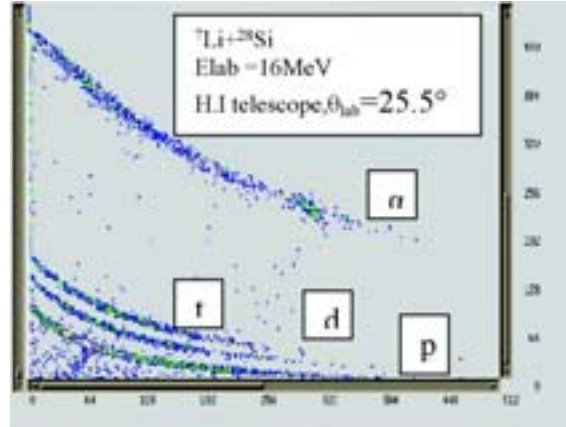


Fig 2 : ΔE -E spectrum for LI telescope

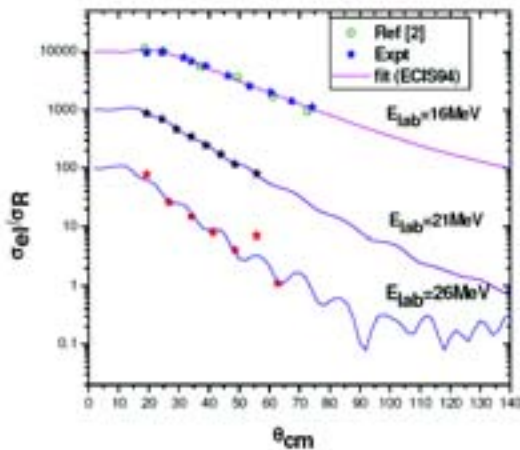


Fig.3 Elastic angular distribution of ${}^7\text{Li} + {}^{28}\text{Si}$

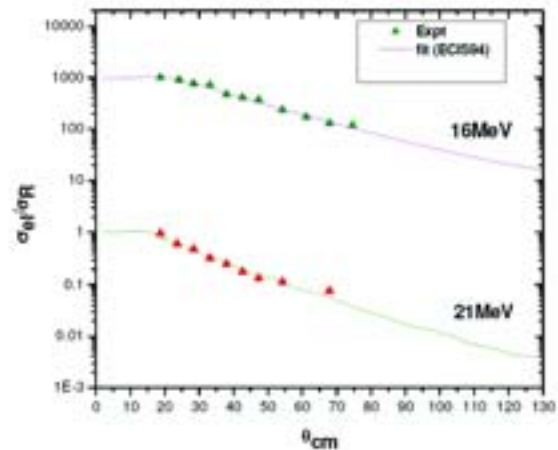


Fig.4 Elastic angular distribution of ${}^6\text{Li} + {}^{28}\text{Si}$

Table 1 Phenomenological potential parameters for ${}^7\text{Li} + {}^{28}\text{Si}$

E_{lab} (MeV)	V (MeV)	r_o (fm)	a (fm)	Ws (MeV)	r_o' (fm)	a' (fm)	σ_{react} (mb)
16	45.97	0.99	0.756	18.75	1.0	0.75	1227
21	48.42	0.99	0.756	14.38	1.0	0.75	1406
26	66.94	0.99	0.756	13.9	1.01	0.69	1557

Table 2 Phenomenological potential parameters for ${}^6\text{Li} + {}^{28}\text{Si}$

E_{lab} (MeV)	V (MeV)	r_0 (fm)	a (fm)	Ws (MeV)	r_0' (fm)	a' (fm)	σ_{reac} (mb)
16	48.64	1.01	0.78	23.94	1.02	0.75	1316
21	45.08	1.01	0.78	26.45	0.99	0.75	1537

REFERENCES

- [1] A. Pakou et al., Phys. Lett., B556 (2003) 21
[2] A. Pakou et al, Phys. Rev C 69, 054602 (2004)

5.1.13 Elastic scattering and fusion measurement of ${}^7\text{Li} + {}^9\text{Be}$ system

S. Verma¹, K.S. Golda², J.J. Das², A. Jhingan², S. Mandal¹, K. Kalita^{1,4}, N. Madhavan², P. Sugathan², J. Gehlot², Ranjit¹, S. Nath², T. Varughese², B.K. Nayak³, A. Saxena³, S.K. Datta², R. Singh¹

¹Department of Physics and Astrophysics, Delhi University, Delhi - 110007

²Inter-University Accelerator Centre, Post Box -10502, New Delhi 110 067

³Nuclear Physics Division, BARC, Mumbai - 400085

⁴Department of Physics, Gauhati University, Guwahati-781014

The effect of breakup of stable and radioactive weakly bound nuclei on fusion has been extensively investigated in recent years both experimentally [1] and theoretically [2,3], but there is not yet a definite conclusion. There is a special interest in this subject due to the recently available radioactive ion beams. Although it is now possible to investigate reaction mechanisms with these exotic nuclei, experimentally such studies are limited due to low intensity of currently available radioactive ion beams. In view of the similarities of weakly bound stable systems with their associate weakly bound radioactive ones, the comprehension of the reaction mechanisms induced by intense beams like ${}^6,7\text{Li}$ and ${}^9\text{Be}$, should be very important for the study of reactions induced by low intensity radioactive ion beams.

Elastic scattering measurements for ${}^7\text{Be}+{}^9\text{Be}$ [4] system has been carried earlier at $E_{\text{lab}}=17, 19$ and 21 MeV. In order to do a comparative study, in the present experiment we have undertaken elastic scattering and fusion measurements for ${}^7\text{Li}+{}^9\text{Be}$ system.

The experiment was done at energies of ${}^7\text{Li}$ as $E_{\text{lab}} = 15.75, 24$ and 30 MeV using the GPSC facility. The elastic scattering measurement at 24 MeV has also been

carried by Weber et. al. [5] . The elastic scattering cross sections were measured in the angular range of 4° to 40° (in lab or 7° to 70° in c.m.) and fusion cross sections were measured at 125° and 150° (in lab). For obtaining fusion cross sections evaporated alpha particles were detected at backward angles so that there is no interference from any other channel. A ΔE -E (Si surface barrier, $13\mu\text{m}+300\mu\text{m}$) detector was mounted on the movable arm to detect alpha particles. For elastic scattering measurements ^7Li was detected using four Si surface barrier detectors of thicknesses $150\mu\text{m}+3\text{mm}$, $25\mu\text{m}+300\mu\text{m}$, $300\mu\text{m}$ and $300\mu\text{m}$ respectively, placed on another movable arm with angular separation of 6° . The first telescope detector was used with an intention to obtain the alpha and other low Z particles along with the ^7Li which completely stops in ΔE detector at the measured energies. The ^9Be target used in the experiment was of thickness 1.368 mg/cm^2 . Overlapped runs were also taken to normalise the solid angles of different detectors. Two monitor detectors were placed at $\pm 10^\circ$. Energy calibration was performed using ^{241}Am and ^{252}Cf sources. The experimental setup is shown in Fig. 1.

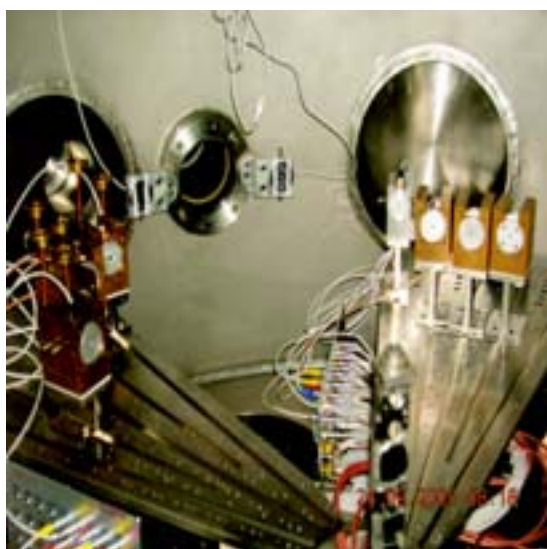


Fig. 1. Experimental set up

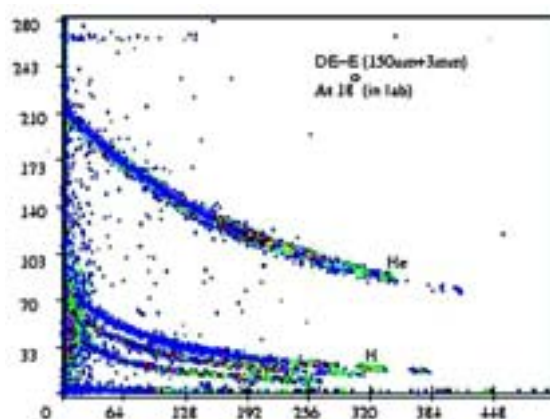


Fig. 2. IC vs E(tot) at $E_{\text{lab}}=24\text{MeV}$

A two dimensional ΔE -E spectrum with target (^9Be) at 24 MeV , as detected by the first telescope ($150\mu\text{m}+3\text{mm}$), placed at 18° (in lab), is shown in fig. 2. The elastic scattering cross section is obtained through the ΔE spectrum, as ^7Li gets stopped completely in ΔE detector at the measured energies. The spectrum shows a clear band of different Z values, possibly resulting from the decay of compound nucleus, transfer or breakup channels. The analysis of data is in progress.

REFERENCES

- [1] J. Takahashi *et al.*, Phys. Rev. Lett. 78 (1997) 30 and references therein.

- [2] C. Dasso *et al.*, Phys. Rev. C 50 (1995) R12.
- [3] M. S. Hussein *et al.*, Phys. Rev. C 46 (1992) 377.
- [4] S. Verma *et al.*, DAE-BRNS symp. On Nucl. Phys. 47B (2004) 340.
- [5] K. A. Weber *et al.*, Nucl. Phys. A186 (1972) 145.

5.1.14 Neutron multiplicity from $^{16}\text{O} + ^{181}\text{Ta}$ at $E_{\text{lab}} = 105 \text{ MeV}$

Hardev Singh¹, Golda K.S.², Pankaj Kumar², A. Jhingan², R.P. Singh², P. Sugathan², Ajay Kumar¹, Gulzar Singh¹, B.R. Behera¹, Mihir Chatterjee³, I.M. Govil¹

¹Department of Physics, Panjab University Chandigarh-160014

²Inter-University Accelerator Centre, Post Box -10502, New Delhi 110 067

³Saha Institute of Nuclear Physics, Kolkata-700064

The properties of heavy nuclei at high angular momentum and high excitation energies are currently areas of great experimental and theoretical activities, partly because of the recent revival of interest in the Super Heavy Elements (SHE) and partly for the sake of detailed understanding of the dynamics of the compound nucleus (CN) formation. Recent experimental data showed the presence of enhanced yield of neutrons [1], protons, alpha and GDR gamma rays as compared to statistical model prediction. This excess yield was explained in terms of time delay involved in the fusion-fission process because of motion of nuclei through viscous medium inside the nucleus.

The Experiment was performed at Inter University Accelerator Centre, New Delhi using 105 MeV pulsed Oxygen beam in General Purpose Scattering Chamber (GPSC). Tantalum target of $320 \mu\text{g}/\text{cm}^2$ thickness was made on $20 \mu\text{g}/\text{cm}^2$ carbon backing by high vacuum evaporation technique. Two large area ($20 \times 10 \text{ cm}^2$) position sensitive multi wire proportional counters (MWPC) were used at angles of 90° and -62° w.r.t. beam to detect complementary fission fragments. The detectors were placed at 57 and 40 cm from the target. Target ladder was kept at 45° w.r.t. beam to avoid the shadowing on either fission detector. Two monitor detectors were used at $\pm 11^\circ$ for beam flux normalization purpose. Four neutron detectors were used outside the chamber at distance of 100 cm from the target and at angles of 30, 60, 90 and 120 degree to detect the fission coincident neutrons. Pulse Shape Discrimination (PSD) technique was employed to reduce the gamma background in the experiment. Time of flight (TOF) of neutrons and fission fragments was measured with respect to RF. The observed TOF of neutrons was converted into energy and was corrected for neutron detector efficiency.

Pre and post-scission component of neutron multiplicity was extracted by

least square fitting of observed neutron energy spectrum with Watt expression [2]. The fits gives $v_{pre} = 2.6 \pm 1$ and $v_{post} = 1.5 \pm 0.12$. One such fit is shown in figure 1.

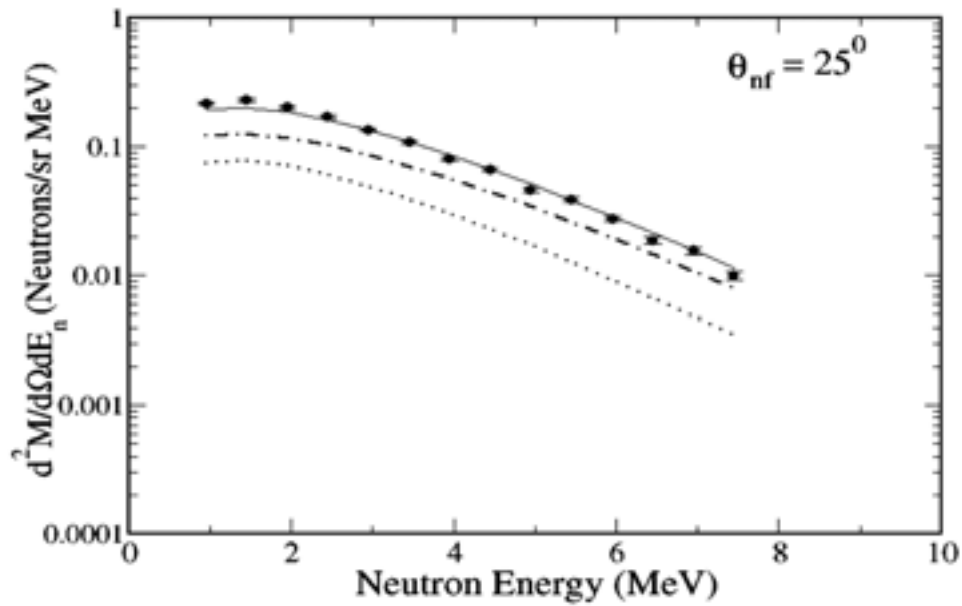


Fig. 1. Neutron energy spectra along with fits for pre-scission (dotted line), post-scission (dash-dotted) component and the sum of the two (solid line)

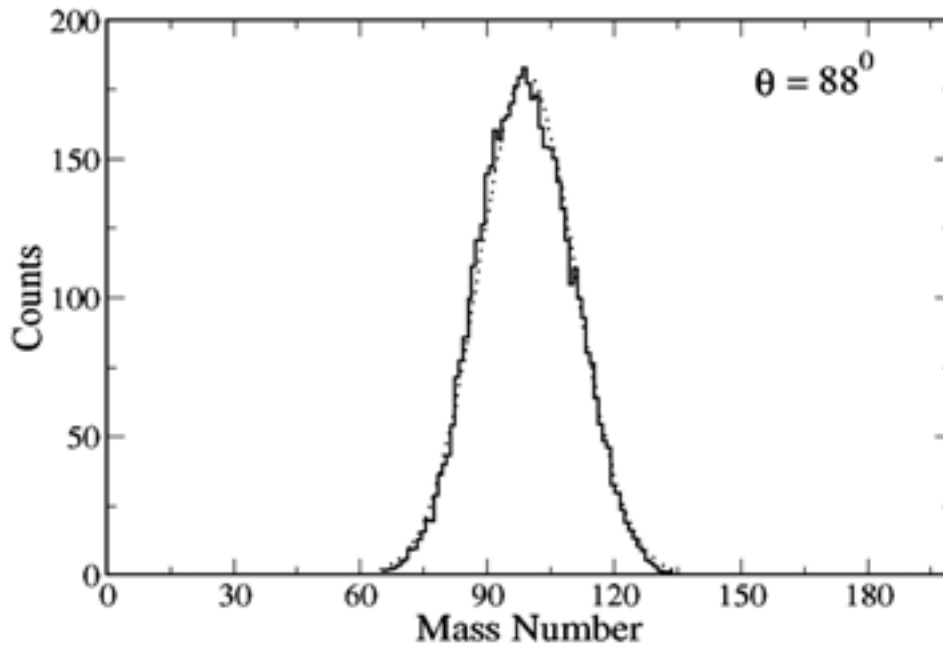


Fig. 2. Mass distribution along with the Gaussian fits (dotted line)

Masses of the fission fragments were determined from flight paths and time difference between complementary fission fragments [3] assuming no particle emission before scission as shown in fig.2.

REFERENCES

- [1] D. J. Hinde et al., Phys. Rev. C 45, 1229 (1992).
- [2] D. Hilscher et al., Phys. Rev. C 20, 576 (1979).
- [3] R. K. Choudhury et al, Phys. Rev. C60, 054609 (1999).

5.1.15 Study of incomplete fusion reaction dynamics: Observation of fast alpha particles in forward cone

Pushpendra P. Singh¹, Bhavna Sharma¹, Unnati¹, D. Singh¹, M.K. Sharma¹, B.P. Singh^{1*}, M.A. Ansari¹, H.D. Bhardwaj², R. Prasad¹, Rakesh Kumar³, K.S. Golda³, R.P. Singh³, S. Muralithar³ and R.K. Bhowmik³

¹A. M. University, Aligarh (UP)-202002

²D. S. N. College, Unnao

³ Inter-University Accelerator Centre, Post Box -10502, New Delhi 110 067

In recent years, there has been an increased interest in exploiting incomplete fusion (ICF) reaction dynamics, for gamma-spectroscopic studies of residues populated, in heavy ion (HI) reactions. One of the reasons for this interest is that ICF reactions offer access to states at relatively high angular momentum ($\ell_{\text{crit}} \leq \ell \leq \ell_{\text{max}}$) which are otherwise inaccessible by standard fusion-evaporation reactions involving stable projectile-target combinations. In ICF reactions, the projectile is assumed to break-up into fragments in the nuclear range of target nucleus. One of the fragments may fuse with the target nucleus leading to the formation of excited composite system and the remaining part may flow in the beam direction with almost the same velocity as that of incident projectile without any significant interaction with the target nucleus. Some of the important characteristics of ICF reaction dynamics are;

- 1) The angular distribution of the PLFs is strongly forward peaked.
- 2) The mean velocity of projectile like fragments (PLFs) is roughly equal to the velocity of projectile.
- 3) The excited composite system has a narrower angular momentum population as compared to complete fusion etc.

ICF reactions were recognized and studied many years ago using strongly bound nuclei like ¹⁶O and ¹²C, which are expected to have cluster structures. These studies were carried out at higher excitation energies ($E_{\text{beam}} = 10$ MeV/nucleon) [1-3]. Recent studies, however, indicated that ICF start competing with complete fusion reaction process at energies even near and slightly above the Coulomb barrier [4-6]. Significant information of ICF processes has been obtained from the studies of excitation functions (EFs), recoil range distributions (RRDs) and angular distributions

(ADs) of the residues [7-10]. In most of these studies the activation technique has been used to identify the residues from their characteristic gamma rays and half-lives. A vast number of channels, which leads to stable residues, could not be studied by the activation technique. As such, the measurements done so far are not complete. More detailed information about the ICF reaction dynamics can also be obtained from in-beam experiments by using particle-gamma coincidence technique. The information obtained from particle-gamma coincidence technique is likely a supplement and complement to the information obtained from the off-line measurements.

With a view to study ICF reaction dynamics, a particle-gamma coincidence experiment in the $^{16}\text{O}+^{169}\text{Tm}$ system at 90 MeV beam energy has been performed by using Gamma Detector Array (GDA) alongwith Charged Particle Detector Array (CPDA) set-up at Inter-University Accelerator Center (IUAC), New Delhi. The GDA consists of 12 Compton suppressed HPGe detectors at angles 45° , 99° , 153° with respect to the beam direction and there are 4 detectors at each of these angles. CPDA is a set of 14 phoswich detectors housed in a 18cm diameter scattering chamber. There are 4 detectors at forward angle (10° - 60°), 4 at backward angles (120° - 170°) and 6 around 90° covering nearly 90% of total solid angle so that the angular distribution of charged particles in $\approx 4\pi$ arrangement may be recorded. Spectroscopically pure Thulium (^{169}Tm) target of thickness $\sim 0.83\text{mg}/\text{cm}^2$ was mounted at 45° with respect to the beam direction inside the CPDA with the help of specially designed target holder. ^{16}O beam of 90MeV energy with beam current $\approx 30\text{nA}$ was used for the bombardment. To stop the evaporation alpha particles a foil of $100\mu\text{m}$ aluminum was employed in front of each forward detector of CPDA. All HPGe detectors of GDA set-up were pre-calibrated by using standard sources of known strength. In-beam prompt gamma-rays spectra were recorded in list mode file by using online data acquisition programme CANDLE of IUAC. The analysis of the data has been performed using INGASORT software. The intensities and area under the peaks of the characteristic prompt gamma-lines were used to determine the production yield and cross-sections for various residues.

Analysis of the data has been done by projecting different gating conditions like, CPDA- α -Forward, CPDA- α - 90° , CPDA-p-Forward, CPDA-p- 90° and CPDA-p-Backward, on all spectra. With gating condition CPDA- α -Forward, fast alpha particles were detected in forward cone which indicate that the ICF process is a dominant reaction dynamics at these moderate excitation energies. Residues, which are found to be strongly populated via ICF reaction channels in $^{16}\text{O}+^{169}\text{Tm}$ system, are $^{176,177,178,179}\text{Re}$, $^{176,177}\text{W}$, $^{175,176,178}\text{Ta}$, ^{172}Lu and $^{175,178}\text{Hf}$ [11]. The spin distributions of these populated residues have also been determined to know the population probability in different spin states and also to look into the side feeding pattern intensities. Some complete fusion and pre-equilibrium emission channels have also been identified with different gating conditions. All these reaction channels have

been confirmed by looking into singles as well gated spectra. Data analysis is still in progress.

REFERENCES

- [1] H. C. Britt, et. al., Phys. Rev. 124, 3 (1961) 877.
- [2] J. Galin, et. al. Phys. Rev. C9 (1974) 113.
- [3] H. Tricore, et. al., Z. Phys. A – Atoms and Nuclei, 306 (1982) 127.
- [4] B. J. Roy, et. al., Nucl. Phys. A, 597 (1996) 151.
- [5] R. I. Bardan, et. al., Euro. Phys. J. A12 (2001) 317.
- [6] S. Mukherjee, et. al., Euro. Phys. J. A12 (2001) 199.
- [7] Sunita Gupta, et. al., Phys. Rev. C61 (2000) 064913.
- [8] M. K. Sharma, et. al., Phys. Rev. C70 (2004) 044606.
- [9] L. Corradi, et. al., Phys. Rev. C71 (2005) 014609.
- [10] Unnati, et. al., Int. J. Mod. Phys. E14 (2005) 775.
- [11] Pushpendra P. Singh, et. al., DAE-BRNS, Symp., V50 (2005) 336.

5.1.16 Study of fission hindrance in ^{200}Pb

P.D. Shidling¹, N.M. Badiger¹, S. Nath², Rakesh Kumar², Akhil Jhingan², R.P. Singh², P. Sugathan², S. Muralithar², N. Madhavan², P.V. Madhusudhana Rao³, K. Kalita⁴, S. Verma⁵, S. Mandal⁵, R. Singh⁵, B.R. Behera⁶, Santanu Pal⁷, A.K. Sinha⁸, S. Kailas⁹, B.P. Singh¹⁰, K.M. Varier¹¹, M.C. Radhakrishna¹²

¹Karnatak University, Dharwad – 580003

²Inter-University Accelerator Centre, Post Box -10502, New Delhi 110 067

³Andhra University, Visakhapatnam – 530003

⁴Guwahati University, Guwahati – 781014

⁵Delhi University, New Delhi –110007

⁶Panjab University, Chandigarh

⁷Variable Energy Cyclotron Centre, Bidhannagar, Kolkata – 700064

⁸UGC-DAE, CSR, Kolkata Centre, Bidhannagar, Kolkata – 700091

⁹Nuclear Physics Division, BARC, Mumbai – 400085

¹⁰Aligarh Muslim University, Aligarh

¹¹Calicut University, Calicut – 673635

¹²Bangalore University, Bangalore – 560056

The time scale of fission for highly excited heavy nuclei resulting from a heavy ion induced fusion reaction has been extensively studied by measuring multiplicities of neutrons [1], charged particles [2] and electric dipole γ -rays [3]. These experiments have shown that the fission process is strongly hindered relative to expectation based on the standard statistical model description of the process.

However, these experiments are not very sensitive about whether the emission occurs mainly before or after the traversal of the saddle point as the system proceeds towards scission. Measurement of evaporation residue formation probability provides a desired separation between pre-saddle and post-saddle dissipation. Evaporation residue spin distribution is also an additional physical parameter to study the dynamical competition between evaporation residue and fission. Thus the combined study of the evaporation residue and spin distribution gives better understanding of fusion fission dynamics. In the present experiment we have measured evaporation residue and spin distribution for $^{16}\text{O} + ^{184}\text{W}$ system in the energy range 84 MeV to 120 MeV.

The experiment was performed in two runs using the Heavy Ion Reaction Analyzer (HIRA) [4] and the 14 element BGO ball (multiplicity filter) at IUAC, New Delhi. In the first run, ^{16}O pulsed beam with the pulse separation of 4 μsec was taken from 15UD Pelletron at IUAC and bombarded on enriched isotopic tungsten target of thickness 200 $\mu\text{g}/\text{cm}^2$ with carbon backing of 100 $\mu\text{g}/\text{cm}^2$. A carbon foil of thickness 40 $\mu\text{g}/\text{cm}^2$ was placed 10 cm downstream from the target to reset the charge states of ERs to statistical distribution after internal conversion processes. Two monitor detectors were placed symmetrically at $\pm 25^\circ$ with respect to the beam direction for normalization purposes. The 14 element BGO multiplicity filter was used at the target chamber to record the gamma fold in coincidence with evaporation residues detected at the focal plane of HIRA using a 2D position sensitive silicon detector (50 \times 50 mm^2). To predict the evaporation residue cross section accurately, precise measurement of the transmission efficiency of HIRA was required. This was performed in the second run using coincident gamma ray method. Top 7 BGO detectors were replaced by single high resolution HPGe detector at the target chamber. Remaining experimental setup was same as that of the previous run. ^{16}O pulsed beam of 100 MeV was bombarded on isotopic ^{184}W target of thickness 200 $\mu\text{g}/\text{cm}^2$. Gamma rays were recorded in singles and in coincidence with evaporation residues detected at the focal plane of HIRA. Three gamma energies of residual nuclei ^{194}Pb and ^{195}Pb were identified. Ratio of coincidence counts and singles counts was taken to determine the transmission efficiency of HIRA and it was found to be 1% for our system. Few energy points were repeated by replacing the HPGe detector with BGO detectors to confirm our results of the first run. Fig. 1 shows the plot of evaporation residue cross section as a function of beam energy. In the analysis of spin distribution data, bit pattern was generated using the CANDLE software [5] for extracting fold distribution of ER gamma rays. Computer program was written following the procedure adopted by Vander Werf [6] to convert the fold distribution into moments of multiplicity distribution. Fig. 2 shows the plot of average gamma multiplicity as a function of beam energy. Using the skewed gaussian distribution function, extracted moments were converted into multiplicity distribution. Transformation of the multiplicity to spin distribution is made assuming evaporation residues to be good rotors with two units of angular momentum carried by each nonstatistical γ -rays. Fig. 3 shows the spin distribution for different beam energies. Theoretical calculation is in progress.

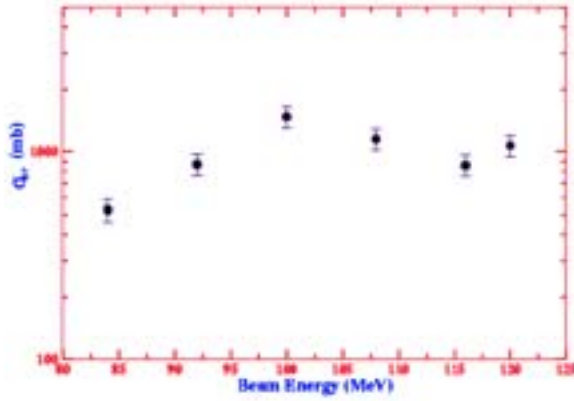


Fig. 1. ER cross section Vs beam energy

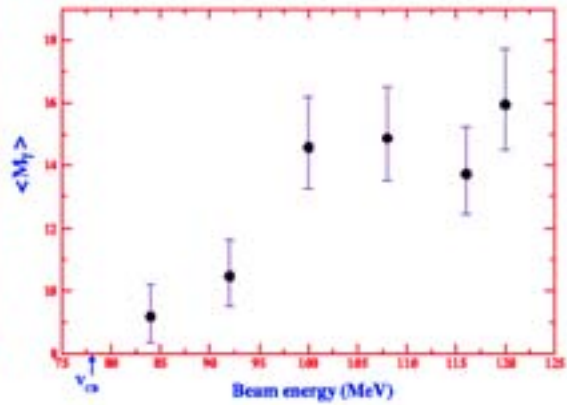


Fig. 2. $\langle M_\gamma \rangle$ Vs Beam energy

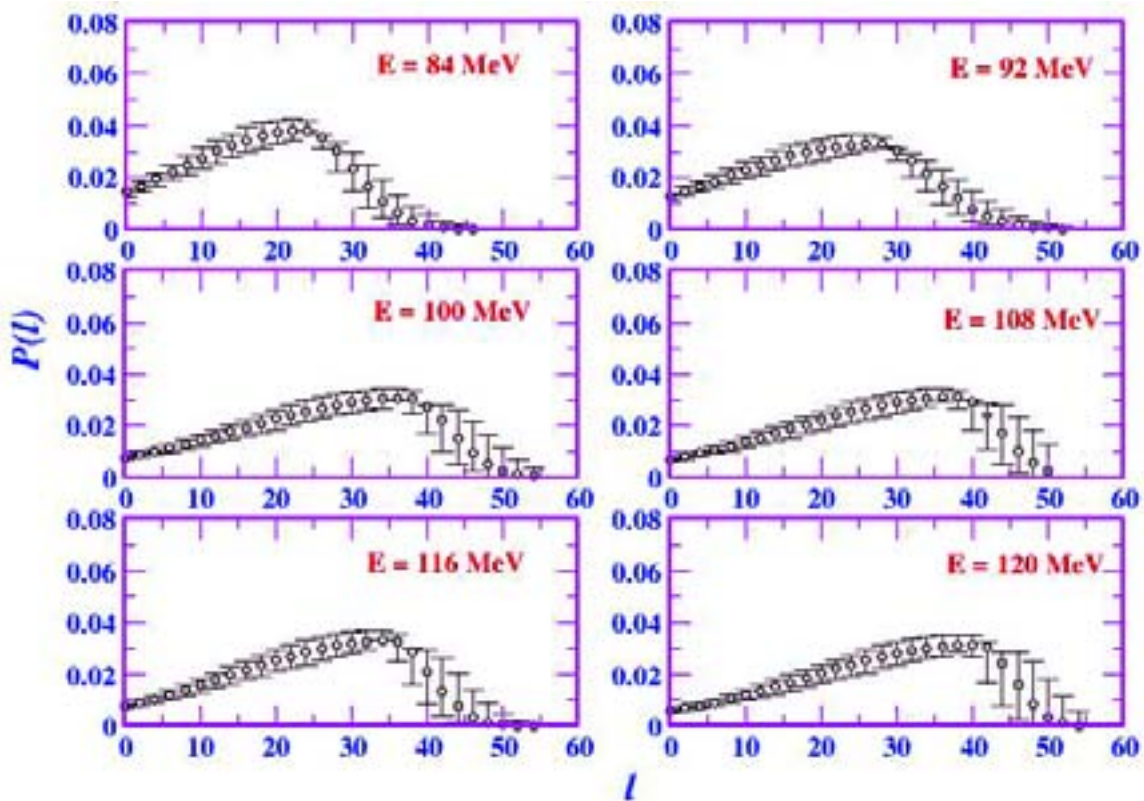


Fig. 3. $P(\ell)$ Vs ℓ

REFERENCES

- [1] D.J. Hinde et al. Phys. Rev. C. 45(1992)1229.
- [2] J. P. Lestone et. al., Phy. Rev. Lett. 67 (1991)1078.
- [3] I. Diószegi et al. Phy. Rev. C. 63 (2000) 014611
- [4] A. K. Sinha et al., NIMA 339 (1994) 543
- [5] CANDLE Version 2.2, developed at Inter University Accelerator Centre , New Delhi
- [6] S.Y. Vander Werf, Nucl. Instr. And Meth. 153 (1978) 221 – 228.

5.1.17 Elastic scattering and fusion cross sections for ${}^7\text{Li}$, ${}^7\text{Be}$ + ${}^{27}\text{Al}$ systems

K. Kalita^{1,4}, S. Verma¹, R. Singh¹, J.J. Das², A. Jhingan², N. Madhavan², S. Nath², T. Varughese², P. Sugathan², V.V. Parkar³, K. Mahata³, K. Ramachandran³, A. Shrivastava³, A. Chatterjee³, S. Kailas³, S. Barua⁴, P. Basu⁵, H. Majumdar⁵, M. Sinha⁶, R. Bhattacharya⁶, A.K. Sinha⁷

¹Department of Physics and Astrophysics, Delhi University, Delhi - 110007

² Inter-University Accelerator Centre, Post Box -10502, New Delhi 110 067

³Nuclear Physics Division, BARC, Mumbai - 400085

⁴Department of Physics, Gauhati University, Guwahati-781014

⁵Saha Institute of Nuclear Physics, Kolkata-700064

⁶Gurudas College, Kolkata-700054

⁷UGC-DAE consortium for Scientific Research, Kolkata-700098

Reactions induced by weakly bound stable as well as radioactive nuclei on a range of targets have been studied in recent years in the energy region around and well above the Coulomb barrier. There has been a focused interest in this field with the aim of studying the effect of break-up of such projectiles on the fusion cross-sections in the context of enhancement and/or suppression. With the intention of making a comparison between the ${}^7\text{Be}$ + ${}^{27}\text{Al}$ and ${}^7\text{Li}$ + ${}^{27}\text{Al}$ systems, we carried out elastic scattering angular distribution measurements at $E_{\text{lab}} = 17, 19, 21$ MeV (for ${}^7\text{Be}$ + ${}^{27}\text{Al}$) and at $E_{\text{lab}}=10,13, 16, 19$ and 24 MeV (for ${}^7\text{Li}$ + ${}^{27}\text{Al}$). For ${}^7\text{Be}$ + ${}^{27}\text{Al}$ system the one proton transfer measurement was also done[1]. This one-proton stripping channel has $Q = +6\text{MeV}$. The alpha-evaporation spectra were also measured for ${}^7\text{Li}$ + ${}^{27}\text{Al}$ system for obtaining the fusion cross sections. It can be noted that ${}^7\text{Be}$ and ${}^7\text{Li}$ are mirror nuclei and have similar cluster structures.

The experiment for ${}^7\text{Li}$ + ${}^{27}\text{Al}$ system was carried out at BARC-TIFR pelletron accelerator facility at Mumbai, with ${}^7\text{Li}$ beam at $E_{\text{lab}}=10, 13, 16, 19$ and 24 MeV. A set of three ΔE -E Si detector telescopes were used for these measurements. The elastic scattering angular distributions were measured at all the above energies covering an angular range from 10° to 72° (in lab) using all the three telescopes. The fusion measurements were performed by detecting evaporated alpha-particles using first two of the telescopes at lab angles of $52^\circ, 72^\circ, 92^\circ, 102^\circ, 112^\circ, 122^\circ, 132^\circ$ (142° at 10 MeV).

Quasielastic scattering and transfer reaction cross section measurements have been done for ${}^7\text{Be}$ + ${}^{27}\text{Al}$ system at $E_{\text{lab}}=17, 19$ and 21 MeV in the angular range $\theta_{\text{c.m.}}=12^\circ$ - 43° . Optical model (OM) analysis of the quasielastic scattering data has been carried out. The fusion cross sections have been derived at these energies by subtracting the integrated transfer cross sections from the reaction cross sections obtained from the fits to quasielastic scattering data.

These fusion cross sections were found to be consistent with those obtained from the coupled channels calculations. Elastic scattering and fusion cross sections have been measured for ${}^7\text{Li} + {}^{27}\text{Al}$ system at $E_{\text{lab}}=10, 13, 16, 19$ and 24 MeV. For elastic scattering the angular coverages were in the $\theta_{\text{lab}}=12^\circ-72^\circ$ range and for fusion the alpha-evaporation spectra from the compound nucleus were measured in the angular range $\theta_{\text{lab}} = 52^\circ$ to 132° (142° at 10 MeV). The elastic scattering angular distributions were subjected to OM analysis (fig 1).

The alpha-evaporation spectra were reproduced with the statistical model calculations and the fusion cross sections were extracted therefrom. The fusion cross sections were also extracted by subtracting the integrated inelastic scattering cross sections from the reaction cross sections obtained from the OM fits to the elastic scattering data and these fusion data were found to be consistent [2].

The CCDEF calculations describe these data quite well. A comparison of the fusion data for the ${}^7\text{Be}$, ${}^9\text{Be}$, ${}^7\text{Li} + {}^{27}\text{Al}$ systems shows a similar and consistent behavior (fig 2).

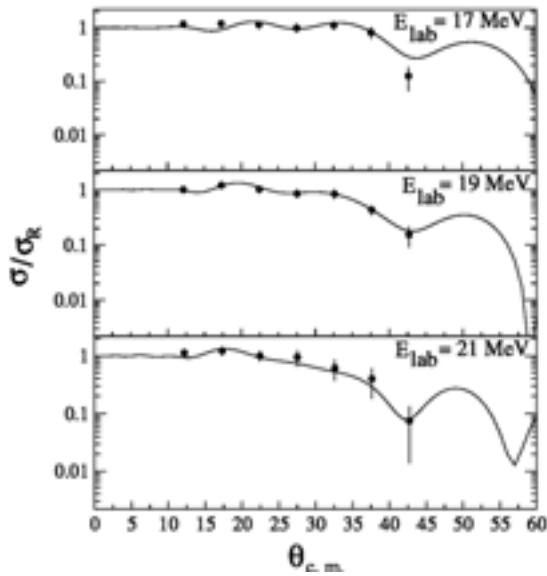


Fig. 1. Angular distributions for elastic scattering of ${}^7\text{Be}$ from ${}^{27}\text{Al}$ at $E_{\text{lab}}=17, 19$ and 21 MeV. The solid curves are OM fits obtained with the SNOOPY code.

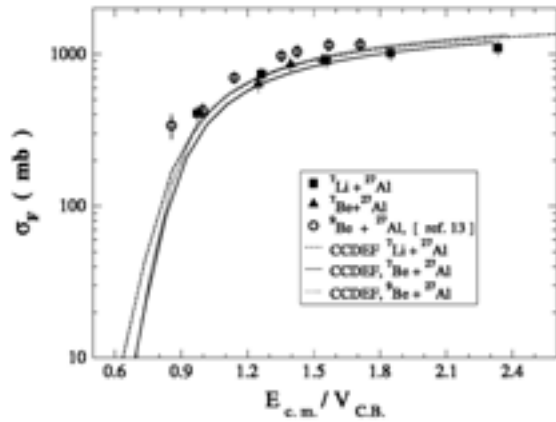


Fig. 2. Reduced fusion excitation functions for ${}^7\text{Be}$, ${}^9\text{Be}$, ${}^7\text{Li} + {}^{27}\text{Al}$ systems with reduced energy scale.

REFERENCES

- [1] K. Kalita *et al.*, Ind. J. Pure Appl. Phys. 43 (2005) 567.
- [2] K. Kalita *et al.*, Phys. Rev. C 73 (2006) 024609.

5.2 SWIFT HEAVY IONS IN MATERIALS SCIENCE

D.K. Avasthi and D. Kanjilal

A large number of experiments in materials science were carried out during the year 2005 by different researchers from various Universities and Institutes.

Among the experiments related to the phenomena of surface and interface modifications, some experiments were performed by on-line ERDA, which has been a unique feature of the laboratory. The electronic sputtering experiments on LiF showed clear effect of the dependence of the electronic sputtering yield on (i) the grain size and the (ii) thickness of the film, which is according to the expectation from thermal spike model. The LiF films of different grain size were specially prepared by varying the deposition conditions specially the substrate temperature. Ion beam mixing in Mo/Si and In/Se system has been performed with clear indications of the mixing at the interface. The availability of AFM from the IRHPA project of DST made it easier to study the nano patterning in NiO thin films under glancing angle swift heavy ion irradiation at low temperatures. There have been indications of the nanostructured surface formed by irradiation of titanium oxide thin layers. The optical and magnetic properties of the SHI irradiated Cr doped ZnS are under study. The effect of SHI irradiation in noble metal particles in silica matrix and the magnetic metal particles are being investigated in detail for the dissolution or the growth of the particles. The change in the shape of the particles leading to the changes in optical and magnetic properties is also under investigation. There are indications that the dissolution of the particles takes place below certain density of particles and the growth of particles takes place beyond a specified density of particles. More experiments are required to be confirmed about it. The Cu fused silica system seems to be resulting in the formation of nanoparticles under SHI irradiation as evidenced by absorption spectroscopy. The changes in magnetic anisotropy are also being studied in the irradiated metallic glasses. The strain due to lattice mismatch between the InGaAs thin film and GaAs substrate has been shown to be reduced by SHI irradiation. The dislocation densities in the irradiated sample of the same system are shown to be decreased as investigated by high resolution XRD. Swift heavy ion irradiation effects are being investigated in semiconductors CdTe, n-InP, GaN, InAs, GaSb etc. for the band gap, structure by XRD and surface morphology. The effect of Li irradiation in Si and GaAs based solar cells have been investigated to roughly simulate the effects of the performance of these in space applications. Controlled irradiation of good quality MgB₂ thin film by 200 MeV gold beam led to an increase of onset temperature with fluence.

The effect of SHI irradiation in Ti⁴⁺ substituted Li_{0.5}Al_{0.1}Fe_{2.4}O₄ is studied and dielectric loss is seen to be increased significantly upto 100 kHz. The effect of SHI irradiation in ITO films is under investigation by XRD and PL. The SHI induced color centers F₂ and F₃⁺ in LiF films having nano size grains are investigated by PL. Degree of crystallinity is shown to be improved at lower fluences in polypyrrole and HCL doped polyanilin films.

Ferromagnetism is observed in SHI irradiated fullerene films, revealed by MFM and SQUID measurements. It is a significant result from the point of view of the magnetism in C based system, which has drawn attention of researchers worldwide for last five years or so. Low fluence irradiation of Fe₃O₄ magnetite films has shown improvement in the magnetization.

5.2.1 Size Effect on Electronic Sputtering of LiF Thin Films

M. Kumar¹, S.A. Khan², F. Singh², A. Tripathi², D.K. Avasthi² and A.C. Pandey¹

¹Department of Physics, University of Allahabad, Allahabad 211 002

²Inter-University Accelerator Centre, Post Box-10502, New Delhi 110 067

The swift heavy ion induced release of atoms from polycrystalline LiF thin film [1] is investigated using 120 MeV Ag²⁵⁺ ions as projectiles. The sputter yield of Li and F for different thickness (10, 20, 40, 80,150 and 265 nm) of the films is measured with online elastic recoil detection analysis technique in lower fluence regime (2×10^{12} ions/cm²) in order to exclude the effect of surface modification [2]. From GAXRD results of pristine films, reduction in the grain size of the films is observed with decrease in the film thickness as shown on left y-axis in figure 1. The reduction in sputter yield, from $\sim 2.3 \times 10^6$ to 2.2×10^4 atoms/ion, is observed with the increase in film thickness as shown on right y-axis in figure 1. It is found that yields are enhanced by about an order of magnitude for the films less than 100 nm thickness.

The results are explained in terms of size effect along with thermal spike model. According to the thermal spike model, the energy is deposited by the projectile ions in the electronic subsystem of the target and the electronic sputtering strongly depends on the efficiency of the transfer of the electronic energy to the lattice, which finally depends on electron phonon coupling strength (g) by the relation,

$$g = \frac{D_e(T_e)C_e(T_e)}{\lambda^2},$$

where D_e is the spatial energy distribution and C_e is the electronic

specific heat of the system. The effective mean free path strongly influence the electron phonon interaction and the electron phonon coupling strength is inversely proportional to the square of the mean diffusion length (λ) of the excited electrons. Now, there are two factors that affect the mean diffusion length, one is the thickness of the film and other one is grain size of the film, influenced by films thickness. When the thickness of the film is less, the motion of the excited electrons will be restricted by the film surface and substrate interface because they act as confinement barrier for the motion of the electrons. The surface and interface scatter the electrons partially or completely resulting in reduction in electron mean free path [3]. Now, on the other hand, the motion of the electrons also gets affected by the smaller grain size

due to grain boundary scattering. As the grain size become smaller, scattering of electrons with grain boundaries influences the mean free path, and since the grains in the films have all the possible orientations, these grain boundaries effectively become electron scatterer [4]. Due to smaller grain size, the λ value will be smaller resulting in the higher value of electron-phonon coupling strength in the context of above relation.

Two different regimes of the electronic sputtering can be understood in terms of grain size effect. Below 50 nm thickness of the film, the grain size is comparable/equal to the film thickness resulting in strong grain boundaries scattering as well as electron scattering from surface and interface of the film and substrate. In case of thicker film the scattering from film surface and interface of the film and substrate is less effective, whereas the grain boundaries scattering still will play an important role. Hence, the temperature spike will be highest in case of the smallest grain size and thickness. In other words, high sputtering yield in regime I is combine effect of reduced thickness and grain size of the film, whereas in regime II, it is due to the change in the grain size of the film rather than the thickness of the films. Thus, both the factors, thickness and the grain size of the film, influence the sputtering yield. Thickness dependence of electronic sputtering has been widely studied in metals [5] and organic materials [6], but the effect of grain size has never been observed earlier.

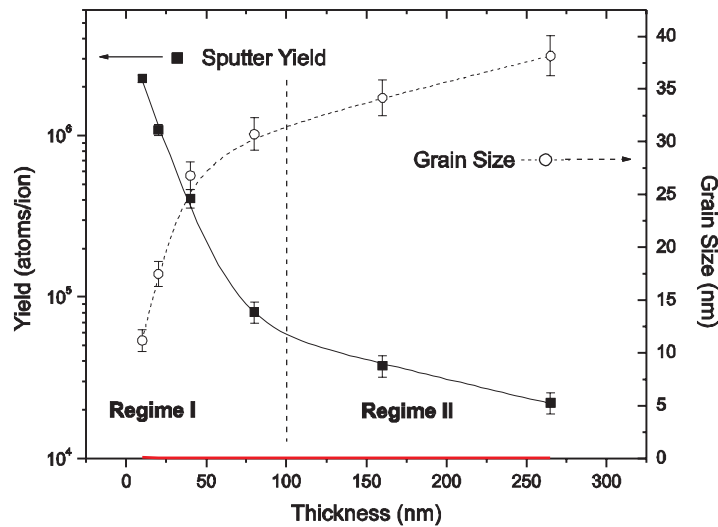


Fig. 1

REFERENCES:

[1] M. Kumar et al., J. Phys. D: Appl. Phys. 38 (2005) 637.
 [2] Toulemonde et al., Phys. Rev. Lett. 88 (2002) 057602.
 [3] M. Ohring, The Materials Science of Thin Films, Academic Press, 1991, Chapter 10.
 [4] A. F. Mayadas and M. Shatzkes, Phys. Rev. B 1 (1970) 1382.
 [5] A. Gupta and D. K. Avasthi. Phys. Rev. B 64 (2001) 155407.
 [6] S. Ghosh et al., Nucl. Instru. And Meth. B 190 (2002) 169.

5.2.2 Au ion irradiation study on Mo/Si surface

I.P. Jain¹, Garima Agarwal¹, Shivani Agarwal¹, Veenu Sisodia¹, Pratibha Sharma¹, Ankur Jain¹, Chhagan Lal¹, Rajkumar Jain¹, D.Kabiraj² and Ambuj Tripathi²

¹Centre for Non-Conventional energy Resources, University of Rajasthan, Jaipur 302004

²Inter-University Accelerator Centre, Post Box-10502, New Delhi 110067

Ion – beam mixing has been considered as an alternate means to form metal contacts in microelectronics devices by implanting energetic ions through metallic thin films deposited on silicon [1]. The method had an additional advantage in forming shallow metal contacts. In addition to a lower processing temperature this technique provides a high degree of spatial selectivity. Metal-semiconductor system is a good choice to study Swift Heavy Ion (*SHI*) induced mixing from the fundamental ion-solid interaction point of view as well as their wide applications. Lot of studies have been undertaken to see the ion beam induced structural modification through high level of linear energy deposition by swift heavy ion at metal/metal or metal/Semiconductor surfaces and interfaces. Several metals e.g Ti, Fe, Co, Mo, Ni, Zr, Pd, Bi etc have been suggested [2] which are S_e sensitive. A number of works have been done using above metals for compounds formation with Si in the form of metal silicide using ion beam.

Refractory silicides have been used in various aspects of very large-scale integrated-circuit devices because of their low resistivity and their ability to withstand the high temperature required for integrated circuit processing [3]. $MoSi_2$ is one of the main silicides that have been selected by the microelectronics industry. Srivastava et al [4] have studied the effect of temperature, up to 750°C on the microstructural changes in the Mo-Si multilayer using a transmission electron microscope (TEM) and high resolution electron microscopy coupled with selected area diffraction pattern. Mo–Si multilayers were heated from room temperature to 750°C. The as-deposited film was found to be quite smooth. Above 400°C, the interfaces start diffusing into one another. They have observed the formation of Mo_5Si_3 and $MoSi_2$ crystalline phases at 750°C.

To investigate the mixing process in more detail, a trilayer system formed by 50nm of Mo deposited on 50nm of Si layer which was deposited onto Si (100) substrate, the whole system is then covered with a top Si layer of 30nm to protect it with oxidation. The deposition was made by electron beam evaporation at vacuum of 4×10^{-8} Torr at NSC, New Delhi. The deposition rate was nearly 0.2 Å/sec for Si while it was around 1.0 Å/sec for Mo. The Si (30nm) / Mo (50nm) / Si (50nm) / Si (100) systems were then irradiated by 120 MeV Au ions using 15 UD Pelletron Accelerator at NSC New Delhi having 10^{-6} Torr vacuum in the Material Science

Chamber at different fluences from 10^{12} to 10^{14} ions / cm^2 at RT. X-Ray Reflectivity (XRR) studies were undertaken to measure the deposited thickness in pristine (unirradiated) system. Measurements were performed using $\text{CuK}\alpha$ ($\lambda=1.54060\text{\AA}$) radiation. Irradiation effect on the surface morphology of the Mo/Si surface has been undertaken with the help of Atomic Force Microscope in tapping mode. Detailed analysis is in progress.

REFERENCES

- [1] Z.L. Liao and W. Mayer, in Treatise on Materials Science and Technology, Academic New York 18 (1980) 17.
- [2] Z.G. Wang, Ch Dufour, E. Paumier and M. Toulemonde, J. Phys: Condens. Matter 6 (1994) 6733-6750.
- [3] T.P. Chow and A. J. Steckl, IEEE Trans. Electron Devices ED- 30, (1983) 1480.
- [4] A.K. Srivastava*, P. Tripathi, M. Nayak, G. S. Lodha and R. V. Nandedkar Current Science, Vol. 83, No. 8 (2002) 997.

5.2.3 Effect of irradiation on In/Se systems

R. Sreekumar¹, C. Sudha Kartha¹, K.P. Vijayakumar¹, S.A. Khan², D. Kabiraj² and D.K. Avasthi².

¹ Department of Physics, Cochin University of Science and Technology, Cochin 682022

² Inter-University Accelerator Centre, Post Box -10502, New Delhi 110 067

Indium selenide, a group III-VI compound semiconductor, attracted researchers because of its wide application in electromemory, photomemory and photovoltaic device fabrication [1]. Simple technique of stack elemental layer technique followed by vacuum annealing was employed to prepare the sample [2]. Thin films of Selenium with thickness 150nm were deposited using chemical bath deposition technique, over which indium film of 56nm was deposited using vacuum evaporated technique. In the present study we tried to explore the effects of swift heavy ion irradiation on these films.

(i) SHI induced mixing in In/Se bilayer system in different energy regime

Interface mixing between metal/semiconductor interface induced by swift heavy ions has been studied extensively [3,4] and found that there exist a threshold value of electronic energy loss (S_e) [5], for the mixing to take place between the systems. In the present study we investigated the interface mixing between In/Se bilayer systems prepared on glass substrate at different electronic energy regime. These samples were irradiated with 90MeV Si, 80MeV Ni and 100MeV Ag ions

respectively using 15UD Pelletron Accelerator. Different fluence from 1×10^{12} ions/cm² to 1×10^{14} ions/cm² were used for irradiation over an area of 1 cm^2 . These films were then characterized using X-ray diffraction (XRD), atomic force microscopy (AFM) and Rutherford backscattering spectroscopy (RBS). Swift heavy ion induced interface mixing between In and Se was observed in the case of 80MeV Ni and 100MeV Ag with a fluence of 1×10^{13} ions/cm². But, no mixing was observed in the case of samples irradiated with 90MeV Si ions upto a fluence of 1×10^{14} ions/cm². Thus threshold S_e is 9.15keV/nm respectively for mixing of In and Se.

(ii) Observation of drastic variation in photoconductivity in γ -In₂Se₃ due to irradiation

Effect of irradiation on γ -In₂Se₃ thin films prepared by annealing In/Se bilayer systems at different temperatures from 100°C to 400°C was studied. 90MeV Si ions with a fluence of 2×10^{13} ions/cm² were used for irradiation. XRD study revealed no significant effect of irradiation on the structural property of the films. Optical absorption studies showed an increase in optical band gap of the material on irradiation. This might be due to the annealing of the defects in the forbidden energy region. Photoconductivity measurements were carried over (using 123X KIETHLY Source Measuring Unit) by giving electrical contacts using the silver electrode pasted on the sample as shown in Fig. 1. Halogen bulb (12 mW/cm^2) was used as illumination source. The interesting observation is the enhancement in photoconductivity. Negative photoconductivity of the sample is converted to positive conductivity on irradiation. This might be probably due to the annealing of electron traps, which is responsible for negative photoconductivity.

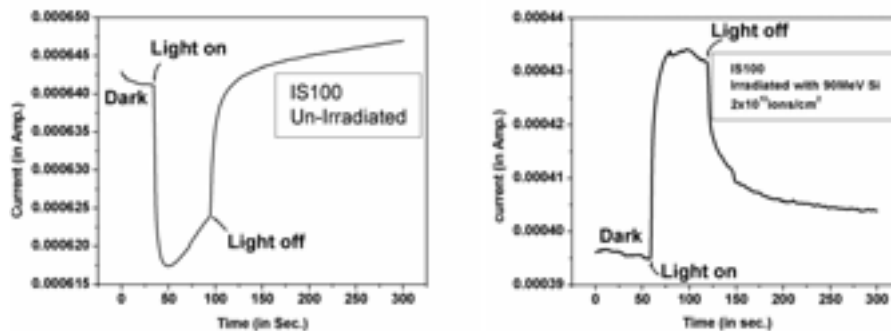


Fig. 1. Photoconductivity spectra of indium selenide film before and after irradiation.

REFERENCES

- [1] S.T. Lakshmikumar and A.C. Rastogi, Sol. Energy Mater. Sol. Cells 32 (1994) 7.
- [2] K. Bindu, M. Lakshmi and C. Sudha Kartha, Semicond. Sci. Tech. 17 (2002) 270.
- [3] Sarvesh Kumar, R.S. Chauhan, R.P. Singh, W. Bolse and D.K. Avasthi et al. Nucl. Instr. and Meth. B 212 (2003) 242

- [4] C. Dufour, Ph. Bauer, G. Marchal, J. Grilhe, C. Jaouen, J. Pacaud and J.C. Jousset, Europhys. Lett. 21(6) (1993) 671
- [5] Saskia Kraft, Beate Schattat and Wolfgang Bolse, J. Appl. Phys.91 (2002) 1129

5.2.4 Swift heavy ion induced surface restructuring of the thin film

D.C. Agarwal¹, A. Gupta¹, S. Kumar¹, S.A. Khan², D. Kabiraj², I. Sulania², R.S. Chauhan¹, D.K. Avasthi² and W. Bolse³

¹Department of Physics, R.B.S. College, Agra, 282 002

² Inter-University Accelerator Centre, Post Box-10502, New Delhi 110 067

³ Stuttgart University, Germany

The restructuring of the surface of NiO thin film after irradiation with 100 MeV Ag ions at LN₂ temperature at an angle of 75° is studied and the effect of different substrate is investigated. The surface morphology of the irradiated surface is studied by Atomic force microscopy (AFM). The films are irradiated at different fluences 1x 10¹³, 3 x 10¹³, 7 x 10¹³, 1 x 10¹⁴, 3 x 10¹⁴, and 6 x 10¹⁴ ions/cm². There are few reports on the restructuring of NiO thin film under the SHI irradiation [1-2].

We observed that the continuous film of NiO show first cracking at low fluence perpendicular to the beam direction and after the application of high fluence the material between the cracks begin to shrink and self-organize into the periodic lamella structure. Fig. 1(a) and 1(b) show the AFM micrograph of the NiO thin film on two different substrate irradiated at fluence of 6 x 10¹⁴ ions/cm². Images show the formation of periodic lamellae structures on surface of NiO thin film induced by swift heavy ion bombardment. The measured width of the lamellae is less in the case of NiO thin film deposited on SiO₂ substrate while it is greater in the case of Al substrate. It is also observed that the cracking and development of lamellae structure are seen at higher fluence in the case of Al substrate.

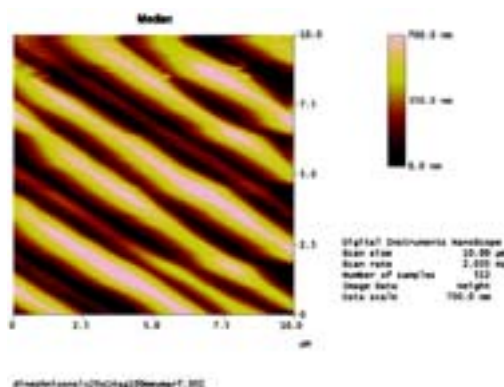


Fig. 1 (a): AFM micrograph of NiO/SiO₂ irradiated at 6 x 10¹⁴ ions/cm²

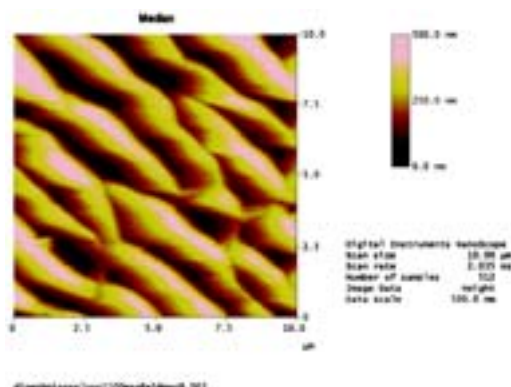


Fig. 1(b): AFM micrograph of NiO/Al irradiated at 6 x 10¹⁴ ions/cm²

REFERENCES

- [1] W. Bolse, B. Schattat and A. Feyh, *Appl. Phys. A* 77(2003)11
- [2] W. Bolse, *Nucl. Instr. and Math. B* 244(2006)8

5.2.5 Formation of nanostructures of TiO₂

Madhavi Thakurdesai¹, John J.², P. Kumar³, T. Mohanty³, Pratap Raychaudhary², V. Bhattacharyya¹ and D. Kanjilal³

¹Department of Physics, University of Mumbai, Vidyanagri, Mumbai-400098

²Tata Institute of Fundamental Research, Homi Bhabha Road, Mumbai-400005

³Inter-University Accelerator Centre, Post Box -10502, New Delhi-110067

Titanium dioxide is a very important transition metal oxide semiconductor. In recent years nanocrystalline TiO₂ is studied extensively due to its interesting physical and chemical properties. TiO₂ is an indirect band gap semiconductor having large energy band gap (3.2eV), excellent visible and IR transmittance, high refractive index and dielectric constant. TiO₂ continues to attract much interest because of its application in photocatalytic, photovoltaic, photochromic devices, gas and chemical sensor, pigments in paints etc. TiO₂ is known to exhibit three crystallographic forms namely anatase, rutile and brookite All the above mentioned properties of TiO₂ depend on specific crystallographic structure it has [1]. Ion beam synthesis is one of the suitable methods of achieving controlled growth of nanoclusters [2].

In the present investigation amorphous thin films of TiO₂ of various thicknesses ranging from 80nm to 300nm were deposited on fused silica substrates by pulsed laser ablation method. The substrate temperature was maintained at 750⁰C. These films were later irradiated by 100MeV gold and silver ion beam obtained from Pelletron facility at IUAC, New Delhi. The fluence of both the ion beams was varied between 10¹² ions/cm² and 10¹³ ions/cm².

The surfaces of pristine and irradiated films were studied by AFM to understand surface morphology. It was observed that the films of thickness 80nm and 100nm after irradiation by the fluence 10¹² ions/cm² form smaller particles in case of both the ion beams. The smallest particle size achieved was 16nm in 100nm film irradiated by Au-10¹² ions/cm² but the more uniform distribution of particles was found in 200nm film irradiated by Ag-10¹² ions/cm². In case of both 80nm film and 100nm film irradiation by Au ion beam formed smaller particles than Ag ion beam. In case of 200nm film irradiation by Ag ion beam formed smaller particles The reason could be smaller S_e value of Ag (11.46 keV/nm) than S_e value of Au (13.4 keV/nm) and the S_e to S_n ratio for Ag ions being 3.5 times more than that of Au ions. Nanoclusters were observed only in the films of thickness upto 200nm for the fluence

of the order of 10^{12} ions/ cm^2 and 10^{13} ions/ cm^2 . 300nm thick film failed to give formation of nanoparticles.

The optical characterization was done by absorption measurement carried on UV-VIS double beam spectrophotometer CARY 5000. The quantum confinement effect increases the band gap of the semiconductor, causing a blue shift of the absorption band edge[1]. The UV absorption spectra of 80nm thick TiO_2 pristine and irradiated film by Ag ion beam 10^{13} on / cm^2 . The 19nm blue shift observed in the spectra indicates the decrease in particle size after irradiation.

As the SHI beam induces structural modification in the target, phase of TiO_2 film was investigated before and after irradiation by GAXRD. The 80nm and 100nm pristine films were amorphous in nature. The 80nm film after irradiation by Au- 10^{13} ions/ cm^2 gave a small peak at $2\theta = 25.2$ which indicates the anatase phase of TiO_2 . The 100nm film after irradiation by Au ion beam of fluence 10^{13} ions/ cm^2 gave a peak at $2\theta = 40.2$ indicating Ti_8O_{15} phase after irradiation. The 80nm film after irradiation by Ag- 10^{13} ions/ cm^2 gave a small peak at $2\theta = 53.9$ which indicates the anatase phase of TiO_2 . Where as 100nm film after irradiation by Ag ion beam of fluence 10^{13} ions/ cm^2 gave a peak at $2\theta = 25.9$ indicating Ti_8O_{15} phase. This change in stoichiometry of TiO_2 indicates little loss of oxygen during irradiation or change in stoichiometry may be due to instability of TiO_2 phase, as it is reported that TiO_2 can be easily reduced to a series of intermediate $\text{Ti}_n\text{O}_{2n-1}$ phases [3]. A conclusion can be drawn that amorphous TiO_2 films after irradiation formed TiO_2 nanophase with stoichiometry slightly changed.

REFERENCES :

- [1] Daocheng Pan, Nana Zhao, Qiang Wang, Shichun Jiang, Xiangling Ji and Lijia An Adv. Mater. Vol.17 (2005) 1991
- [2] T. Mohanty, A. Pradhan, S Gupta and D Kanjilal Nanotechnology 15 (2004) 1620
- [3] Naoto Koshizaki, Aiko Narazki and Takeshi Sasaki Appl. Surf. Sci. 197-198 (2002) 624

5.2.6 Irradiation induced effects on the optical and magnetic properties of transition metal doped ZnS nanoparticles

U. Das¹, D. Mohanta¹, F. Singh², A. Tripathi², D. K. Avasthi², A. Choudhury¹

¹Department of Physics, Tezpur University, P.O. Napaam, Assam -784 028

²Inter University Accelerator Centre, Post Box -10502, New Delhi 110 067

Diluted magnetic semiconductors (DMS) are promising candidates for magnetic memories, sensors and other spin-based devices [1,2]. Such semimagnetic and semiconducting structures, where carrier and spin confinement is possible provides

a matchless system for spin manipulation and spin transportation [3].

Mn and Cr doped ZnS nanoparticle samples were prepared in polymer matrix by simple chemical process [3] and films were casted on glass substrates. These nanoparticle samples irradiated with 150-Mev Ti^{+11} ion with different fluence values in the range 5×10^{10} - 3.2×10^{12} ion/cm².

Swift heavy ion induced modification were studied by transmission electron microscopy, photoluminescence and magnetic force microscopy. The high resolution electron microscopic images provide information relating to irradiation-led modification in nanoparticle systems. Due to irradiation, aligned grain growth was observed in the ZnS nanoparticle systems. The PL response of pristine and ion irradiated ZnS:Cr nanostructures. It depicts three distinct bands around 475 nm, 540 nm and 700 nm. We ascribe the emission peak ~ 475 nm to donor-acceptor (D-A) pair transition and the band at ~ 700 nm corresponds to surface state led fluorescence activation, in consistency with our recent work in ZnS:Mn systems [4].

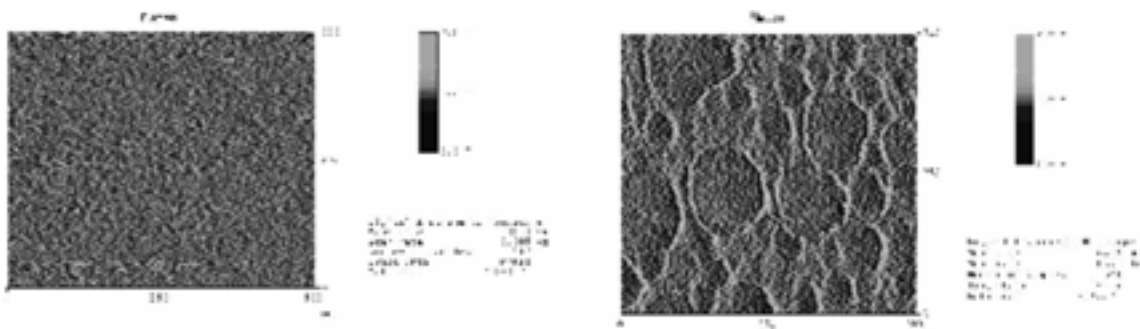


Fig. 1. MFM images of unirradiated and irradiated (5×10^{10} ions/cm²) ZnS:Cr nanostructures

To exploit magnetic properties, we have carried out magnetic force microscopic studies on irradiated ZnS:Cr nanosystems. In un-irradiated nonoclusters doped with Cr does not show appreciable results on the magnetic domains owing to matrix encapsulation which prevents from detecting magnetic domains by the tip of the MFM. Where as after irradiation, elongated domain like structures are distinctly visible which correspond to individual ZnS:Cr nanostructures.

REFERENCES

- [1] G.A. Prinz, Science 282 (1998) 1660
- [2] D.P. Divincenzo, J. Appl. Phys. 85 (1999) 4785
- [3] T. Dietl, Braz. J. Phys. 34 2B (2004)
- [4] D. Mohanta, G.A. Ahmed, A. Choudhury, F. Singh and D.K. Avasthi, J. Nanopart. Res, 8(4) (In press, 2006).

5.2.7 Investigation of swift heavy ion effects on metallic nanoparticles embedded in silica

F. Singh¹, Y. Mishra¹, D.K. Avasthi¹, J.C. Pivin², S. Esnouf³, P. Berthet⁴

¹Inter University Accelerator Centre, Post Box -10502, New Delhi 110 067

²CSNSM, 91405 Orsay Campus, France,

³ LSI -DRECAM, CEA Saclay, 91191 Gif sur Yvette, France

⁴LPCES-ICMMO, Bât.410, Université Paris Sud, 91405 Orsay Cedex, France

Nanometric particles of metals embedded in insulators exhibit properties depending on their size, shape and volume fraction. A few studies showed that these parameters may be modified by swift heavy ion irradiation [1, 2], but little is known of the dissipation mechanism of the energy deposited by ions in composite materials. A detailed investigation of the effects of the ions stopping power and velocity and of the initial characteristics of systems made of silica containing Ag, Au or Fe particles was undertaken for a fundamental purpose as also for applications. Indeed, these types of composite systems are useful in non-linear optics, magnetic recording of information and the synthesis of metallic nano-wires.

The studied materials during 2005 were films with a thickness of the order of 500 nm deposited by magnetron co-sputtering or sol-gel chemistry. Some of the films were submitted to annealing treatments in Ar:H₂ to reduce the metal (case of Fe) and increase the size of the particles in the system before the irradiation (the particles size was determined by using the X-ray diffraction set-up recently installed at IUAC). They were irradiated with 120 MeV Ag or Au ions delivered by the Pelletron accelerator of IUAC or swifter ions provided by the UNILAC accelerator of GSI.

Measurements of the optical absorption of Ag and Au particles in the visible, related to their surface plasmon resonance, or of the magnetization of SiO₂:Fe films, showed that particles are dissolved when their mean diameter is in the range of 1-5 nm (smaller than that of ion tracks) and the atomic fraction of the metallic element is limited to 3-5%. Fe particles in low concentration are not dissolved under irradiation by 120 MeV Ag or Au ions when their size reaches about 8 nm. These results concerning the size effect are in agreement with calculations based on a thermal spike formalism. On basis of the few series of targets investigated until now, the volume fraction of precipitated metal increases, if part of the metal atoms were still in solid solution before the irradiation, or remains constant, when the concentration of the metallic element exceeds 10% [3]. The new particles (with a small size) which are formed under irradiation from targets in which the metal is initially in concentrated solid solution, are aligned along the ion tracks, as shown by transmission electron microscopy observations.

Changes in the anisotropy of these systems need a more detailed modelization, taking into account the likelihood that some of the particles grow at the expense of smaller ones, when they are close enough (effect of the concentration), and the various effects of stress on the particle shape (creep) or intrinsic properties (lattice parameter...). $\text{SiO}_2\text{:Ag}$ and $\text{SiO}_2\text{:Au}$ samples, containing particles of size 20 nm (much larger than ion tracks) and with a high filling factor of 15%, were for instance irradiated at an oblique incidence in order to be able to observe an effect of a change in their shape with a polarized light. A significant shift of their plasmon resonance peak to smaller energy is observed when the angle between the electric field is parallel to the projection of the ion trajectory onto the surface (Figure 1) indicating the occurrence of an elongation of the particles along the irradiation axis.

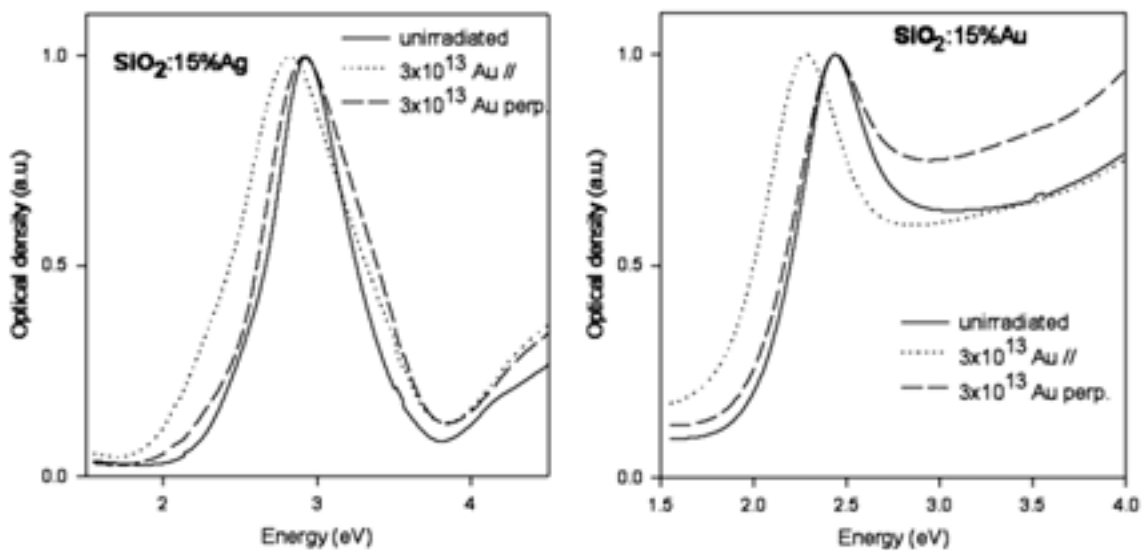


Fig. 1. Spectra of optical absorption recorded with polarized light from films irradiated with 120 MeV Au ions at oblique incidence

A change in the magnetic anisotropy of Fe particles is also observed when they are larger than ion tracks and their concentration is below 10%, without significant change in their shape. Their easy magnetization axis becomes aligned parallel to tracks, as evidenced by a tilt of the minimum in the field of ferromagnetic resonance with respect to the film surface. This effect is ascribed to the anisotropic deformation of the matrix (hammering) [4] and may be useful for increasing the density of magnetic recording. Unfortunately this magnetostriction effect is cancelled when increasing the Fe concentration, because of the strong in-plane dipolar correlation between the particles.

REFERENCES

- [1] C. D'Orleans, J.P. Stoquert, C. Estournès, C. Cerutti, J.J. Grob, J. L. Guille, F. Haas, D. Muller and M. Richard-Plouet, Phys. Rev. B67 (2003) 220101
- [2] J.J. Penninkhof, A. Polman, L.A. Sweatlock, S.A. Maier, H. Atwater, A.M. Vredenberg, B.J. Kool, Appl. Phys. Lett. 83 (2003) 4137
- [3] J.C. Pivin, S. Esnouf, F. Singh, D.K. Avasthi, J. Appl. Phys. 98 (2005) 1.
- [4] F. Singh, D.K. Avasthi, O. Angelov, P. Berthet, J.C. Pivin: Proceedings of International Conference Swift Heavy Ion Modification of Materials, Nucl. Instr. and Methods. (in press)

5.2.8 Optical properties in the Cu-fused silica system irradiated with swift heavy ions

Ranjana C. Gupta¹, D.C. Kothari¹, R.J. Choudhari², Ravi Kumar², P.K. Sahoo³, K.P. Lieb³ and S. Klaumünzer⁴

¹Department of Physics, University of Mumbai, Vidyanagari, Santacruz East, Mumbai 400 098

²Inter University Accelerator Centre, Post Box -10502, New Delhi 110 067

³II. Physikalisches Institut, Universität Göttingen, Friedrich-Hund-Platz 1, D-37077 Göttingen, Germany

⁴Hahn-Meitner Institut, Glienicke Str. 100, D-14109 Berlin, Germany

In the present work, we study the role of S_e in producing nano-clusters. Substrates of fused silica covered with 10-nm Cu films were irradiated using beams of 120-MeV Ag^{+9} ions or 350-MeV Au^{+26} ions at various fluences. The dual purpose was to form tracks in silica, which could act as nucleation sites, and to introduce Cu into silica by ion beam mixing induced by electronic stopping. UV-VIS absorption spectroscopy was used mainly to characterize the samples.

High-purity silica glass plates, 10 mm × 10 mm × 1.5 mm in size, were chosen as substrates. Copper films of 10 nm thickness were deposited on the substrates using vacuum evaporation at a pressure of 3×10^{-5} mbar. The coated samples were then irradiated using either a 120-MeV Ag^{+9} beam, provided by the tandem accelerator of the Nuclear Science Center, Delhi, or the 350-MeV Au^{+26} beam of the ECR/RFQ/cyclotron facility of the Hahn-Meitner-Institut, Berlin. An electronic energy loss of $S_e = 11$ keV/nm and 21 keV/nm in SiO_2 (at the Cu/ SiO_2 interface) for the two ion species was estimated with the SRIM code. These S_e values clearly exceeded the 1 keV/nm threshold value for track formation in fused silica; tracks of 3 nm radius were formed for $S_e = 8$ keV/nm. Thus both ion energies were sufficient to produce tracks of radii greater than 3 nm in fused silica. The Ag^{+9} -ion fluences ranged from 4×10^{13} to 1×10^{14} cm⁻², while the Au^{+26} -ion irradiation was carried out for a fluence of 2×10^{13} cm⁻². After irradiation, 30-min annealings in an Ar atmosphere were performed at temperatures ranging from 500 to 1200 K.

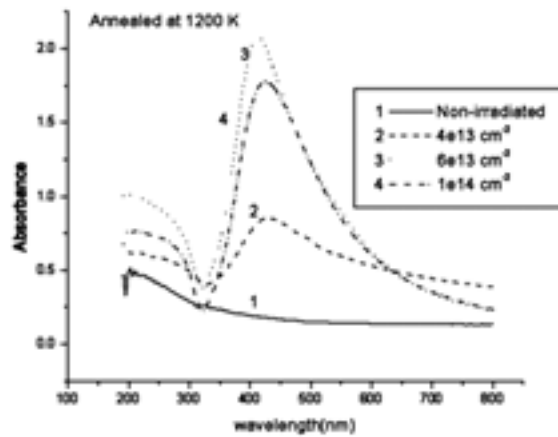


Fig.1. UV Absorption Spectra for quartz samples annealed at 1200 K (1) and irradiated with 120 MeV Ag ions at fluences (2) 4×10^{13} ; (3) 6×10^{13} (4) 1×10^{14}

UV-Vis spectra spectra of the irradiated samples show two peaks at 215 and 245 nm arising from the E' and B₂ defect centres created in the SiO₂ substrates . These types of defects were also observed after the 350-MeV Au⁺²⁶ irradiations. The E' centre is due to an oxygen vacancy opposite an electron in a dangling Si-sp³ orbital, while the B₂ centre is due to the Si-vacancy-Si configuration. Fig. 1, illustrate the effects of thermal annealing on the UV-Vis spectra, indicate that after annealing the 215 and 245 nm peaks disappeared and the peak due to Cu₃ cluster appeared. At the highest annealing temperature of 1200 K, Cu₄ clusters and larger-size particles are formed. Irradiation fluences of more than 4×10^{13} cm⁻² and annealing temperatures exceeding 1100 K appear to be more effective in forming larger nanoclusters. It may be concluded that the swift heavy-ion irradiations create E' and B₂ defects in Cu-coated, fused silica. Post-irradiation annealing helps to eliminate these defects and form Cu clusters.

5.2.9 Modification of magnetic anisotropy in metallic glasses using high-energy ion irradiation

Kavita Amrute¹, D.C. Kothari¹, D. Kanjlilal²

¹Department of Physics, University of Mumbai, Santacruz, Mumbai, 400098.

²Inter University Accelerator Centre, Post Box-10502, New Delhi 110 067

This research work is based on the following two observed facts; 1) in magnetic materials heavy ion irradiation induces the change in magnetic anisotropy [1]; and, 2) In metallic glasses, heavy ion irradiation induces stress which results in the irreversible macroscopic dimensional change [2]. M. Sorescu et al. [3], have studied metallic glasses by exposing it isochronally to pulsed-excimer-laser beam, and found that at moderate values of repetition rate and pulse energy, controlled magnetic anisotropy could be induced in the higher magnetostriction samples, whereas,

random orientation of magnetic moment was obtained in the lower magnetostriction coefficient sample.

Here, in ferromagnetic metallic glasses, we expect both type of changes, the macroscopic dimensional change and change in the magnetic anisotropy, due to heavy ion irradiation. In our previous work, [4, 5] we found that the growth in the sample dimensions perpendicular to the direction of ion beam, is due to the residual stress induced by swift heavy ions. The change in the direction of magnetic moment shows a correlation with the induced stress and increases with the increasing stress. This effect is similar to that of magnetostriction, but the stress induced here is not mechanical but introduced by swift heavy ion irradiation. The origin of the induced perpendicular magnetic anisotropy was interpreted in terms of magnetoelastic effects due to strong stresses generated by the reaction of the nonirradiated region to the anisotropic deformation of the irradiated amorphous material [6].

We have used Mossbauer Spectroscopy to study the modification of magnetic anisotropy because it gives direct information about the hyperfine field distribution and the orientation of magnetic moment. The metallic glass preserves its amorphous nature after heavy ion irradiation. The magnetic anisotropy in metallic glass changes considerably after high-energy heavy ion irradiation. As received samples display orientation of the magnetic moments nearly parallel to the surface of the ribbon, which rotate to nearly random orientation.

In the earlier run, in Dec.'04, ^{197}Au beam of 190 MeV energy has been used for irradiation. ^{197}Au has been selected to increase Se in the material, which would increase the residual stresses induced by irradiation. The irradiation has been done at liquid nitrogen temperature to retain the stresses in the sample. The metallic glass samples have been thinned by electro polishing, reducing their thickness up-to 12 microns, to avoid the effect of un-irradiated bulk. The range of ^{197}Au beam of energy 190 MeV have range up-to 10 microns in these metallic glasses.

Two samples from both type of metallic glass are also irradiated at room temperature and liquid nitrogen temperature with the same fluence 3×10^{12} , to investigate the difference in induced anisotropy. The Mossbauer study of all these irradiated samples reveals the correlation between the change in magnetic anisotropy by irradiation induced stress and fluence of irradiation. The hyperfine magnetic field increases slightly with the dose and becomes narrower indicating reduction in disorder by atomic rearrangements. As fluence increases, the magnetic moments turn in perpendicular direction i.e. at the direction of ion beam. As irradiation is done at low temperature, the stresses retain in the sample and does not dissociate.

In the previous run, in Jan'06, few samples have been irradiated at an angle of a 45 degree. The irradiation with an angle would help the find out the reason behind the turning of magnetic moments in the direction perpendicular to the direction

of macroscopic dimensional growth. This is to find out whether the change in anisotropy is due to the shear stress/ local melting along the ion track or due to the elastic stress in the direction parallel to ion beam, generated by irradiation. Two samples each from the same compositions have been irradiated at same fluences, by keeping them at 90 and 45 degree to the beam and then the induced change in anisotropy has been measured by using Mossbauer Spectroscopy. The difference the values of canting angle have been observed in both the cases. Definite results will get published after further characterization with CEMS, DSC, XRD and TEM.

REFERENCES

- [1] F. Studer et.al., Nucl. Instr. Meth. B 82(1993) 91
- [2] S. Klamunzer et.al., Phys. Rev. Lett. 57 (1986) 850.
- [3] M. Sorescu et. al., Phys. Rev. B 49(1994) 3253
- [4] K. V. Amrute et. al. , PRAMANA 58,5-6 (2002)1093.
- [5] K.V. Amrute et.at., Surf.Coat. Tech. 196 (2005) 135.
- [6] J. Juraszek et. al., Jour. Appl. Phys., 89-6, (2001) 3151.

5.2.10 Ion Beam Analysis of Defects and Strain in Heavy Ion Irradiated InGaAs/ GaAs Heterostructures

S Dhamodaran¹, N Sathish¹, A P Pathak¹, S A Khan², D K Avasthi², T Srinivasan³, R Muralidharan³, B Sundaravel⁴, K G M Nair⁴

¹School of Physics, University of Hyderabad, Hyderabad – 500 046.

² Inter University Accelerator Centre, Post Box -10502, New Delhi 110 067

³Solid State Physics Laboratory, Lucknow Road, Timarpur, Delhi – 110 054

⁴Materials Science Division, IGCAR, Kalpakkam – 603102

The lattice mismatch between the layer and the substrate in such a structure is accommodated by strain. The strain in the epilayer due to tetragonal distortion improves the device performance. Beyond a certain thickness the strain relaxes giving rise to defects in general and misfit dislocations in particular. These defects deteriorate the device performance and reduce their lifetime. Hence defect generation in these structures need a basic understanding to control their concentration and to grow high quality epitaxial layers for device applications. The defects present at the interface and the type of defect can be identified by the incident beam energy dependence of the dechanneling parameter (DP) and the additional peak that is produced by the defects. Swift Heavy Ion (SHI) modification of materials is of great interest for about a decade now. We have studied effects of irradiation on defects at the interface [1,2].

The SHI irradiation was performed at room temperature by 150 MeV Ag¹²⁺ ions with a fixed fluence of 1×10^{13} ions/cm². RBS/Channeling experiments were performed by using He⁺ ions with energies between 2 and 4.1 MeV from a 1.7MV

Tandetron at IGCAR, Kalpakkam. Axial channeling along $\langle 001 \rangle$ was carried out for dechanneling analysis and angular scans along $\langle 110 \rangle$ direction was also recorded for strain analysis. The dechanneling parameter is calculated from the normalized back scattering yield to see its energy dependence for defect analysis.

RBS/C spectra recorded, varying incident energy of Helium ions have been analyzed. Dechanneling by defects of InGaAs/GaAs heterostructures with layer thickness 36 and 96 (both U & I) has been studied and the $E^{0.5}$ dependence of dechanneling parameter was attributed to the presence of dislocations (Table.1). The dislocation densities were also calculated the dislocation densities were less in irradiated samples compared with the unirradiated ones (not shown). This was attributed to the diffusion of indium and/or irradiation induced damages in the substrate region close to the interface. The energy dependence of DP and the power fit of experimental data points, $E^{-0.23 \pm 0.25}$ and $E^{-0.14 \pm 0.15}$ dependence for U and I samples is observed. In view of the error bars in the power dependence, it is neither E^0 (stacking faults) nor $E^{-0.5}$ (point defects). To cross check the possibilities of point defects angular scans from both, the layer (In-signal) and the substrate (Ga/As-signal) regions were investigated. If indium existed as interstitials, the yield will show a peak at the axial tilt angle instead of a dip, generally referred as flux peaking in the angular scans. Absence of flux peaking in the present case for either of the axial scans reflected the absence of interstitials. Hence the possibility of point defects may be ruled out to some extent and the dechanneling may be attributed to stacking faults like defects in 60nm thick sample. Fig.2 shows the energy dependence of DP for 96nmI sample, $E^{0.5}$ dependence for both 36 and 96nm thick samples were attributed to dislocations. This indicates a thickness dependence of defects contrary to the expected misfit dislocations due to strain relaxation.

A set of InGaAs/GaAs samples varying thickness as 36, 60 and 96nm has been investigated using RBS/C for defect analysis. The dechanneling parameter shows $E^{0.5}$ dependence, which has been attributed to the presence of dislocations. The dislocation density calculated shows that it has been reduced after irradiation. Though an exact E^0 dependence is not observed in 60nm thick samples, the possibility of point defects is ruled out to some extent from the angular scan analysis and the observed dependence may be attributed to stacking fault like defects.

Table.1: Type of defects and strain of $\text{In}_{0.18}\text{Ga}_{0.82}\text{As}/\text{GaAs}(001)$ samples

Sample Id	Layer Thickness (nm)	Approximate Energy Dependence of DP (both U & I)	Strain (ϵ_t %)	
			U	I
0903	36	Dislocations ($E^{0.5}$)	1.1997	1.151
1003	60	Stacking Faults (E^0)	0.793	0.7799
1103	96	Dislocations ($E^{0.5}$)	0.5475	0.5167

REFERENCES

- [1] S Dhamodaran, N Sathish, A P Pathak, S A Khan, D K Avasthi, T Srinivasn, R Muralidharan, B Sundaravel, K G M Nair and D Emfeitzoglou, Nucl. Instr. Meth B (in press).
- [2] S Dhamodaran, N Sathish, A P Pathak, S A Khan, D K Avasthi, T Srinivasn, R Muralidharan, B Sundaravel, K G M Nair, Nucl. Instr. Meth B 244 (2006) 174.

5.2.11 High Resolution XRD Study of Swift Heavy Ion Irradiated InGaAs/GaAs Heterostructures

S Dhamodaran¹, N Sathish¹, A P Pathak¹, S A Khan², D K Avasthi², T Srinivasan³, R Muralidharan³ and B M Arora⁴

¹School of Physics, University of Hyderabad, Hyderabad-500046.

²Inter University Accelerator Centre, Post Box-10502, New Delhi-110067

³Solid State Physics Laboratory, Timarpur, Delhi-110054

⁴Tata Institute of Fundamental Research, Homibhabha Road, Mumbai-400005.

Strain relaxation and consequent defect generation in strained heterostructures has evoked interest for over two decades by now. InGaAs/GaAs is the most studied material in this direction, due to its potential applications in opto-electronics. Ion beams to modify semiconductor properties is a well established tool. Recent interest is on material modification using Swift Heavy Ions (SHI) (ion energy $E > 1$ MeV/nucleon) from both fundamental and application points of view. SHI irradiation of InGaAs/GaAs heterostructures characterized by HRXRD and analyzed using dynamical theory based simulations.

The $\text{In}_{0.18}\text{Ga}_{0.82}\text{As}$ layers were grown on GaAs(001) substrate by molecular beam epitaxy (MBE), varying the layer thickness as given in Table.1. The critical thickness calculated from Matthews and Blakeslee's model to a single epilayer is approximately 10nm. The heavy ion irradiations were done at room temperature with 150 MeV Ag^{12+} ions fixing the fluence at 10^{13} ions/cm². The X-ray scans were recorded on a Philips X'Pert system having a channel cut, four crystals Ge (220) (Bartels type) monochromator for $\text{CuK}_{\alpha 1}$ X-ray beam ($\lambda = 1.5406 \text{ \AA}$) of divergence 12 arc sec in the scattering plane and a 2⁰ open detector. Five reflections (004), (115) L & H and (224) L & H (L = Low and H = High incidence respectively) were recorded for each sample after optimizing the tilt and azimuth angles. The data for both unirradiated and irradiated samples were analyzed for the out of plane and in plane strains ϵ_{\perp} and ϵ_{\parallel} respectively by least square analysis. The dislocation density (ρ) has also been calculated using the in plane strain (Table.1).

The sample details and calculated parameters are given in Table.1. The outcome of the strain analysis using the separation between the substrate and InGaAs layer peak positions are given in Table.1. It is seen that there is considerable ϵ_{\parallel} which

increases with layer thickness as ϵ_{\perp} decreases, indicating substantial relaxation of strain. The FWHM value of the InGaAs layer peak is quite higher than the expected natural broadening. The FWHM of the layer peak measured from the experimental (004) scans are given in Table.1. The rocking curve FWHMs are extremely sensitive to the defects near the interface regions particularly for thin samples ($t < 1\mu\text{m}$). Observed increase of FWHM with the increase of thickness is attributed to poor layer quality due to higher strain relaxation and consequent generation of defects [1]. Additional peaks appearing in the rocking curves are attributed to a continuous variation of inter-planar spacing producing X-ray interference effects and not due to regions of distinct lattice spacings. In the present study, the additional peak has been deconvoluted assuming a four layer model as a function of depth for distinct energy loss of the incident ions. Different mismatch was assumed and the misfit has been varied editing the database of the simulation program. A trial and error method was used to optimize these values and a satisfactory fit was obtained. The dislocation density (ρ) calculated are less in the irradiated samples compared with the ones in the unirradiated samples (Fig.1). This may be due to the effect of damage created by the SHI in the GaAs substrate close to the interface region of InGaAs/GaAs heterostructure. It is possible that damage enhances the diffusion of indium across the heterostructure interface and hence reduces the relative mismatch at the interface. This in turn would lead to the observed improvements in the quality of the layer – a sort of dynamic annealing [1].

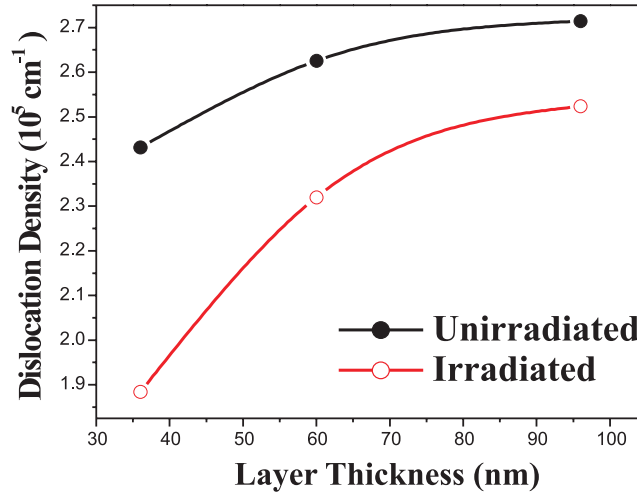


Fig. 1. Dislocation density as function of thickness for U & I samples.

Table. 1: Strain and dislocation density of the samples

Sample ID	Sample Thickness (nm)	ϵ_{\perp} (%)		ϵ_{\parallel} (%)		ρ (10^5 cm^{-1})	
		Unirradiated	Irradiated	Unirradiated	Irradiated	Unirrad.	Irrad.
0903	36	2.3311±0.05	2.3040±0.05	0.9091±0.05	0.7680±0.04	2.2728	1.9199
1003	60	2.1025±0.03	2.1069±0.06	1.0701±0.05	0.9455±0.05	2.6753	2.3638
1103	96	1.9340±0.03	1.9574±0.03	1.1062±0.05	1.0287±0.02	2.7656	2.5716

REFERENCE

- [1] S Dhamodaran, N Sathish, A P Pathak, S A Khan, D K Avasthi, T Srinivasan, R Muralidharan, B M Arora, (Communicated).

5.2.12 Raman Studies of SHI Irradiated InGaAs/GaAs Heterostructures

S Dhamodaran¹, N Sathish¹, A P Pathak¹, S A Khan², D K Avasthi², T Srinivasan, R Muralidharan³, R Kesavamoorthy⁴

¹School of Physics, University of Hyderabad, Hyderabad – 500 046.

²Inter University Accelerator Centre, Post Box -10502, New Delhi 110 067

³Solid State Physics Laboratory, Timarpur, Delhi – 110 054.

⁴Materials Science Division, IGCAR, Kalpakkam – 603 102.

InGaAs/GaAs heterostructures are important due to its built-in strain and the extra degree of freedom that it gives for variety of applications in opto-electronics. Enormous amount of work has been reported on the characterization of strain and the strain relaxation mechanisms of heterostructures grown beyond critical layer thickness. Raman spectroscopy is a reliable technique to characterize such heterostructures. Since the lattice dynamics are affected by stress induced lattice deformation, the strain in epitaxial layers and its relaxation can be analyzed through the evaluation of the phonon frequencies in the Raman spectrum [1].

The In_{0.18}Ga_{0.82}As layers were grown on GaAs by Molecular Beam Epitaxy (MBE) with thicknesses of 12, 36, 60 and 96 nm. The layers were grown at 500°C with a growth rate of 0.2nm/s. SHI irradiation was done at room temperature with 150 MeV Ag¹²⁺ ions with a fluence of 1x10¹³ ions/cm² from 15MV pelletron at IUAC. To avoid heating of samples a low beam current (0.5 – 2 pA) was maintained. The samples were oriented at an angle of 5° with respect to the beam axis to minimize channeling. The Raman scattering measurements were carried out at room temperature in backscattering geometry with 514.5nm argon-ion laser beam of 75mW power. Figure 1 shows some of the Raman spectra. InAs type modes were hardly observed, probably due to less indium concentration. In the present experimental configuration, the GaAs type TO mode is forbidden. However, a weak TO mode at about 270 cm⁻¹ appears due to strain relaxation induced defects in the samples. The usual intense peak of GaAs type LO mode around 290 cm⁻¹ is also observed. The results are discussed in the light of penetration depth of the probe laser beam used in the experiment. The penetration depth of 514.5 nm laser beam in GaAs is about 55nm and in InAs is about 15nm in defect free crystals. These values are significantly reduced by disorder present in the crystal. Hence, in the present study, the interface of 12nm and 36nm thick samples is within the penetration depth. However, for 60 and 96nm thick samples, the interface is beyond the penetration depth of the probe beam.

The bulk equivalent (strain free) GaAs type LO mode (ω_0) for $\text{In}_{0.18}\text{Ga}_{0.82}\text{As}$ is taken from literature as 287.54 cm^{-1} and is used for strain measurements. Blue shift for compressive strain (negative ϵ) is observed and the strain values are calculated. For the unirradiated samples, the strain decreases as a function of thickness, this indicates that the onset of strain relaxation is around 12nm. Very low strain values for thick samples indicate a strong relaxation of strain in the near-surface regions. After irradiation, blue shift of the Raman mode implying an increase of strain in thin layers and red shift implying a decrease of strain in thick layers were observed. This is probably due to the difference in the ion beam modifications near the interface and near the surface. Also different effects of ion beams at the interface and near-surface regions suggests that initial strain energy plays a crucial role in such modifications.

The FWHM of GaAs type LO modes decreases for thin samples and increases for thick samples upon irradiation. An intense LO mode comparable to that of as-grown samples was observed and the TO mode intensity has decreased after irradiation. This highlights that in the present work, the modifications are solely by the electronic energy loss and that discernable lattice damage has not been created due to irradiation. For thin samples, the SHI irradiation results in decrease of FWHM, increase of strain values and decrease of TO/LO mode intensity ratio (not shown). This may be attributed to the reduction in defect density and probably not to the inhomogeneity in strain and/or composition. In contrast, for thick samples, the FWHM increases, strain value decreases and there is no significant change in the TO/LO mode intensity ratio after irradiation. This may be due to inhomogeneity in strain and/or composition.

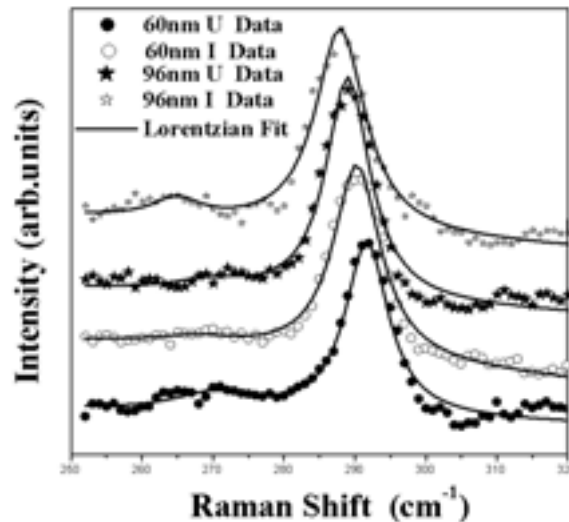


Fig. 1. Raman Spectra of 60 and 96nm thick unirradiated (U) and irradiated (I) Samples.

REFERENCE

- [1] S Dhamodaran, N Sathish, A P Pathak, S A Khan, D K Avasthi, T Srinivasan, R Muralidharan, R Kesavamoorthy, (Communicated).

5.2.13 Effect of Ion Beam Irradiation on the Properties of Cadmium Telluride (CdTe) Thin Films

R. Sathyamoorthy¹, S. Chandramohan¹, D. Kanjilal², D. Kabiraj² and K. Asokan²

¹R&D Department of Physics, Kongunadu Arts & Science College, Coimbatore, Tamilnadu 641 029

²Inter University Accelerator Centre, Post Box -10502, New Delhi 110 067

CdTe is one of the leading candidates for the development of high efficiency solar cells in regard of its notable properties such as optimum direct band gap of 1.5 eV, high absorption coefficient etc. Different processing steps have been adopted by various research groups to enhance the efficiency of CdTe based solar cells. Ion Beam Irradiation is an efficient tool to modify the properties of thin films. In the present work we made an attempt to study the effect of ion beam irradiation on the properties of CdTe thin films and also on the performance of CdTe/CdS solar cells.

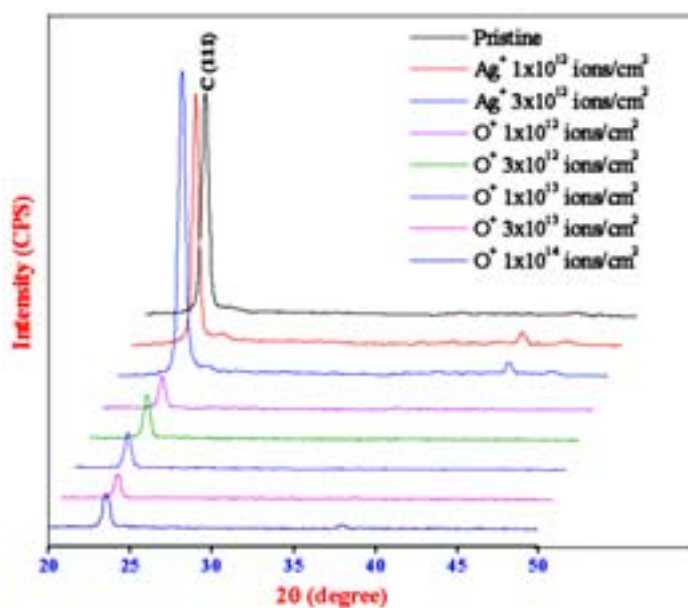


Fig. 1. XRD spectrum of CdTe films irradiated with 100 MeV Ag⁺ and 80 MeV O⁺¹⁶ ions

CdTe thin films were prepared by thermal evaporation on glass substrates. The films were irradiated with 100 MeV Ag⁺⁷ ions and 80 MeV O⁺¹⁶ ions at different ion fluence ranging from 1x10¹² to 1x10¹⁴ ions/cm². The XRD spectrum of CdTe films irradiated with Ag⁺⁷ and O⁺¹⁶ ions is shown in fig.1. An intense (111) reflection has seen in all the samples, which is due to the oriented growth of the crystallites along the (111) direction of cubic phase CdTe. The intensity of the dominant (111)

peak for Ag^{+7} ion irradiated films evidently increases with increase in ion fluence. This implies that most of the irradiation energy might take on the constructive role, improving the crystalline quality of the film. Another interesting feature observed from the spectra is a slight gradual shift in the (111) peak position towards higher diffraction angle. This shift is due to the change in the residual stress, associated with the difference in thermal expansion coefficient and lattice mismatch between the thin film layer and underlying substrate [1]. In contrast to these results, an opposite trend has been noticed for O^{+16} ion irradiated films, where the intensity of the (111) plane decreases due to irradiation. We have also seen a progressive shift in the peak position towards lower diffraction angle for O^{+16} ion irradiated films up to 1×10^{13} ions/cm², while the trend is quite opposite beyond this fluence. By considering the FWHM values, the grain size was calculated using Debye-Scherrer formula. The estimated grain size for as-grown film is 206 Å, which upon irradiation decreases up to 190 Å. This might be due to the recrystallization of the film due to irradiation [2].

The surface topography of CdTe films before and after irradiation has been analyzed by Atomic Force Microscopy. At higher fluences the grains coalesce with each other forming clusters on the surface of the films. This result indicates an increase in the surface roughness with increasing ion fluence.

The optical transmittance spectra of as-grown and irradiated films shows that the band edge of the irradiated films shift towards higher wavelength with a large decrease in the transmittance. The optical band gap energy was found to decrease from 1.53 eV for the as-grown film to 1.49 eV for film irradiated with 80 MeV oxygen ions at a maximum ion fluence of 1×10^{14} ions/cm². The decrease in band gap energy with increase in ion fluence is attributed to the creation of trap levels within the forbidden gap [3,4]. Similar effect was observed on films irradiated with Ag ions.

REFERENCES

- [1] B. Bhattacharya M.J. Carter, Thin Solid Films 288 (1996) 176.
- [2] P.M. Ratheesh Kumar, Teny Theresa John, C. Sudha Kartha and K.P. Vijayakumar, Nucl. Instr. and Meth. in Phys. Res. B 244 (2006) 171.
- [3] Yatendra S. Chaudhary, Saif A. Khan, Rohit Shrivastava, Vibha R. Satsangi, Sathya Prakash, D.K. Avasthi and Sahab Dass, Nucl. Instr. and Meth. in Phys. Res. B 225 (2004) 291.
- [4] Maninder Singh Kamboj, G. Kaur, R. Thangaraj and D.K. Avasthi, J.Phys. D: Appl. Phys. 35 (2002) 477.

5.2.14 Studies of swift iron ($^{56}\text{Fe}^{7+}$) ion irradiated n-InP surfaces

S.K. Dubey¹, A.D. Yadav¹, R.L. Dubey¹, T. Mohanty² and D. Kanjilal²

¹Department of Physics, University of Mumbai, Santacruz(E), Mumbai-400098

²Inter University Accelerator Centre, Post Box-10502, New Delhi-110067

The n-type InP wafers of <100> orientation were irradiated with 100 MeV $^{56}\text{Fe}^{7+}$ ions at fluences of 5×10^{12} , 1×10^{13} , 5×10^{13} , 1×10^{14} and 2×10^{14} ions cm^{-2} , using the 15 UD Pelletron. During irradiation, the beam current was held at 3 to 4 pA (Particle nano-ampere). Atomic Force Microscopy (AFM), X-ray Diffraction (XRD) and Fourier Transform Infrared (FTIR) measurements were carried out on these irradiated samples.

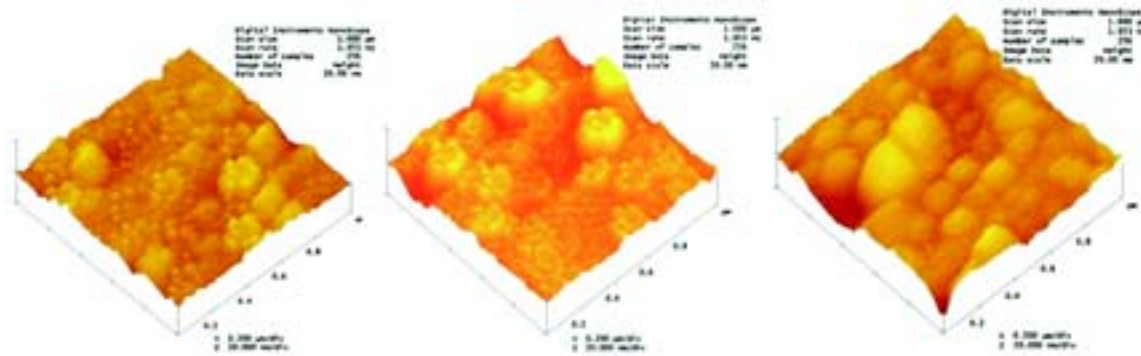


Fig. 1 (a) 5×10^{12} ions cm^{-2} (b) 5×10^{13} ions cm^{-2} (c) 2×10^{14} ions cm^{-2}

AFM micrographs of the non-irradiated and samples irradiated with 5×10^{12} , 1×10^{13} , 5×10^{13} , 1×10^{14} , 2×10^{14} ions cm^{-2} were recorded. The representative AFM images of the InP surface irradiated with low (5×10^{12} ions cm^{-2}), medium (5×10^{13} ions cm^{-2}) and high (2×10^{14} ions cm^{-2}) fluences are presented in Figs 1(a), 1(b) and 1(c) respectively. Non-irradiated sample showed very smooth micrograph with root means square (rms) roughness of 0.326. After irradiation, the hills of nano-size surrounded by the crater type features have been observed in all irradiated samples [1-2]. However, the shape, size and density of these features were found to be increasing with ion fluence. The density and radius of the clusters were measured from 2D AFM micrographs for all irradiated samples using analysis software. The density of cluster having radius ~ 90 nm was found to be 80.61 %, 69.26 %, 63.07 % and 77.90 % respectively for the ion fluences 5×10^{12} , 1×10^{13} , 5×10^{13} and 2×10^{14} ions cm^{-2} .

Normal XRD and high resolution XRD (HRXRD) spectra for Fe irradiated samples with different fluences were recorded. The decrease in intensity of XRD peaks with respect to the ion fluences is attributed to the lattice disordering of the samples. The peak corresponding to the damaged layer was not observed for both the reflections; however the peak shifts towards the higher Bragg's angle. The lattice constants for (200) and (400) reflections computed from XRD spectra using the Bragg's law [3] were found to vary from 5.855 \AA to 5.854 \AA with respect to ion fluence. HRXRD spectra of the samples irradiated with different fluences varying 5×10^{12} to 2×10^{14} ions cm^{-2} for (004) reflection revealed that the radiation induced defect density increases with respect to ion fluence. High energy ion irradiation processes lead to various types of defects such as broken bonds, voids, screw dislocations, edge dislocations divacancies etc. The screw dislocation density in the

samples estimated from the FWHM was found to vary from 1.32×10^7 to 2.38×10^7 cm^{-2} [2]. The substrate and damaged peaks was distinguished in the sample irradiated with 2×10^{14} ions cm^{-2} . The out of plane strain for reflections (004) determined from the separation between substrate and damaged layer peaks ($\Delta\omega_{L,S}$) was found to 0.365×10^{-3} .

FTIR transmission spectra of the samples irradiated with different fluences showed that the optical density increases with respect to fluence over the entire photon energy range, which indicates the increase in defect concentration with increasing ion fluence.

REFERENCES

- [1] R.L. Dubey, S.K Dubey, A.D. Yadav, S.D. Pandey, S.J. Gupta, A. Tripathi, T. Mohanty, D. Kanjilal; Proc. Of the DAE Solid State Physics Symp. 50 (2005) 449.
- [2] R.L. Dubey, S.K Dubey, A.D. Yadav, T. Mohanty, D. Kanjilal, J. Appl. Phys. (submitted)
- [3] E.M. Jackson, G.I. Boishin, E.H. Aifer, B.R. Bennet, L.J. Whitman, Journal of Crystal Growth 270 301 (2004)

5.2.15 Effect of High energy Oxygen ion Irradiation on CdTe Polycrystalline Thin films prepared by Chemical Spray Pyrolysis.

Ison V. Vanchipurackal¹, A. Rangarao¹, Dinesh Agarwal³, D.K. Avasthi², V. Dutta¹.

¹C.E.S, Indian Institute of Technology, Hauz Khas New Delhi.

²Inter University Accelerator Centre, Post Box -10502, New Delhi 110 067

³Dept of Physics, Agra University, Agra.

The high energy heavy ion irradiation is a useful tool to study materials in view of its ability to modify the structural [1], optical [2,3] and electrical [4,5,6] properties due to the interaction of the swift heavy ions with target atoms. In the energy range of our interest the effect of nuclear energy loss is insignificant and the electronic energy loss plays the major role. Cadmium telluride is a compound semiconductor, which is used extensively in the field of solar photovoltaic, nuclear detectors etc. This study is focusing on the effect of ^{16}O heavy ion irradiation on CdTe polycrystalline thin films prepared by chemical spray pyrolysis. We irradiated the samples with ^{16}O beam of charge state 5+ at energy 60 MeV. The beam current was around 3 pA. The samples are irradiated at different levels of fluences from 10^{11} to 10^{14} ions/ cm^2 .

The structural characterization using X-ray diffraction is recorded using Glancing Angle X-ray Diffractometer (Rigaku-Giegerplx-D/max-RB-RU200) with

monochromatic Cu K α radiation. CdTe is having a cubic zinc-blende structure. X-ray diffraction data shows that after heavy ion irradiation (at different levels of fluences), the basic crystal structure is not changing. Also, the lattice constant is remaining as a constant quantity (6.511 Å). The variation in the relative peak intensity is insignificant.

The optical studies are done using a UV-VIS-NIR spectrophotometer. It is observed that the band gap of the CdTe films are decreasing with increase of fluence. The band gap is decreased from 1.47 eV to 1.32 eV with increase of fluence from 10^{11} to 10^{14} ions/ cm².

The resistivity of the samples are determined using a Keithley electrometer and measuring the thickness using a Talystep. It is found that the resistivity of the samples are increasing with increase of fluence. The resistivity increased from 648 Ω m to 7600 Ω m by increasing the fluence level from 10^{11} to 10^{14} ions/ cm². This can be identified as due to the formation of defect levels in the band gap which act as traps of charge carriers.

Surface morphology is done using Atomic Force Microscopy. Swift Heavy ion does not induced any noticeable changes in the roughness or the grain size of the films. At higher fluences also the situation is the same.

REFERENCES

- [1] H.C.Barshilia et.al Thin solid films 258 (1995) 265.
- [2] M.S.Kamboj et.al. NIM B 211 (2003) 369.
- [3] M.S.Kamboj et.al. J. Phys. D 35 (2002) 477.
- [4] P.M.Ratheesh Kumar et.al Journal of Applied Phys. 97 (2005) 013509
- [5] P.C. Srivastava et.al NIM B 156 (1999) 1105.
- [6] B.Balmurugan et.al J. Phys D Appl. Phys 92 (2002) 3304.

5.2.16 Zinc Sulfide nano particles in a matrix and their ion induced modifications

Sandeep Nagar¹, Lokendra Kumar¹, A.C. Pandey¹ and A. Tripathi²

¹Physics Department, University of Allahabad, Allahabad- 211 002

²Inter University Accelerator Centre, Post Box -10502, New Delhi 110 067

Zinc Sulfide has been extensively studied for its optical and structural properties in the past and research is even continuing till date for determining band gap behavior using ab-initio calculations [1-3]. Making them in nanometer scale significantly change their optical [4] and magnetic properties due to large surface to volume ratio and quantum confinement [5]. Doping significantly change the optical

properties of the materials as now the excited electron get an option to de-excite through dopant levels [6-7].

In present work, we have synthesized doped and undoped ZnS nanoparticles in SiO_2 matrix by chemical method and coated onto the glass and quartz substrates by spin coating system. ZnS thin films have been irradiated with 100 Mev (Ag/Au) ions at different fluences. The range of ions has been calculated using SRIM-2003. A significant change has been found in the optical and structural properties of the ZnS thin films. In order to determine the change in the surface morphology of the films after SHI irradiation, we performed AFM (fig.1. and 2) also. Structural characterization is carried out by XRD and small angle x-ray scattering (SAXS) methods which has been confirmed by the electron microscopic images. Luminescence properties of the ZnS:Mn nanoparticles have been investigated at room temperature.

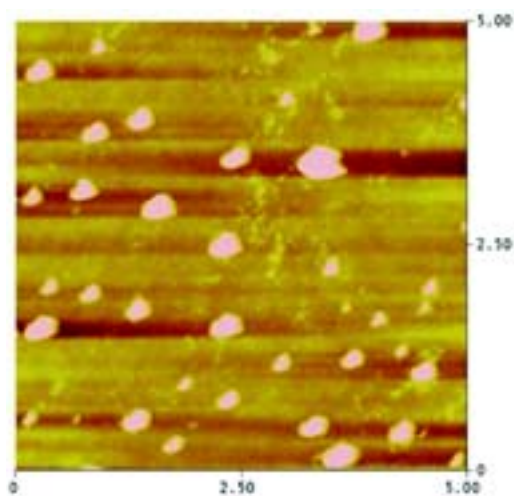


Fig. 1 : AFM picture of chemically grown ZnS: Mn nanocrystals μm (in SiO_2 matrix) thin films.

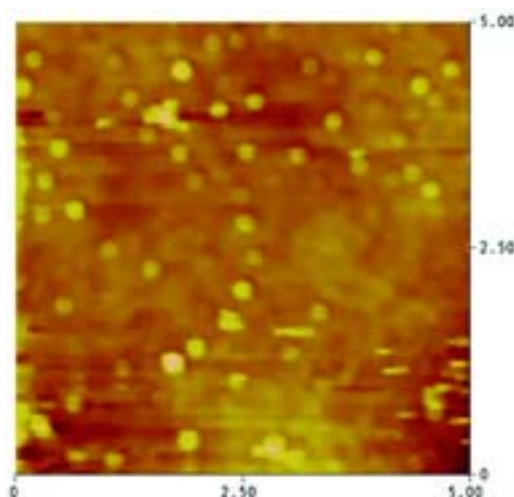


Fig. 2 : AFM picture of chemically grown ZnS: Mn nanocrystals (μm in SiO_2 matrix) thin films irradiated with Ag ions.

REFERENCES:

- [1] Bal K. Agrawal, P. S. Yadav, Savitri Agrawal Phys. Rev. B 50 (1994) 14881
- [2] Jaffe Phys. Rev. B 47 (1993) 6299
- [3] Nazzal and Qteish Phys. Rev. B 53 (1996) 8262
- [4] R. N. Bhargava and D. Gallagher Phy. Rev. Lett 72 (1994) 416
- [5] Y. Wang and N. Herron J. Phys. Chem. 95 (1991) 525
- [6] Bol and A. Meijerink Phys. Review B 58 (1998) R 15997
- [7] Brian A Smith and Jin Z. Zhang Phys. Review B 62 (2000) 2021

5.2.17 Investigations on the influence of 100 MeV Au⁸⁺ ion and 40 MeV Li³⁺ ion irradiation on MOCVD grown Gallium nitride epilayers

V. Suresh Kumar¹, I. Sulania², V. Baranwal², T. Mohanty², F. Singh², A. Tripathi², D. Kanjilal², K. Asokan², and J. Kumar¹

¹Crystal Growth Centre, Anna University, Chennai – 600 025

²Inter University Accelerator Centre, Post Box -10502, New Delhi 110 067

Gallium nitride exhibits wurzite crystal structure and has a direct band gap value of 3.4 eV. It is mainly used in high temperature optoelectronic devices [1]. Swift heavy ion irradiation (SHI) in GaN is a subject of current research interest and is of technological importance. During irradiation, damage is created in the near surface region layer leading to amorphization and stress in the microelectronic structure causing material cracking, anomalous diffusion of dopants and void formation [2].

The samples used in this study are 3 μm thick n-GaN epilayers grown by Metal Organic Chemical Vapour Deposition technique on Sapphire substrates. The mobility and carrier concentration of grown GaN layer are 600 cm² V.s and 6 E 16 cm⁻³ respectively. The computer code Stopping Range of Ions in Matter (SRIM) calculations were used to calculate the depth distributions of the irradiated ions. For 100 MeV Au⁸⁺ ions and 40 MeV Li³⁺ ions are 15 μm and 181 μm in GaN. For 100 MeV Au⁸⁺ ions, electronic energy loss (S_e) and nuclear energy loss (S_n) are calculated as 1.3 eV/Å and 2.9eV/Å. For Lithium beam, S_e is 1.3 eV and S_n is 7.6 eV/Å. These GaN samples were irradiated with 100 MeV Au⁸⁺ ions and 40 MeV Li³⁺ ions of fluence 10¹² and 10¹³ ions cm⁻² at room temperature using 15 UD Pelletron Accelerator. 100 MeV Au⁸⁺ ion beam irradiation were carried out in room temperature. 40 MeV Li³⁺ ion beam irradiation were carried out in room temperature and also 77 K.

XRD measurements were carried out on irradiated samples using D8 Brucker AXS X-ray diffractometer with Cu K_α source. The XRD spectrum of pristine GaN sample exhibits c-plane texture and its full width half maximum (FWHM) is 0.087°. After 100 MeV Au⁸⁺ ion irradiation with the fluence of 10¹² ions.cm⁻² and 10¹³ ions.cm⁻², it was found that the GaN and sapphire substrate XRD peak intensity

decreased. The FWHM of irradiated GaN increases with increasing fluence. From these studies GaN surface amorphization were confirmed. This amorphization of crystalline surface leads to surface tracks [4]. The surface tracks are created from the ion induced melt due to the mechanical stress arising from the thermal expansion.

The effect of 100 MeV Au⁸⁺ ion beam and 40 MeV Li³⁺ ion beam on GaN surface is visible from the changes in the surface morphology as observed using Digital nanoscope III A SPM. The root mean square (rms) value of surface roughness has been evaluated from the AFM data. As grown GaN sample shows pillar like growth leading to high surface roughness which is 1.5 nm. This sharpness of the surface pattern of pristine GaN layer gets damage after ion irradiation. The surface roughness values of irradiated samples increase with increasing fluence. 40 MeV Li³⁺ ion beam irradiated GaN AFM images show uniform nano tracks formation on the GaN surfaces after irradiation. The nano tracks dimension is around 82 nm.

We have investigated the effect of 100 MeV Au⁸⁺ ion beam and 40 MeV Li³⁺ ion beam irradiation carried out on MOCVD grown GaN samples by X-ray diffraction and AFM measurements.

REFERENCES

- [1] Kucheye S.O, Williams J.S, Pearton S.J, 2001, Mater. Sci. Eng., R 33, 51
- [2] Singh J.P, Singh R, Kanjilal D, Mishra N.C and Ganesan V. 2000, J. Appl. Phys. 87, 2742
- [3] Suresh Kumar V et. al., 2006, Nucl. Inst. Meths. B, 255, 145
- [4] Szenes G. Nucl. Inst. Meths. B, 2002,191, 27
- [5] Mohanty T, Mishra N.C, Singh F, Tiwari U. and Kanjilal D, 2003, Nucl. Inst.Meths. B 212, 179
- [6] Zhang, J. Peng X, Wang X, Wang Y, Zhang L, 2001, Chem. Phys. Lett 345, 372

5.2.18 Study of Li ion irradiation on Si and GaAs solar cells

Jayashree. B¹, Ramani¹, M.C.Radhakrishna¹ and Saif Ahmad Khan²

¹Department of Physics, Bangalore University, Bangalore-560056

²Inter University Accelerator Centre, Post Box-10502, New Delhi 110067

The influence of high-energy Lithium ion irradiation on the performance of the solar cells, designed for space application has been investigated. The space-grade Si and GaAs solar cells with thickness and size of 200 μm & 4x7 cm^2 and 145 μm & 2x4 cm^2 respectively are used for our work. The Si solar cells are of N/P type with 1 Ωcm base resistivity, made by diffusion process where as GaAs cells are of P/N configuration, grown on Ge substrate by metal organic vapour phase epitaxy (MOVPE) technique. The cover glass of the cells has been removed to study the radiation damage effects on the bare cells. The cells are irradiated with Li³⁺ ion beam of 15

& 40 MeV at room temperature in vacuum at fluences ranging from 1×10^{10} to 5×10^{12} ions cm^{-2} in the general purpose scattering chamber (GPSC) at IUAC New Delhi. The cell is scanned with ion beam to ensure uniform irradiation. The solar cells are characterized before and after irradiation using X-25 sun simulator with illumination intensity at 135.3 mWcm^{-2} , i.e. illuminated I-V characteristics under air mass zero (AM0) condition (at $\approx 28^\circ\text{C}$) and the dark properties of the cells are measured using Keithley 2420, 3A source meter. Annealing of the irradiated samples is performed for 16 hours in nitrogen flow atmosphere at 60°C . Figure 1 shows the illuminated I-V characteristics of Si and GaAs solar cells before and after irradiation. With increase in the fluence, the short circuit current (I_{sc}), the open circuit voltage (V_{oc}) and the power maxima (P_{max}) of the cell decreases. The fill factor (FF) is a measure of how “square” the output characteristics are which also decreases as the fluence increases.

The decrease in the short circuit current I_{sc} under Li^{3+} irradiation (Table: 1 & 2) could be related to the lifetime of minority carriers. The lifetime of minority carriers is sensitive to the radiation-induced effects, and the decrease in the minority carriers would reduce the electric properties of solar cells.

The change in the open circuit voltage of the cells, irradiated with 40 MeV Li ions is related to the damage of P-N junctions. The efficiency of the cells decreases with increase in the fluence indicating degradation of the cell performance due to irradiation induced defects.

Table 1: Electrical parameters of Si cell before and after irradiation of 40 MeV Li^{3+} ions.

Fluence	Isc in mA		Voc in mV		Pmax mWcm^{-2}		FF		Efficiency	
	Before	After	Before	After	Before	After	Before	After	Before	After
5×10^{10}	1034.0	778.7	594.8	535.0	402.3	317.4	65%	74%	11.44%	9.02%
1×10^{11}	1041.6	722.5	595.1	522.7	463.1	279.9	74%	69%	13.17%	7.96%
5×10^{11}	1026.9	601.6	594.4	500.5	481.8	217.1	78%	64%	13.70%	6.17%
1×10^{12}	1031.8	546.3	595.3	502.5	458.9	144.3	75%	47%	13.05%	4.10%
5×10^{12}	1031.8	191.5	595.3	480.1	459.4	36.9	74%	40%	13.06%	1.05%

Table 2: Electrical parameters of GaAs cell before and after irradiation of 40 MeV Li^{3+} ions.

Fluence	Isc in mA		Voc in mV		Pmax mWcm^{-2}		FF		Efficiency	
	Before	After	Before	After	Before	After	Before	After	Before	After
1×10^{10}	255	250	1007.2	987.6	196.26	186.95	76.4%	75%	17.80%	16.95%
5×10^{11}	256.6	166.1	1020.3	715.2	194.68	73.84	74%	62%	17.66%	6.70%
1×10^{12}	251.6	175.8	1019.4	777.8	196.20	77.39	76.4%	57%	17.79%	7.02%
5×10^{12}	255.3	92.5	1038.6	588.4	187.91	31.58	70%	56%	17.04%	2.86%

With increase in the fluence of Li^{3+} ions, the effect of change in the internal resistance on I_{sc} would dominate gradually in dark I-V characteristics. The fill factor variation in the I-V curves of Fig.1 confirms the increase in the resistivity, which causes the increase of series resistance [1]. The saturation current I_0 of the cell and the ideality factor n increases as the fluence increases (n for Si cell increases from 2.08 to 2.92 at the highest fluence $5 \times 10^{12} \text{ cm}^{-2}$). This suggests that as there is no serious reduction in the V_{oc} of the solar cell, the diode saturation current (I_0) and ideality factor, the damage caused to the cell is uniform, which is related to change in the minority-carrier diffusion length. With increase in the fluence the dark current reduces. A dramatic decrease is seen for the highest fluence of $5 \times 10^{12} \text{ cm}^{-2}$ compared to the lowest fluence. A further increase in the fluence has to be made, to check whether the cell practically behaves as the insulator.

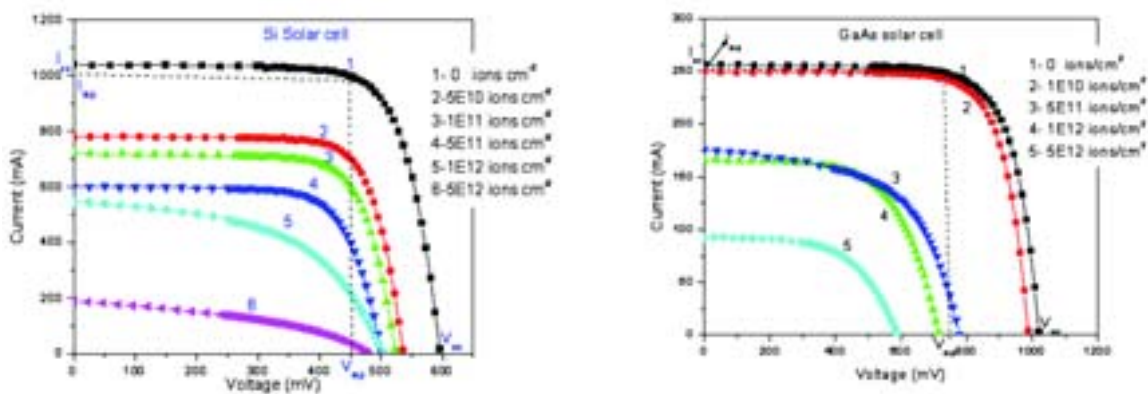


Fig. 1. Illuminated I-V curves for Si & GaAs solar cells irradiated with 40 MeV Li^{3+} ion

The observation reveals that the effect of high energy Li ion irradiation on the electrical characteristics of the solar cells is similar to that of high-energy proton irradiation. Ambient increase in the cell parameters can be seen after annealing, there by passivating the cell defects. It can be concluded that the rate of degradation of P_{max} , I_{sc} , V_{oc} is more for 40 MeV Li^{3+} ion irradiation than 10 MeV proton irradiation due to the large difference in electronic energy loss.

REFERENCES

- [1] J.C. Bourgoin and M.Zazoul, "Irradiation-induced degradation in solar cell: Characterization of recombination centres," *Semicond.Sci.Technol.*17 (2002) 453-460.
- [2] Zhenyu Hu,Shiyu He, Dezhung Yang "Effect of <200 keV proton radiation on electric properties of solar cells at 77K" *NIMB* 217(2004) 321-326.

5.2.19 Nano magnetism in swift heavy ion irradiated ferromagnetic metal/silicon interface

P.C. Srivastava¹, J.K. Tripathi¹ and P.S. Pandey¹

¹Department of Physics, Banaras Hindu University, Varanasi-221005 (INDIA)

The use of carrier spin in semiconductors is promising root towards new device functionality and performance [1]. Ferromagnetic semiconductors are promising materials in this endeavor. The prominent success during the last decade in using the ion beam to modify the structure and properties of materials has attracted considerable interest from both the scientific and technological point of view. This technique allows us to overcome either thermodynamic or kinetic barriers by employing energetic particles to surpass the limit of solid solubility and to produce compositional and structural metastability. Ion irradiation of magnetic bilayers and multilayers has shown to modify the extrinsic magnetic properties such as magnetic anisotropy, coercivity and magnetic exchange coupling [2,3]. Recently [4], it has been shown that in the case of FePt₃ upon irradiation (with 700 keV N⁺ ions at a fluence of 1X10¹⁶ ions cm⁻²), the chemical order is destroyed and ferromagnetism is induced. It has also been shown that an antiferromagnetic to ferromagnetic transition can be induced through ion irradiation without destroying the film crystallinity.

pSi <100> wafers of 8-10 Ωcm has been used for the fabrication of Fe/pSi and Fe₂₀Ni₈₀/pSi devices. Electron beam evaporation technique has been used for metallization. A thin layer (of ~ 50 nm) of Fe (99.999) and Fe₂₀Ni₈₀ was deposited on the pSi substrates. The above fabricated Fe/pSi and Fe₂₀Ni₈₀/Si interface devices were irradiated by 100MeV Fe⁷⁺ ions for a fluence of ~10¹⁴ cm⁻² at 15 UD pelletron facility. The pristine and irradiated devices have been characterized from XRD and SEM and the M vs H data has been obtained from a VSM facility.

The XRD of the Fe/Si and Fe₂₀Ni₈₀/pSi before and after the irradiation clearly shows that in Fe/Si, Fe₅Si₃ compound is formed but interesting is that FWHM (full width at half maxima) is increased after the irradiation to show the reduction in the grain size. Whereas in Fe₂₀Ni₈₀/Si, it is found that FeSi₂ (101) peak emerges with highest intensity followed by Ni₂Si (042) peak. The grain size has been calculated from the Scherrer formula [5] which is found to be in range of 17 nm to ~ 70 nm after the irradiation. The observed phase can be understood due to the ion beam induced atomic mixing. High energy ion almost instantly produced (i.e., within 10⁻¹⁰ to 10⁻¹² s) a highly disordered and kinetically active zone across the interface due to the thermal spike which allows rapid but transient atomic motion possible. The process can be also considered as fast quenching process. This lead to an alloying of elements in neighbouring layers. The SEM micrographs of the top surface of Fe film deposited on Si substrate before and after the irradiation were recorded. The granular structure is clearly observed for the irradiated whereas the unirradiated also show the mixed phase. The Fe/Si pair is reactive and there is mixing even at room temperature due to high chemical activity of the pair. The SEM feature shows the reacted phase which has been identified as Fe₅Si₃ from the XRD data. The grain formed after the swift heavy ion irradiation has been found to be of ~ 100 nm from the SEM micrograph. Thus it seems that nano-granular particles are formed after the swift heavy ion irradiation as result of intermixing of Fe/Si pair.

To study the magnetization, M vs H curve for the irradiated pair (Fe/Si) was obtained from a VSM (vibration sample magnetometer) facility. It is interesting to note that the M-H curve does not show any hysteresis and coercivity .The saturation magnetization is 1.17 emu/gm. The value is less because the weight in denominator is of the entire sample (i.e., Fe film on crystalline substrate). However only the mixed phase in the neighboring region of Fe/Si interface seems to form the magnetic nano particles and large amount of silicon is still unmixed and non-magnetic. So if the weight division of the mixed phase is only done the saturation magnetization shall increase by a large factor. The observed behavior in M-H variation also shows the presence of magnetic nano particles [6] . In nano particles, the formation of domain walls is energetically unfavorable and the particle stays in a single domain configuration below a certain size. For the small particle system above certain temperature (known as blocking temperature, TB), thermal fluctuations dominate and particles can spontaneously switch its magnetization from one easy axis to another. Such a system of superparamagnetic particles does not show hysteresis in the M-H curve above T_B . It seems that for our system, T_B is below room temperature. For TiO_2 films doped with Co, showing nano-sized superparamagnetic clusters, a T_B of 200 K has been observed [7] .

REFERENCES

- [1] Kioseoglou George, T Hanbicki Aubrey, M. Sullivan James, M J Van't Erve Olaf, H Li Connie, C Erwin Steven, Mallory Robert, Yasar Mesut, Prtrou Athos and T Jonker Berend, Nature Materials 3 (2004) 799
- [2] M Cai, T Veres, S Roorda, R Abdouche, R W Cochrane and M Sutton, J. Appl. Phys. 81 (1997) 5200
- [3] C Chappert, H Bernas, J Ferre, V Kottler, J P Jamet, Y Chen, E Cambрил, T Devolder, F Rousseaux, V Mathet and H Launois , Science 280 (1998) 1919
- [4] S Maat , A J Kellock, D Weller , J E E Baglin and Eric E Fullerton J. Magn. Mater. 265 (2003) 1
- [5] J P Eberhart Analyse Structurale et Chimiques des Materiaux (Paris : Bordas) 1989
- [6] M.R. Zachariah, ML Aquino, R.D. Shull and E.B. Steel, Nano Structured Materials 5 (4) 1995
- [7] S R Sinde, S B Ogle, J S Higgins, H Zheng, A J Millis, V N Kulkarni, R Ramesh, R L Greene and T Venkatesan, Phys. Rev. Lett. (In Press)

5.2.20 Silicon Ion Induced Structural and Surface Modifications on InAs, InSb and GaSb Single Crystals

S. Sudhakar¹, V. Ganesh¹, S. Suresh¹, T. Mohanty², Pawan Kulariya ², Indra Sulania², K. Asokan², D.K. Avasthi² and K. Baskar¹

¹Crystal Growth Centre, Anna University, Chennai – 600 025

²Inter University Accelerator Centre, Post Box -10502, New Delhi 110 067

Several implantation and irradiation techniques have been applied to modify the electrical properties of III-V semiconductors [1-5]. In the present investigation, single crystals of InAs, InSb and GaSb of size 1cmx1cm and about 250 μ m thickness were used for high-energy ion irradiation. The samples have been irradiated at liquid nitrogen temperature to avoid local heating and thermal effects. Silicon ion has been used to irradiate the samples with fluence of 10^{10} , 10^{11} , 10^{12} and 10^{13} ions/cm². Irradiation was carried out at a background pressure of 9×10^{-7} torr and the beam current was maintained at 3PnA. To study the structural characteristics, XRD was recorded for all the samples. BRUKER-D8 Advanced XRD system at a glancing angle of 1° has been used. AFM images were recorded by Digital Nanoscope Instrument with a scan rate of 1.502Hz in tapping mode.

The FWHM of the XRD peak for InAs gets gradually decreases with the increase of ion fluence from 10^{10} to 10^{13} ions/cm². This shows that there is improvement in the crystalline nature of InAs sample with the increase of ion fluence. This is also evident from the reduction in the value of r.m.s surface roughness from 8.2nm to 2.3nm as discussed below.

The full width at half maximum (FWHM) values corresponding to different ion fluences for all the samples are given in Table 1.

Sample	FWHM for as grown crystal in arc sec	FWHM for samples irradiated at different ion fluences in arc sec			
		10^{10} ions/cm ²	10^{11} ions/cm ²	10^{12} ions/cm ²	10^{13} ions/cm ²
InAs	468	198	198	156	144
InSb	70	90	72	72	
GaSb	126	180	1620	468	684

Table 1 FWHM for samples before and after irradiation

In the case of InSb, there is an increase in the value of FWHM for irradiation at 10^{10} fluence and the FWHM almost remains constant for the higher fluences of 10^{11} and 10^{12} . Whereas in the GaSb sample there is a large increase in the value of FWHM at 10^{11} fluence and this may due of the creation of defects in the sample and is evident from the appearance of new peaks at 64°. The FWHM decreases at 10^{12} and again increases at 10^{13} fluence. The intensity of the peak at 29° gets increases with the increase of ion fluence. Detailed analysis to identify the nature of defects and their influence in the structural modification due to irradiation is in progress. AFM images were recorded for all the samples.

Our investigation of the effect of Si ion irradiation was carried out on single crystals of InAs, InSb and GaSb at different ion fluences revealed that there is

degradation in the crystalline quality as a result of heavy-ion irradiation. Surface morphology was studied by AFM shows that the roughness value decreases in the case of InAs with the increase of ion fluence. Detailed analysis is in progress.

REFERENCES

- [1] Y.K.Su, U.H.Liaw, T.P.Sun, G.S.Chen, J. Appl. Phys. 81 (1997) 739.
- [2] S.Chadda, A.Datye, L.R.Dawson, J. Appl. Phys. 73 (1993) 4232.
- [3] H.Gernstenberg, W.Glaser, Phys. Status Solidi A 118 (1990) 241.
- [4] M.V.Rao, P.E.Thompson, R.Echard, S.Mulpuri, A.K.Berry and H.B.Dietrich, J. Appl. Phys. 69 (1991) 4228.
- [5] G.Kuri, B.Sundaravel, B.Rout, D.P.Mahapetra, B.N.Dev, Nucl. Inst. and Methods, B 111; G. Kuri *et al* J. Appl. Phys. (1996) 234.

5.2.21 Effect of SHI irradiation on dielectric behaviour of Ti^{4+} -substituted $\text{Li}_{0.5}\text{Al}_{0.1}\text{Fe}_{2.4}\text{O}_4$ spinel

M.C. Chhantbar¹, K.B. Modi¹, Ravi Kumar² and H.H. Joshi¹

¹Department of Physics, Saurashtra University, Rajkot-360005 (Gujarat) India

²Inter University Accelerator Centre, Post Box-10502, New Delhi 110067

Lithium ferrite $\text{Li}_{0.5}\text{Fe}_{2.5}\text{O}_4$ is a high resistivity, low mobility semiconductor that has low eddy-current losses. Modifications of the properties of $\text{Li}_{0.5}\text{Fe}_{2.5}\text{O}_4$ due to substitution of different ions, which are dependent upon nature and number of substituted ions, are fundamental importance for microwave devices [1]. Swift heavy ion irradiation is known to create controlled defects in the ferrite material and being used to understand the damage structure and modifications in their dielectric properties [2]. In the present study, we investigated the dielectric properties of the system $\text{Li}_{0.5(1+x)}\text{Ti}_x\text{Al}_{0.1}\text{Fe}_{2.4-1.5x}\text{O}_4$ ($x = 0.0$ to 0.3) ferrites before and after irradiation.

The polycrystalline samples of the spinel system $\text{Li}_{0.5(1+x)}\text{Ti}_x\text{Al}_{0.1}\text{Fe}_{2.4-1.5x}\text{O}_4$ ($x = 0.0$ to 0.3) were prepared by the double sintering ceramic technique. For Irradiation, we used lithium beam of energy 50 MeV with fluence 5×10^{13} ions/cm² at IUAC, New Delhi. The dielectric measurements were made using Agilent 4284 A Precision LCR Meter. Thermoelectric power studies were carried out over a temperature range 300-500 K. The details regarding sample preparation and the effect of irradiation on structural and magnetic properties have been given in our earlier paper [3].

The variation of dielectric constant (ϵ') were studied as a function of an a.c. field in the frequency range 100Hz-1MHz for unirradiated and irradiated two representative compositions $x = 0.1$ and 0.3 . The variation of dielectric constant (ϵ') with frequency reveals the dispersion due to Maxwell-Wagner interfacial polarization

[4] which in the agreement with Koops phenomenological theory [5]. The values of dielectric constant (ϵ') initially decrease rapidly with increase in the frequency but beyond 100KHz remain fairly constant for unirradiated as well as irradiated samples but after irradiation it is decreased in magnitude from that of the unirradiated samples. This is evident because the fact that only species (Fe^{3+}) contributing to polarisability are bound to be lagging behind the applied field at higher frequency.

After the SHI irradiation, for the frequency range studied there is a considerable decrease in the magnitude of dielectric constant (ϵ') but nature remains constant before and after irradiation. The observed reduction in the magnitude for irradiated samples may be due to the fact that point defects hinder the polarization process-taking place. In other words exchange holes may trap in defects. It is interesting to note that after irradiation, dielectric loss increases considerably particularly up to frequency of 100KHz after which it coincides with unirradiated curve.

REFERENCES

- [1] S. A. Mazen et al, J. Phys D: Appl. Phys. 30 (1997) 1799.
- [2] Anjana Dogra et al, Nucl. Instr. And Meth. B 207 (2003) 296.
- [3] M. C. Chhantbar et al, Nucl. Instr. And Meth. B (2006) (In Press)
- [4] K. W. Wagner, Ann. Physik 40 (1917) 817.
- [5] C. G. Koops, Phys. Rev. 83 (1951) 121.

5.2.22 Effect of shift heavy Au^{8+} ions on Indium doped Tin Oxide (ITO) thin film

N.G. Deshpande¹, S.D. Chavhan¹, R.R. Ahire¹, A.A. Sagade¹, F. Singh², A. Tripathi², D.K. Gautam³, J.C. Vyas⁴ and R.P. Sharma¹

¹Dr. Babasahab Ambedkar Marathwada University, Aurangabad- 431004

²Inter University Accelerator Centre, Post Box-10502, New Delhi 110 067

³Department of Electronics, North Maharashtra University, Jalgoan.

⁴Bhabha Atomic Research Centre, Anushaktinagar, Mumbai.

In the present study spray deposited Indium doped Tin Oxide (ITO) thin films have been irradiated with 100MeV Au^{8+} ions at different fluency from 1×10^{11} to 1×10^{13} ions/cm². There are few reports on shift heavy ions induced modification (SHI) on structural and optical properties of ITO [1] material. Analysis of the change in structural and optical properties of ITO thin films under the defect production has continuing interest.

Fig .1 shows the XRD patterns of pristine and irradiated ITO films. The (h k l) values are in good agreement with the JCPDS card [6], which confirms the

formation of ITO thin films. The XRD patterns of ITO thin films Show prominent peaks along (221), (400), (331), (441) in the pristine as well as in ion-irradiated films. After irradiation the peak intensity of (221), (400), (441) increases while the peak intensity of (331) decreases as the ion fluence increases. It also reveals that the grain size and texturing of the film increases after irradiation.

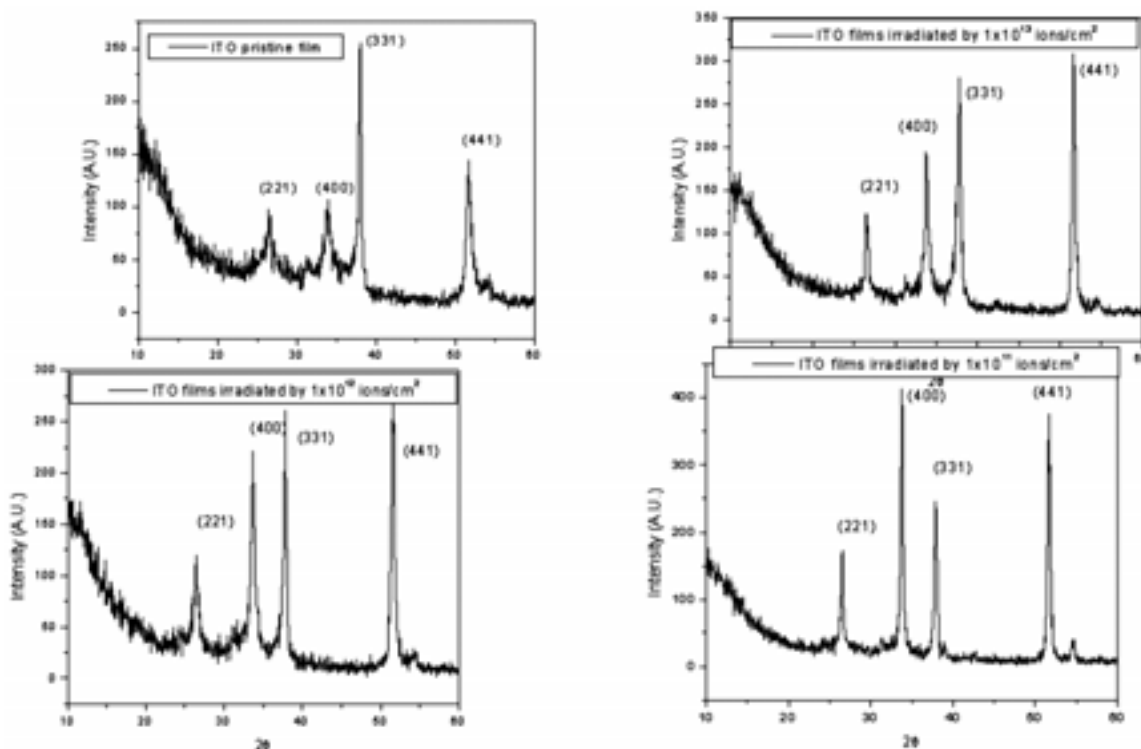


Fig. 1.

The PL spectra of the as grown and Au ions of 100MeV irradiated ITO recorded at room temperature. The films are displaying the defects related emission in the PL spectra. After irradiation there is an increase in the PL intensity and a red shift is observed due to the defect created by ion beam.

REFERENCES

- [1] M. Maaza, O. Nemraoui, A.C. Beye, C. Sella, T. Derry, Solar Energy Materials & Solar Cells 90 (2006) 111.
- [2] JCPDS Data card no. 39-1058.

5.2.23 160 MeV Ni¹²⁺ ion irradiation effects on HCl doped polyaniline conducting polymer

A.M.P. Hussain¹, A. Kumar¹, F. Singh² and D.K. Avasthi²

¹Dept. of Physics, Tezpur University, Napaam, Tezpur, Assam-784 028

²Inter University Accelerator Centre, Post Box -10502, New Delhi 110 067

The swift heavy ion (SHI) irradiation is an effective technique for enhancement of the electrical conductivity of both insulating and conducting polymers and generation of active sites for physical and chemical modification of polymers [1]. To the best of knowledge of authors the swift heavy ion irradiation with high energy (>80MeV) and enhancement of electrochemical stability of polypyrrole electrodes after swift heavy ion irradiation has been reported for the first time by us [1,2].

The electro-polymerization of the conducting polymer polyaniline film is carried out potentiodynamically on indium tin oxide (ITO) coated glass substrate with film surface area of 1 cm². Films of thickness 20-25 μm were irradiated with 160 MeV Ni¹²⁺ ion beam with three different fluences of 5X10¹⁰, 5X10¹¹ and 3X10¹² ions/cm². The cyclic voltammetry of the polymer films before and after SHI irradiation are carried out at 50 mV/sec scan rate using potentiostat/galvanostat. The dc conductivity of the polyaniline films is measured by using a four probe setup (Scientific Instruments Inc., India). The scanning electron micrograph and X-ray diffractogram of the polymer films are recorded before and after irradiation for morphological studies.

The cyclic voltammograms (CV) of HCl doped unirradiated and irradiated polyaniline polymer films at 50mV/sec scan rate in an electrochemical cell containing an aqueous electrolyte with HCl concentration kept same as in synthesis. The CV is observed to be related with the electrochromism of the conducting polymer. The shapes of the cyclic voltammogram of the unirradiated and irradiated polymer films are same with oxidation and reduction occurring at the same potential 790 mV and -380 mV respectively. The redox response of the irradiated polyaniline films remains the same as for the unirradiated films upon SHI irradiation. However, there is an increase in the magnitude of the oxidation and reduction currents.

The conductivity of the polyaniline films shows an increasing trend with the increase in ion fluence and increases up to 70% upon SHI irradiation (Table 1). The increase in conductivity of the polymer films after SHI irradiation could be ascribed to the inter-chain cross linking due to huge electronic energy loss [3]. The inter-chain electron hopping required for conduction between chains, which is a source of resistivity in conducting polymers, is reduced due to the cross linking of the polymer chains upon SHI irradiation. Defect sites in the molecular structure of the polymer chains created by SHI irradiation may also contribute dc conductivity enhancement as charge accumulation occurs at the defect sites producing charge carriers. The increase in the degree of crystallinity of the polymer films also contributes to the increase in conductivity upon SHI irradiation [4].

The X-Ray diffraction pattern of the polymer films before and after SHI

irradiation with fluences of 5×10^{10} , 5×10^{11} and 3×10^{12} ions/cm² were recorded. The unirradiated polyaniline conducting polymer films are semi-crystalline. The degree of crystallinity of the polyaniline films after SHI irradiation shows significant increase (Table 1). The increase in the degree of crystallinity of polymer films could be attributed to systematic alignment of polymer chains by chain folding or by the formation of single or multiple helices, for at least part of their length [4]. As these regions possess long range order and are therefore crystalline. In SHI irradiation the density of the polymer increases making the polymer more compact which may have produced closely packed regions by chain folding, cross linking of polymer chain or by the formation of single or multiple helices which produces more crystalline regions in the polymer films resulting in increase in degree of crystallinity. The degree of crystallinity increases with increase in ion fluence. These crystalline regions give easy path for electron conduction in the polymer films, which is consistent with the dc conductivity measurements.

Table 1: Conductivity and degree of crystallinity of polyaniline films after SHI irradiation with 160 MeV Ni¹²⁺ ions at different fluences

Fluence	Conductivity (S/cm)	Degree of crystallinity (K)
Unirradiated	36 ± 2.3	29.3%
5×10^{10} ions/cm ²	45.4 ± 2.2	34.7%
5×10^{11} ions/cm ²	54 ± 2.9	40.2%
3×10^{12} ions/cm ²	61 ± 1.8	44.9%

REFERENCES

- [1] A.M.P. Hussain, D. Saikia, F. Singh, D.K. Avasthi and A. Kumar, Nucl. Instr. and Meth. B, 240 (2005) 834.
- [2] A.M.P. Hussain, A. Kumar, D. Saikia, F. Singh and D.K. Avasthi, Nucl. Instr. and Meth. B. 240 (2005) 871.
- [3] E. H. Lee, Nucl. Instr. and Meth. B 151 (1999) 29.
- [4] Applications of Electroactive Polymers ed. by Bruno Scrosati, Chapman & Hall, London (1993).

5.2.24 Swift Heavy Ion Induced structural and Chemical Changes in BOPP Film

S. Chawla¹, A.K. Ghosh², S. Ahmad³, D.K. Avasthi⁴

¹Amity School of Engineering and Technology, New Delhi, India

²Centre for Polymer Science and Engineering, Indian Institute of Technology, New Delhi

³Materials Research Laboratory, Chem.Dept., Jamia Millia Islamia, New Delhi

⁴Inter University Accelerator Centre, Post Box-10502, New Delhi 110 067

The objective of this work is to study the structural and chemical changes in BOPP induced by swift Si^{7+} and Ag^{9+} ion irradiation. The optimum experimental conditions for creating residual active sites on PP for its efficient graft copolymer synthesis have been presented. "Grafting" is a process whereby chemical groups are attached by covalent bonds to a polymer backbone usually via an aliphatic carbon atom. If the ion incidence is normal to the surface, then circular islands corresponding to the grafted domains are seen [1]. Moreover, in response to a stimulus, the grafted domains are transformed from an expanded conformation to compact ball leading to an increase or decrease in the pore size and thus can be used for the production of permeability – adjustable membranes. These are also called as "intelligent" membranes. Their potential applications include the controlled release of drugs [2].

Commercially available biaxially oriented polypropylene (BOPP) film, 15 mm thick, samples were irradiated in vacuum at room temperature using 80 MeV Si^{7+} and 120 MeV Ag^{9+} ion beams in the fluence range of 10^{10} to 10^{13} ions/cm². Infrared absorption measurements were carried out on a Perkin Elmer FTIR RX1 (4000 – 500 cm⁻¹) spectrophotometer at a 4.0 cm⁻¹ resolution. Ultraviolet spectroscopy measurements were performed using a Perkin Elmer UV-Visible EZ-201 (The 400-190 nm) spectrometer at a 4 nm resolution. The calorimetric measurements were carried out on a Perkin Elmer Pyris-6 series differential scanning calorimeter (DSC) under a nitrogen atmosphere with a uniform heating or cooling rate of 10 °C / min.

A considerable volume of BOPP around the ion projectile is influenced by the interaction between the Si or Ag ions and the BOPP electrons. This results in the production of active chemical species such as cations, anions, electrons and radicals along ion path in the BOPP film. The coulombic attraction and repulsion among these active species cause violent bond stretching and segmental motion in the polymer chains, which lead to distortion of PP's crystal lattice as well as bond breakage [3]. As a result of these bond cleavages, free hydrogen radical and some other radicals are formed in latent track. Subsequently, gaseous molecular species are formed by the combined mechanisms of direct recombination of radicals and by recombination of diffusing radicals [4]. The proposed mechanism is supported by the appearance of a broad OH band at 3400 cm⁻¹ with a shoulder at 3555 cm⁻¹ characteristic of hydroperoxide (OOH) groups [5] in the FTIR spectrum. The peroxides and hydroperoxides can be activated by elevated temperature to form radicals at the desired time. These radicals can be used for graft copolymerization of polypropylene with suitable reactive monomers.

The melting temperature, enthalpy of melting and percentage crystallinity decrease after irradiation of BOPP with 80 MeV Si^{7+} (at $\Phi = 1 \times 10^{10}$ ions/cm²) In the FTIR spectrum of this sample a new peak is observed at 734 cm⁻¹. This peak can be

attributed to propyl branches in the irradiated BOPP [6]. Thus, the observed crystallization behavior and melting characteristics are related to branches which reduce the regular close packing. Furthermore a new peak at 1219 cm^{-1} appeared in the FTIR spectrum which indicates that 14 monomer units are in helical sequences in Si ion beam irradiated BOPP (at $\Phi = 10^{11}\text{ ions/cm}^2$) instead of 12 in the un-irradiated BOPP [7]. The increase in conformational order leads to higher crystallinity and higher enthalpy of melting (Table 1). Moreover the intensity of band centered around 2900 cm^{-1} decreases when BOPP is irradiated with Si^{7+} (at $\Phi = 3 \times 10^{12}\text{ ions/cm}^2$) or Ag^{9+} (at $\Phi = 10^{12}\text{ ions/cm}^2$) respectively. This can be attributed to the reduction in molecular mass.

REFERENCES

- [1] N.Betz, S.Dapz, M.J.Guittet, Nucl. Instrum. and Meth. B 131 (1997) 252.
- [2] N.I.Shtanko, V.Ya.Kabanov, M.Yoshida, Nucl. Instrum. and Meth. B 151 (1999) 416.
- [3] E.H.Lee, Nucl. Instrum. and Meth. B 151 (1999) 29.
- [4] M.P.de Jong, A.J.H.Maas, L.J.Van Ijzendoorn, S.S.Klein and M.J.A. de Voigt, J.Appl.Phys.82 (1997) 1058.
- [5] R.A.V.Raff, Crystalline Olefin Polymers, Part I, Interscience Publishers (1965) 795
- [6] T.R.Crompton, The Analysis of Plastics, 1st edn., Pergamon Press (1984) 145.
- [7] X.Zhu, D.Yan and Y.Fang, J.Phys.Chem.B 105 (2001) 12461.

5.2.25 Effect of swift heavy ion irradiation on the optical properties of semi organic non-linear optical crystal-K [CS (NH₂)₂]₄ Br

V. Krishnakumar¹, R. Nagalakshmi², D.K. Avasthi³, P.K. Kulriya³, Fouran Singh³

¹Department of Physics, Periyar University, Salem-636 011, India

²Department of Physics, Nehru Memorial College, Puthanampatti-621007, Tiruchirappalli

³Inter University Accelerator Centre, Post Box -10502, New Delhi 110 067

Semi organic crystals of Potassium tetrakis thiourea bromide (KTTB) are subjected to swift heavy ion irradiation of Ag^{14+} 100 MeV and Li^{3+} 50 MeV from the 15 UD Pelletron Accelerator at Inter University Accelerator Centre (IUAC), New Delhi having 10^{-6} torr Vacuum in Material Science chamber of fluence 10^{10} to 10^{12} ions/cm². The irradiated samples are characterized by employing various techniques. The effect of irradiation on the dielectric and non-linear optical properties has been studied. The optical transmission spectra of as grown and ion irradiated single crystals have been recorded at room temperature and shown in Fig.1. Optical band gap of ion irradiation crystals give better results compared to as grown crystals. The dielectric measurement of heavy ion irradiated crystal reveals the change in dielectric values with frequency. The changes in dielectric constant and dielectric loss frequencies

have also been calculated. The values of dielectric constant are found sensitive to ion fluence and Se. Fig.2 gives photoluminescence spectra of the as grown and Ag and Li ion bombarded crystals. A shift in PL peak is attributed to the defect created by the ion beam. The very high value of energy transferred induces a usual density of defects in the material. Analysis of the change in optical properties of the crystal under the defect production has continuing interest. SEM images show some morphological modifications after irradiation. The second harmonic relative efficiency has been slightly increased after irradiation and it is given in Table.1. Further detailed studies on the comparison of pre and post-irradiated data are in progress

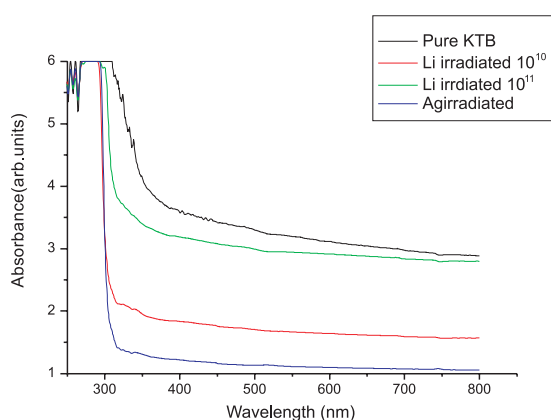


Fig. 1 Optical transmission spectra of pure and irradiated KTTB

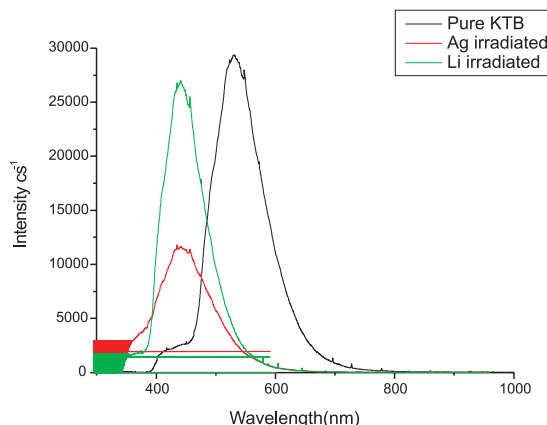


Fig. 2 Photoluminescence spectra of pure and irradiated single crystals of KTTB

Table. 1 Comparison of second harmonic output

Input power mJ/pulse	Pure KTTB mV	Li irradiated mV	Ag irradiated mV
5.7	7	9	7.32

REFERENCES

- [1] A.P. Bhat, P. Sreeramana Aithal, P. Mohan Rao, D.K. Avasthi, Nucl. Instr and Meth. B166-167 (2000) 964.
- [2] P. Sreeramana Aithal, H.S. Nagaraja, P. Mohan Rao, D.K. Avasthi, Asiti Sarma., Vaccum 48 (1997) 991.
- [3] P. Sreeramana Aithal, H.S. Nagaraja, P. Mohan Rao, D.K. Avasthi, Asati Sarma., J.Appl.Phys.,81(1997)7526.
- [4] F. Singh, A. Sarma, R.M. Montereali, F. Bonfigli, G. Baldacchini, D.K. Avasthi., Radiation Measurements 36(2003) 675.

5.2.26 Effect of Li³⁺ irradiation on the structural and transport properties of La-Bi-Mn-O type CMR material

S. Chattopadhyay^{1,2}, S. Taran², B.K. Chaudhuri², A. Sarkar³, Ravi Kumar⁴ and P.K. Bhattacharyya¹

¹Department of Physics, University of Calcutta, 92 A.P.C. Road, Kolkata-700009

²Department of Solid State Physics, Indian Association for the Cultivation of Science, Jadavpur, Kolkata 700 032

³Department of Physics, Bangabasi Morning College, 19 Rajkumar Chakraborty Sarani, Kolkata-700 009

⁴Inter University Accelerator Centre, Post Box-10502, New Delhi 110 067

The mixed valence rare-earth manganite system $R_{1-x}A_xMnO_3$ (R is La, Sm, etc. and A is Pb, Ca etc.) has recently been a subject of substantial interest due to their various magnetotransport properties [1]. Recent study [2-4] shows that defects, disorder and local structural modification by ion-beam irradiation can be useful for tailoring the transport properties of such system by affecting Mn³⁺-O-Mn⁴⁺ network and also by changing the Mn⁴⁺ content and hence the resulting carrier concentration.

Polycrystalline La_{0.62}Bi_{0.05}Ca_{0.33}MnO₃ samples have been prepared by ceramic method. The samples have been irradiated by 50 MeV Li³⁺ beam with three different fluences viz. 5×10^{13} , 1×10^{14} and 2×10^{14} ions/cm². Those fluences have been coded as low, medium and high fluence. The samples have been characterized by powder X-ray diffraction (XRD) and scanning electron microscopy (SEM) techniques. The resistivity of the unirradiated and irradiated samples has been measured by usual four-probe technique in presence and absence of 1.2 T magnetic field down to liquid nitrogen temperature. We have also investigated the temperature and field dependent resistivity and temperature dependent thermoelectric power of the unirradiated and irradiated samples.

The X-ray diffraction study shows that with increasing fluence, the most intense manganite peak shifts towards higher $2q$ value which implies vertical compression or in plane expansion. A significant change in the surface morphology is observed in SEM images. The temperature dependent resistivity data of the unirradiated and two irradiated samples are shown in fig.1. The pristine sample shows metal to insulator transition (MIT) near $T \sim 239$ K. In the low dosed system no noticeable change of MIT is observed but a little increase in the width of the transition and peak resistivity is clear. The resistivity behavior of the medium dosed sample shows a broad MIT and a shoulder just below the T_{mi} . For the sample irradiated with highest dose (not shown in the figure) there is no evidence of MIT up to 80K.

One of the most common ways to study the carrier type in the system is to

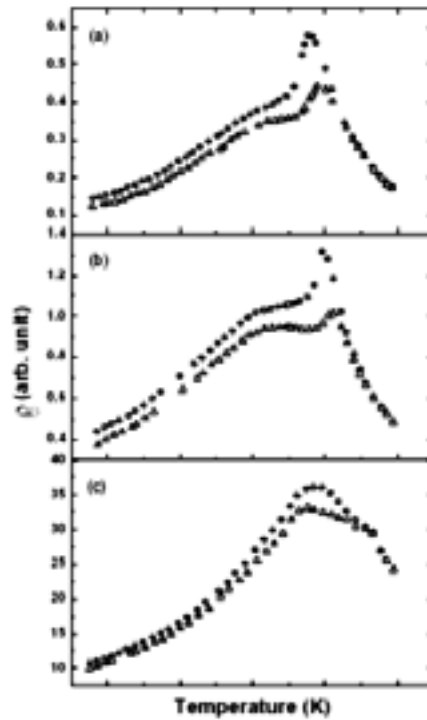


Fig. 1 B vs. T plot for the samples irradiated with (a) unirradiated, (b) low and (c) medium fluence in presence (triangle) and absence (circle) of 1.2 T magnetic field.

investigate the nature of thermoelectric power. For the unirradiated system, the sign of S is negative throughout the temperature range. It shows a sharp increase near MIT temperature and below $T \sim 200\text{K}$, S has almost constant zero value up to lowest temperature which suggests a spin ordered (metallic) state. In case of the system irradiated with low dose, the nature of S is almost similar to that of unirradiated system with a little increase in magnitude of S . The S - T behavior of medium dosed system is interesting showing negative value below $T \sim 190\text{K}$, with a crossover from negative to positive nature up to temperature $T \sim 125\text{K}$ and then saturates at constant zero value. Thermopower of the high dose system (not shown in the figure) shows activated type nature ($1/T$) over the entire temperature range. The change in the nature of thermopower of the irradiated system relative to that of the unirradiated system can be understood by considering the radiation damage induced defects and disorder in this system.

REFERENCES

- [1] C.N.R. Rao, A.K. Raychoudhuri, in: C.N.R. Rao, B. Raveau (Eds.), Colossal Magnetoresistance, Charge Ordering and Related Properties of Manganese Oxides, World Scientific, Singapore, 1998.
- [2] C.H. Chen, V. Talyansky, C. Kwon, M. Rajeswari, R.P. Sharma, R. Ramesh, T. Venkatesan, John Melngailis, Z. Zhang, and W.K. Chu, Appl. Phys. Lett. 69 (1996) 3089.

- [3] S. B. Ogale et al., J. Appl. Phys. 84 (1998) 6255.
[4] S. Chattopadhyay, A. Sarkar, Aritra Banerjee, S. Karmakar, D. Banerjee, Ravi Kumar and B.K. Chaudhuri, Nucl. Instr. Meth. B. 226 (2004) 274

5.2.27 Effect of SHI on RF plasma polymerized thin films

Rajeev. R. Ashokan¹, M.R. Anantharaman¹, D.K. Avasthi², F. Singh², Ambuj Tripathi², Mohan Jacob³

¹Department of Physics, Cochin University of Science and Technology, Cochin, 682 022

²Inter University Accelerator Centre, Post Box -10502, New Delhi 110 067

³Department of electrical engineering, James Cook University, Townsville, Queensland, Australia

Tea tree oil is natural oil which is abundant in the Australian subcontinent. Products based on tea tree oil are antifungicides, solvents, food flavors and traditional medicines. Both of them are nontoxic and hence it is an ideal candidate to be used as biocompatible polymer coating for drug delivery and targeting. Moreover they contain many active components and some of them are optically and electrically active. Hence scope exists to convert them into electronic grade materials. An initial investigation carried out here at CUSAT, Cochin on the plasma polymerisation of this oil by using rf and ac resulted in optically transparent semi conducting films. Any application of these thin films necessitates that the electrical conductivity and optical properties are suitably modified. Swift heavy ion irradiation on RF plasma polymerized tea tree oil thin films might result in cluster formation, bond breaking and thus modify the optical and electrical properties. With this objectives in mind thin films of RF polymerized tea tree oil (TTO) are irradiated with 90 MeV Si⁸⁺ Swift Heavy Ion in the fluence range 1×10^{11} ions/cm² to 1×10^{12} ions/cm² at the material science beam line provided by 15UD Pelletron accelerator. Optical bandgap variation is analyzed using UV-VIS spectroscopic technique and a red shift is observed for both pristine and iodine doped samples. The optical band gap is found to be decreasing with increase in fluence both in pristine and doped samples but in Iodine-doped samples absorption edge modified considerably along with decrease in bandgap. Bandgap is shifted from 3.9 eV to 2.8 eV for undoped samples and that for iodine doped samples are 3.6 eV to 2.6 eV.

Radio frequency polymerized Tea tree oil (TTO) samples in pristine, iodine doped and SHI irradiated form are subjected to photoluminescence study under the excitation 325 nm using He-Cd laser source. FTIR analysis is carried out to identify the optically active group. Observed PL peaks are tabulated and correlated with the induced defect level due to doping and SHI induced nano carbon cluster energy level.

The pristine, doped and irradiated thin films are analyzed using AFM and SEM. At the fluence 1×10^{11} a reduction in roughness is observed and that is an indication of surface smoothening at lower fluence regime. In pristine form the crater formation and mass transport starts at the fluence 3×10^{12} and the defects formation found to be increase with increase in fluence. The induced cluster formed as result of iodine doping consists of 2-3 identical islands each having a diameter of 171 nm-273 nm. The island diameter was reduced in ion irradiated samples and an individual island diameter is found to be 89 nm for the fluence 3×10^{12} . The unusual crater with a diameter 148 nm in the iodine doped samples were obtained at the fluence 1×10^{12} is due to multiple ion impact. Further analysis is in progress.

5.2.28 Structural and mechanical properties of ion irradiated polycarbonate membranes

Y.K. Vijay¹, Vaibhav Kulshrestha¹, Kamendra Awasthi¹, N.K. Acharya¹, M. Singh¹, Balram Tripathi¹, Anil Kumar¹, Rashi Nathawat¹, P. Kuleria², P. Barua² and S.A. Khan²

¹Department of Physics, University of Rajasthan, Jaipur-302 004

²Inter University Accelerator Centre, Post Box-10502, New Delhi 110 067

The interaction of the ions with polymer leads to bond breaking, formation of free radicals and various phenomena that are induced by the complex secondary chemicals processes along the trajectory of the ions. The breaking of atomic bonds and the rearrangements of polymer structure around the swift ion path result in a heavily modified cylindrical area, which is called latent track.

These Polycarbonate membranes were irradiated at the fluence $10^6 - 4 \times 10^{11}$ ion/cm² by 100 MeV Ag⁺⁷ ions. The irradiation was performed under high vacuum of order 10^{-6} torr at Inter University Accelerator Centre (IUAC). The lower dose was achieved by a scattered beam using rotating flywheel arrangement and higher dose by the scanned beam of dimensions, width 1 cm and 1 cm of length.

The diffraction pattern of virgin PC sample indicates that this polymer is amorphous in nature and shows prominent X-ray peak at $2\theta = 17.04^\circ$. The irradiated samples show an identical diffraction pattern except shift of this peak towards lower angle and broadening of this XRD peak with increase in dose [1]. The broadening of peak suggests an evolution of the polymer towards a more disorder state and also a change in crystallite size by irradiation of ions [2]. The crystallite size in the case of virgin sample is 9.13 Å, but in the case of 4×10^{11} ion/cm² irradiated film, the crystallite size decreases and goes to 7.91 Å. The details are shown in table 1.

Table 1: X-ray diffraction results on particle size and reduction in particle size, for virgin and irradiated PC membranes

S.No.	PC (Fluence ion/cm ²)	Particle size (Å)	Reduction in particle size
1.	Unirradiated	9.13Å	—
2.	2x10 ¹⁰	8.56 Å	6.18%
3.	2x10 ¹¹	8.27 Å	9.4%
4	4x10 ¹¹	7.91 Å	13.3%

REFERENCES

- [1] C Liu, Z Zhu, Y Jin, Y Sun, M Hou, Z Wang, X Chen, Z Chonghong, J Liu, B Li, Y Wang, Nucl. Inst. and Meth. in Phy. Res. B 166-167 (2000) 641-645.
- [2] Vaibhav Kulshrestha, Kamalendra Awasthi, N.K. Acharya, M. Singh, P.V. Bhagwat, Y.K. Vijay, Polymer Bulletin 56, 427-435 (2006)

5.2.29 Spintronic materials synthesis using SWIFT heavy ion irradiation

Kavita Bajaj¹, D C Kothari¹, Ajay Gupta²

¹Department of Physics, University of Mumbai, Vidyanagari, Mumbai 400098

²IUC for DAE Facilities, University Campus, Khandwa Road, Indore 452017.

Thin films of TiO₂ were deposited on LaAlO₃ single crystal substrates by pulsed laser deposition. Target was made from 99.9% pure TiO₂ powder & was sintered at 1250 °C. The laser energy density kept was between 2 to 2.5 J/cm². Base pressure was 10⁻⁵ to 10⁻⁶ Torr. The thickness of the films obtained from PLD ranges between 250 nm to 600 nm as measured by profilometer.

The resistivity of the films was measured by four probe method. The resistivity values are in the range of 0.01 Ohm-cm to 40 Ohm-cm. Structural properties of the TiO₂/LaAlO₃ samples were studied by XRD. 250 nm thick films exhibited pure Anatase structure, while remaining relatively thicker films also showed minor Rutile phase (3%-12%).

Two different set of Fe/TiO₂/LaAlO₃ structures were prepared by depositing 10 nm Fe⁵⁷ and 4 nm Fe⁵⁶ on TiO₂/LaAlO₃ samples respectively. These structures were irradiated using 120 MeV Ag ions at fluences ranging between 2x10¹³ cm⁻² to 8x10¹³ cm⁻². Some samples were implanted using 30 keV Fe at a fluence of 1x10¹⁶ cm⁻². Irradiated & implanted structures were analyzed again for resistivity, structure and composition.

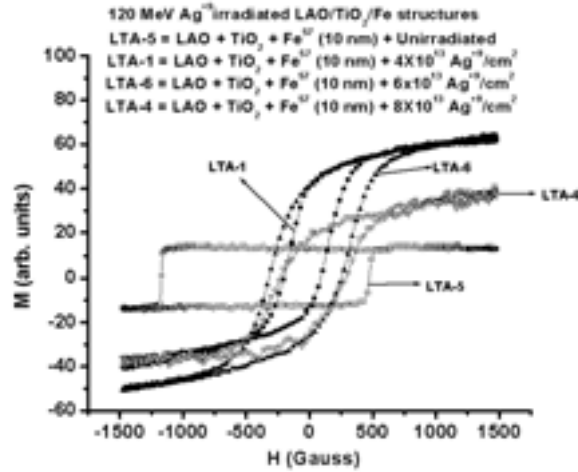


Fig. 1.

The resistivity of Irradiated films show insulating character, while there was little or no change in the structures implanted with Fe at low energy. Also there was no change in the crystal structure of implanted samples, while irradiated films have become completely amorphous. The concentration of Fe⁵⁷ was found to be 6% of Ti & that of Fe⁵⁶ was 16% of Ti as determined by EDS technique. The systems were characterised via MOKE to study magnetic properties. The hysteresis loop obtained from MOKE confirmed that the irradiated and unirradiated Fe/TiO₂/LaAlO₃ structures are ferromagnetic and there is anisotropy (Fig.1). Coercivity decreased after irradiation.

5.2.30 Swift heavy ion irradiation induced effects on MgB₂ thin films

Ravindra Kumar¹, H.M. Agrawal¹, R.P.S. Kushwaha¹ and D. Kanjilal²

¹Department of Physics, G.B.P.U.A & T. Pantnagar, 263145C

²Inter University Accelerator Centre, Post Box -10502, New Delhi 110 067

The discovery of superconductivity with $T_c \approx 40\text{K}$ in MgB₂ [1] has attracted a great attention in scientific community due to its unusual properties such as strongly coupled grain boundaries [2], time dependent electronic anisotropy [3] and multiple superconducting gap structure [4-5]. This material is also good candidate for numerous potential applications due to its encouraging value of T_c , coherence length and critical current density. In view of this, new experiments are being proposed to understand the mechanism of superconductivity in this material. Swift heavy ion (SHI) beams are versatile tools for modification and depth profiling of materials. The interaction of SHI can influence the material properties, which may be desirable in research and technology. The results so far obtained [6-9] on irradiation effects are mixed and there is no unanimous theory to explain the observed effects due to SHI. Therefore,

any experimental data that can shed light on the mechanism of superconductivity on this material are of keen interest.

For the present study, high quality MgB₂ thin films High quality MgB₂ thin films were procured from Superconix Inc (USA), which were fabricated by hybrid physical chemical vapor deposition (HPCVD) on Al₂O₃ (0001) substrate . The film thickness was ~ 300-400 nm. To confirm the MgB₂ phase, XRD was carried out by using Cu- K α radiation. The X- ray diffraction pattern before irradiation showed a randomly oriented growth of MgB₂ hexagonal phase. SRIM (the stopping and range of ions in mater) code was run to choose the ion energy such that no ion implantation takes place. For the present ion energy combination, the electronic energy loss $Se \approx 23$ keV/nm was also chosen to be high to create the desired defects. The samples were irradiated by 200 MeV ¹⁹⁷Au beam from 14 MV tandem Pelletron accelerator at IUAC, New Delhi. The irradiation was carried out at fluences of 5×10^{11} and 1×10^{12} particles/cm².

Precise four probe electrical resistance measurements before and after irradiation was carried out using a fully automated electrical resistance measurement system comprising of a closed cycle refrigerator. The results of resistance – temperature measurements before and after irradiation are shown in figure 1, which shows a sharp transition at around 39 K before irradiation. After irradiation the onset temperature increases with increase in the fluence. It becomes 44.3 K for MgB₂ sample irradiated with fluence 5×10^{11} ions/cm² and to 57.9 K for the sample irradiated with fluence 1×10^{12} ions/cm². But the temperature at which the resistance becomes zero decreases with irradiation by fluence 5×10^{11} ions/cm² from ~ 38 K to 30.3 K and nearly no change was found by 1×10^{12} ions/cm². Figure 1 also shows resistance vs. temperature in a very narrow region near transition temperature.

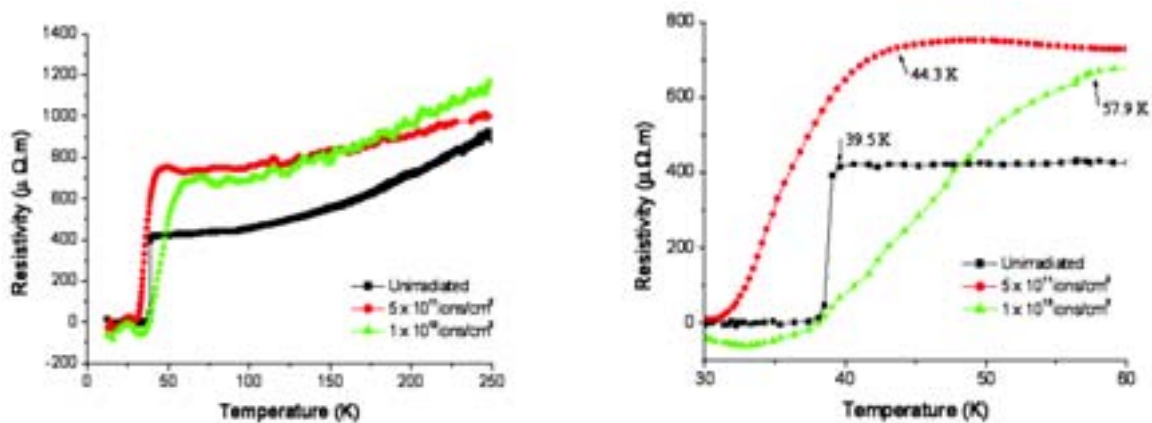


Fig. 1. R-T measurement before and after irradiation

Atomic Force Microscopy (AFM) and Scanning Electron Microscopy (SEM) were carried out to see the change in the surface morphology. The surface morphology

seems to be composed of small grains agglomerating into bigger ones. After irradiation, the roughness of the surface and size of grains have changed.

Further, the critical current density measurements before and after irradiation by SQUID are under way.

REFERENCES

- [1] J. Nagamatsu, N. Nakagawa, T. Muranaka, Y. Zenitani, and J. Akimitsu, *Nature (London)* 410, 63 (2001).
- [2] D. C. Larbalestier, et.al., *Nature (London)* 410, 186 (2001).
- [3] S. Patnaik, et.al., *Supercond. Sci. Technol.*, 14, 315 (2001).
- [4] P. Szabo et.al, *Phys. Rev. Lett.*, 8713, 7005 (2001).
- [5] F. Giubileo et.al, *Phys. Rev. Lett.* 8717, 7008 (2001).
- [6] Y. Bugoslavsky, L. F. Cohen, G. K. Perkins, M. Polichetti, T. J. Tete, R. Gwilliam, and A. D. Caplin, *Nature*, 411, 561 (2001).
- [7] H. Narayan, S. B. Samanta, A. Gupta, A. V. Narlikar, R. Kishore, K. N. Sood, D. Kanjilal, T. Muranaka, and J. Akimitsu, *Physica C*, 377, 1 (2002).
- [8] N. Chikumoto, A. Yamamoto, M. Konczykowski, and M. Murakami, *Physica C*, 378, 381 (2002).
- [9] S. R. Shinde, et.al.,, *Appl. Phy. Lett.*, 84 (13) 2352 (2004).

5.2.31 Photoluminescence properties of SHI induced F_2 and F_3^+ color centers in LiF thin films having nano grains

M. Kumar¹, F. Singh², S.A. Khan², A. Tripathi², D.K. Avasthi³, A.C. Pandey¹

¹Department of Physics, University of Allahabad, Allahabad, India 211002

²Inter University Accelerator Centre, Post Box-10502, New Delhi 110067

Photoluminescence (PL) properties of swift heavy ions induced F_2 and F_3^+ color centers in nano-grains LiF thin film were studied. Luminescence of F centers aggregates, F_2 and F_3^+ color centers, exhibits well resolved spectral bands (at 534 and 665 nm, respectively) compared to optical absorption spectrum as F_3^+ band, observed at a maximum of 458 nm, almost overlapped with F_2 absorption band at 445 nm. The overlapping of these bands allowed exciting F_2 and F_3^+ color centers simultaneously by a single pumping wavelength. The LiF films deposited on glass substrate were irradiated with 120 MeV Ag^{9+} and 80 MeV Ni ions at room temperature RT and liquid nitrogen temperature LNT, whereas film deposited on quartz substrate were irradiated with with 120 MeV Au^{9+} at RT. The Ni ion irradiation was performed at LNT at fluences of 7×10^{11} , 1×10^{12} and 3×10^{12} ions/cm². Thin films (150 nm) with different grain size were irradiated by 120 MeV Ag ions at a fluence of 3×10^{11} ions/cm².

PL studies were performed using excitation by 442 nm. The PL spectra showed well resolved bands at 535 and 665 nm corresponding to F_2 and F_3^+ color centers as shown in figure 1. Figure 2 (a) and (b) show the PL intensity behavior of these two bands as a function of fluence for different ions. The intensities of both the color centers increase with fluence followed by some decrease in the luminescence for all the cases. As the fluence increases, concentration of color centers increases resulting in increase in the luminescence intensity. An interesting finding of the experiment was increase in the luminescence intensity ratio of F_3^+ and F_2 color centers with irradiation fluence (Figure 2 (c) & (d)). At higher fluence, the luminescence intensity of F_3^+ color center was nearly twice as strong as the F_2 color center intensity. At LT irradiation, the intensity of color centers decreases. The concentration ratio between F_3^+ and F_2 can be increased by irradiation at low temperature even at lower fluence.

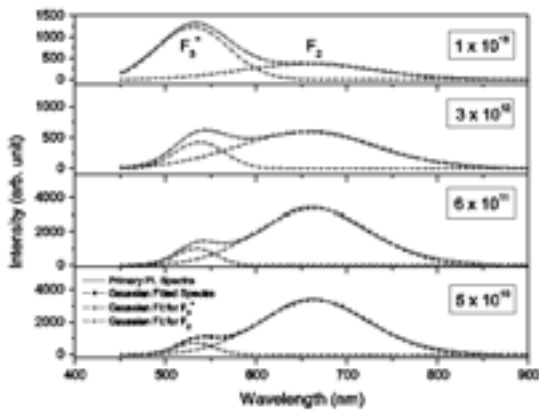


Fig. 1. PL spectra of irradiated samples.

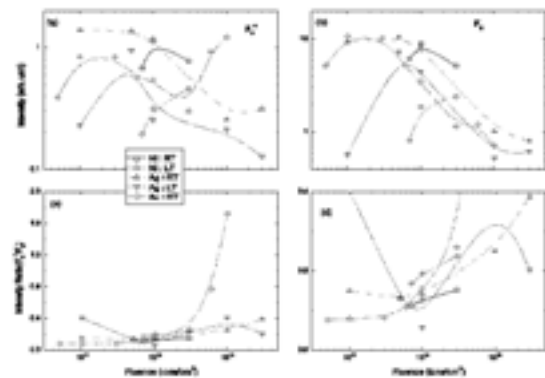


Fig. 2. (a) & (b) Variation in PL intensity, (c) & (d) intensity ratio of F_3^+ and F_2 color centers.

Figure 3 shows PL intensity of F_2 and F_3^+ color centers in LiF thin films having different grain size and irradiated with 120 MeV Ag ions at a fluence of 3×10^{19}

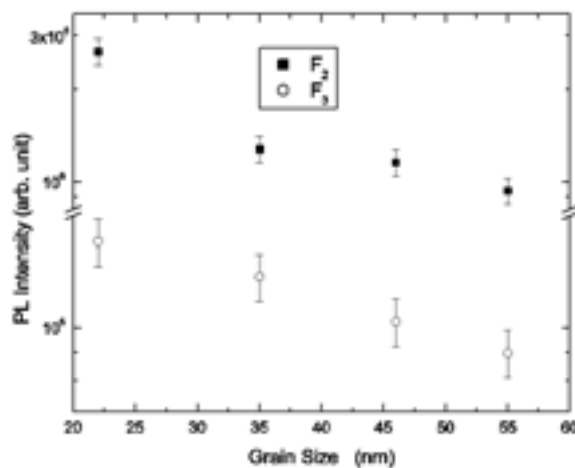


Fig. 3. PL behavior with grain size of the films.

10^{11} ions/cm². The PL intensity of the color centers was found to increase with reduction in the grain size. No significant change in the intensity ratio of F₃⁺ and F₂ color centers could be observed with grain size. The variation in intensity with grain size can be understood in terms of grain size effect in nanometer sized thin films.

5.2.32 Ferromagnetism induced by swift heavy ion irradiation in fullerene films

J.C. Pivin¹, Amit Kumar², D.K. Avasthi², A. Tripathi², F. Singh²

¹CSNSM, 91405 Orsay Campus, France

²Inter University Accelerator Centre, Post Box-10502, New Delhi 110067

A permanent magnetization of various carbon phases has been reported recently as a result of treatments under extreme conditions of pressure or temperature, or of ion implantation [1, 2]. This rather weak ferromagnetism may find interesting applications in medicine for the detection of tumors or the targeted delivery of drugs.

Irradiation experiments have been performed on fullerene films for testing the formation of a magnetic phase under the effect of the polymerization and or amorphization of the molecular structure by electronic excitations with a high density. Irradiation with 92 MeV Si ions leads actually to a drastic change in the magnetic response of the studied films, as shown in figure 1. The unirradiated samples, which are diamagnetic before irradiation, become paramagnetic, due to the formation of defects in the Si substrate. In addition, a ferromagnetic signal, characterized by an

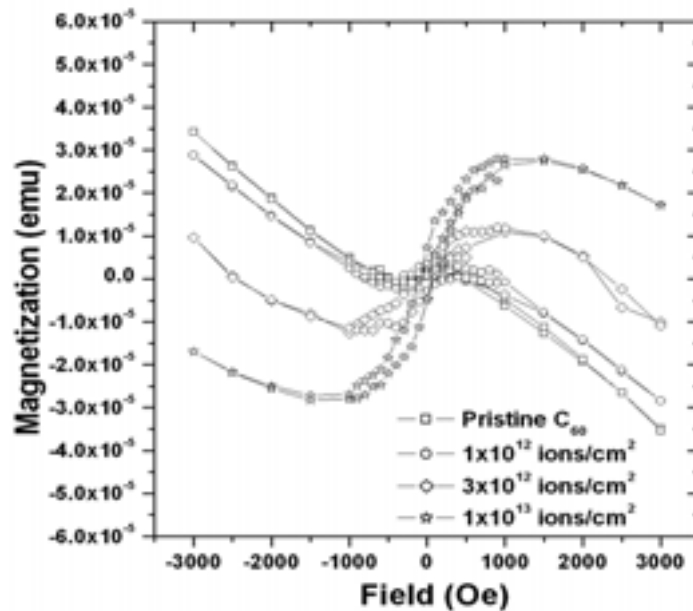


Fig. 1. SQUID measurement on C₆₀ films irradiated with 92 MeV Si ions at indicated fluences.

hysteresis and a residual magnetization under zero applied field, arises and its strength increases progressively with the ion fluence. A correlation with the observed changes of structure indicates that the magnetic phase is made of amorphous carbon, contrarily to the hypothesis proposed in previous papers, ascribing the magnetism of fullerenes treated under high pressure to their polymerization [1].

Magnetic force microscopy imaging of the films shows that the magnetic phase is heterogeneous. The magnetic contrast observed in figure 2 indicates that the magnetized material is concentrated at the periphery of carbon islands with a random magnetic order. The observed grains or columns boundaries (with an irregular shape and larger size than individual tracks) find probably their origin in some kind of topological order, typical of amorphous materials, such as a segregation of dangling bonds.

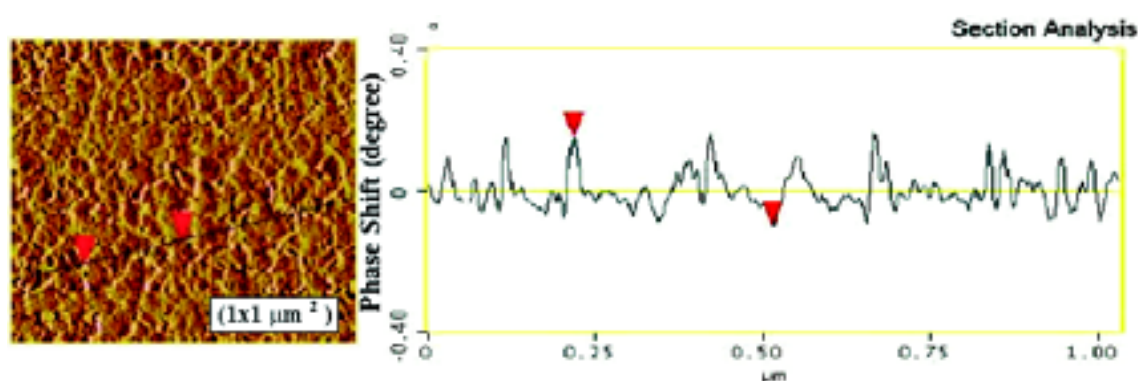


Fig. 2. MFM image and diagonal profile of magnetic force gradient in a fullerene film irradiated at the fluence of 1×10^{13} Si ions/cm².

REFERENCES

- [1] T. L. Makarova B. Sundqvist, R. Höhne, P. Esquinaz, Y. Kopelevich, P. Scharff, V.A. Davydov, L.S. Kashevarova, and A.R. Rakhmanina, *Nature (London)* 413, 716 (2001).
- [2] S. Talapatra, P. G. Ganesan, T. Kim, R. Vajtai, M. Huang, M. Shima, G. Rmanath, D. Srivastava, S. C. Devi, P. M. Ajayan, *Phys. Rev. Lett.* 95, 097201 (2005).

5.2.33 SHI induced modifications in magnetite thin films

Ravi Kumar¹, M. Wasi Khan², J.P. Srivastava², S.K. Arora³, I.V. Shvets³ and R.J. Choudhary³

¹Inter University Accelerator Centre, Post Box -10502, New Delhi 110 067

²Department of Physics, Aligarh Muslim University, Aligarh 202 002

³SFI, Department of Physics, Trinity College, Dublin-2, Ireland

Recently, there has been a renewed interest in the study of half metallic oxide such as magnetite, rare earth manganites and CrO_2 due to the rich phenomenological and technological applications [1]. There is a growing interest found in Fe_3O_4 thin films due to its favorable Curie temperature ($T_c \sim 858\text{K}$)² combined with its high spin polarization and presence of first order metal-insulator transition at 120K. Further, epitaxial Fe_3O_4 films grown on MgO substrate are known to contain antiphase boundaries (APBs). The effect of swift heavy ion (SHI) irradiation on solid can generate structural disorder and localization strain in the lattice. To the our best knowledge there have been no previous studies on the above properties with the effect of SHI irradiation on magnetite thin films.

We have grown the epitaxial thin films of Fe_3O_4 (Thickness $\sim 70\text{nm}$) on MgO single crystal substrate $\langle 100 \rangle$ oriented using an oxygen plasma assisted molecular beam epitaxy (MBE). The well-characterized films were irradiated at room temperature with 190MeV ^{107}Ag ions using the 15UD pelletron accelerator. The HRXRD, magnetometry and electrical transport measurements were performed on pristine and irradiated samples. The HRXRD results for (400) Bragg plane of Fe_3O_4 common to (200) of MgO for pristine and 190 MeV Ag^{15+} ion irradiated films with fluence values in the range of 5×10^{10} to 1×10^{13} ions/cm². It is clearly evident that the separation between the substrate (200) peak and the (400) peak of Fe_3O_4 thin films is marginally decreasing up to the fluence value 5×10^{11} ions/cm², which indicates that the tensile strain in the films is decreasing. However, as the ion fluence is further increased to 1×10^{12} ions/cm², the HRXRD spectra are modified to a great extent and the (400) peak splits into three peaks which indicates the structural disorder and onset of the phase transition. At higher fluence values such as 1×10^{13} ions/cm² the (400) peak disappeared and the system transforms from magnetite (Fe_3O_4) phase to more oxidized magnetite phase i.e. the maghemite (Fe_2O_3) phase.

In case of the rocking curves at (622) plane for pristine and irradiated thin films, again similar results were obtained. At low fluence in the range from 5×10^{10} to 5×10^{11} ions/cm² the (622) peak is showing slight deformation/ shift suggesting that the strain is partially relaxed but the Fe_3O_4 phase is retained. In the fluence range of 1×10^{12} to 5×10^{12} ions/cm² there is an appreciable shift in (622) peak indicating the increased relaxation of strain and transformation towards the maghemite phase. Finally with increasing fluence (at 1×10^{13} ions/cm²) the (622) peak disappeared which indicates the presence of disorder and the complete loss of epitaxial relationship between the substrate and the thin film.

Figure 1 shows the resistivity as a function of temperature and inverse of temperature for pristine and 190 MeV Ag^{15+} ion irradiated Fe_3O_4 thin films respectively. It is clearly evident from Fig. 1 that the Verwey transition temperature T_v of these films increases with the ion fluence values from 109K (for pristine) to 117K for the film irradiated with 5×10^{11} ions/cm². Our explanation to this result is that the SHI irradiation changes the structure of the antiphase boundaries, possibly

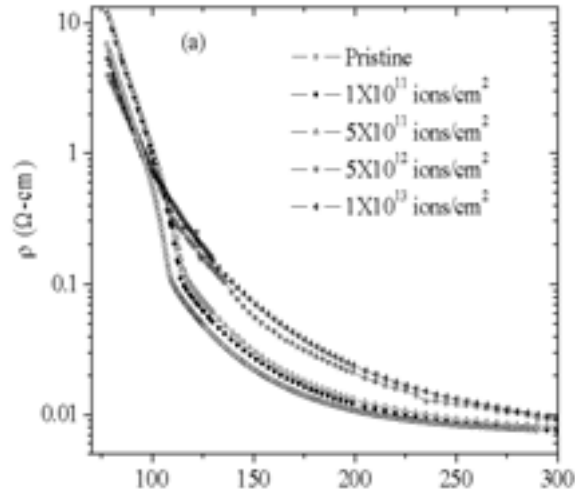


Fig. 1. ρ vs. T

even anneals out some of the boundaries. However, at higher fluences the films do not show Verwey transition down to 77K and the resistivity value is higher than that of the pristine film, demonstrating again that the SHI irradiation induced structural disorder in the film (in agreement with XRD results). It is also evident from the resistivity results that at higher fluences, where the *structural transformation* takes place, the resistivity attains a higher value.

The isothermal dc magnetization hysteresis at 300K for pristine Fe_3O_4 and 190 MeV Ag^{15+} ion irradiated films shows that the magnetization for the optimized fluence value (5×10^{11} ions/cm²) is higher than that of the pristine film. At fluence above 5×10^{12} ions/cm² the magnetization decreases rapidly which is consistent with the formation of iron oxide phases other than magnetite. The films exposed to highest fluence (1×10^{13} ions/cm²) show the lowest saturation magnetization (151 emu/cm³), which is even lower than that of $\gamma\text{-Fe}_2\text{O}_3$ phase ($M_s = 360$ emu/cm³). The results of the magnetic force microscopy (MFM) measurement of pristine and irradiated Fe_3O_4 thin films show that the film irradiated with 5×10^{11} ions/cm² fluence has maximum contrast, which is consistent with the magnetization data.

REFERENCES

- [1] J. P. Hong, S.B. Lee, Y.W. Jung, J.H. Lee, K.S. Yoon, K.W. Kim, C.O. Kim and C.H. Lee, Appl. Phys. Lett. 83, 1590 (2003)

5.2.34 Characterization of Conducting Polymers and their Structural, Electrical, Optical Properties by using Swift Heavy Ions

R.C. Ramola¹, J.M.S. Rana¹, Subhash Chandra¹, S. Annapoorni², Raksha Sharma², Alqudami Abdullah², R.G. Sonkawde³, F.Singh³, D.K. Avasthi³

¹Department of Physics, H.N.B. Garhwal University, Badshahi Thaul Campus, Tehri Garhwal – 249 199

²Department of Physics and Astrophysics, University of Delhi, Delhi – 110007

³Inter University Accelerator Centre, Post Box -10502, New Delhi 110 067

Conducting polymers have recently attracted much attention due to their unique properties like high strength to weight ratio, low cost, easier processability, lightness and tremendous projected technological applications [1-6]. The end uses of the polymers are based on their physical and chemical properties. Effects of ion beam irradiation on conducting polymers at low and high fluences have attracted large interest in the last decade [6-9]. Polyaniline and polypyrrole are most common conducting polymers. In present experiment, these polymers were irradiated with 50 MeV Lithium and 90 MeV Carbon ions at various fluences. The spectroscopic measurements such as UV-Visible spectrometry and electric properties of these materials were performed before and after the irradiation. These materials were also characterized by XRD for their structural properties. Scanning Electron Microscopy (SEM) analyses of the polymer films were made before and after irradiation in order to understand the changes on the surface of polymers.

The X-ray analyses of both the polymer films show that the irradiation by SHI induces the crystallinity in the polymers at low fluences. It turns to amorphous at high fluence. The induction of crystallinity is due to chain folding, cross linking of polymer chains or the formation of single or multiple helices after SHI irradiation. Similar pattern was observed for both Lithium and carbon ion beams with small variation in degree of appearance of scattered peaks after the irradiation.

The changes in surface morphology after SHI irradiation was observed by SEM images of polyaniline and polypyrrole films. The SEM images of polypyrrole films show that the film surface was smoother at lower fluence but the craters were observed at higher fluence. The grains of polypyrrole film surface change to joint and pressed structure after the irradiation.

The surface conductivity of both the polymer films (polyaniline and polypyrrole) was found to increase with increasing fluence of SHI irradiation. However, the decreasing trend in surface conductivity was observed at intermediate range of fluences. This decrease in surface conductivity may be due to formation of crystallinity at intermediate range of fluences. Random growth of crystals at the surface of polymer film may have affected the flow of current due to scattering and collision in the path. The surface conductivity was found to depend on the surface roughness, chain breaking, cross linking and the degree of planarity loss at the surface of polymer films. The surface conductivity increases again at high fluences due to remixing and cross linking of bonds with irradiation. The remixing by SHI pressure tends to smooth the polymer surface and thus increase the surface conductivity of the film. The pattern is observed same for both the films irradiated with Lithium and carbon ions.

The UV visible spectrum of the doped polyaniline was recorded in the reflectance mode. A small reduction of the band gap was observed after the irradiation by 50 MeV Lithium ions. The band gap was found to increase for higher fluences. The results are in well agreement with the surface conductivity of the film, which increases with increasing fluence and decreases thereafter. However, polyaniline films irradiated with Carbon ions does not exhibit any shift in the reflectance mode.

REFERENCES

- [1] A.J Heeger, Philos. Trans. R. Soc. A314 (1985) 19.
- [2] W.S. Huang, B.D. Humphrey, A.G. MacDiarmid. *J Chem Soc. Faraday Trans* 82 (1986) 2385.
- [3] E.M. Genies, *New J Chem.* 15 (1991) 373.
- [4] E.M. Genies, A. Boyle, M. Lapkoski and C. Tsintavis, *Synth. Met.* 36 (1990) 139.
- [5] A.G. MacDiarmid, J.C. Chiang, A.F. Richter and A.J. Epstein, *Synth. Met.* 18 (1987) 285.
- [6] S.R. Forrest, M.L. Kaplan, P.H. Schmidet, T. Venkatesan and A.J. Lovinger., *Appl. Phys. Lett.* 41 (1982) 708.
- [7] G.E. Wnek, M.S. Dresselhaus and B. Wasserman, *Mater. Res. Soc.* 27 (1984) 413.
- [8] G. Marletta, S. Pignataro and C. Oliveri, *Nucl. Instr. Meth.* B39 (1989) 773.
- [9] A.N. Aleshin, A.V. Gribanov, A.V. Dobrodunov, A.V. Suvoronov and I.S. Shlimak, *Sov. Phys. Solid State* 31 (1989) 6.

5.2.35 Investigations on the effect of Shift Heavy Ion (SHI) on the optical and structural properties of organic nonlinear optical Benzimidazole (BMZ) Crystals

T. Kanagasekaran¹, P. Srinivasan¹, N. Vijayan², G. Bhagavan Narayana², T. Mohanty³, D. Kanjilal³, R. Gopalakrishnan¹ and P. Ramasamy⁴

¹Department of Physics, Anna University, Chennai 600025

²Materials Characterization Div., National Physical Laboratory, New Delhi-110012

³Inter University Accelerator Centre, Post Box-10502, New Delhi 110067

⁴SSN College of Engineering, Kalavakkam

The 50MeV Si ion irradiation induced modifications on structural, and optical properties of Vertical Bridgman grown BMZ crystals have been studied. The high Resolution X-ray diffraction studies show that amorphization and lattice mismatch increase on increasing fluence of ion irradiation. The scanning electron micrographs show the collapse of the grain boundaries on irradiation.

The cut and polished BMZ crystals have been irradiated by 50MeV Si ion beam delivered from 15MeV Pelletron Accelerator. Optical absorption studies were performed on 50MeV Si ion irradiated BMZ crystals. The UV-Vis spectra of virgin

and irradiated crystals were recorded using shimadzu UV-Vis spectrometer as shown in fig. 1. The unirradiated BMZ crystals show their characteristic peak at around 305nm, which is a $\tilde{\Gamma}-\tilde{\Gamma}^*$ transition of the heteroatomic benzene ring. The characteristic peaks at 312nm and 318nm are observed for irradiated BMZ crystals at fluences of 5×10^{11} ions/cm² and 5×10^{12} ions/cm² respectively. The increase in absorbance of irradiated BMZ crystals can be explained by decrease in absorption co-efficient (α) on increasing the radiation dose.

HRXRD shows that irradiation produces amorphisation and lattice mismatch increases on increasing fluences. Scanning electron microscopy analysis is carried out using Jeol stereo scan microscope. Since organic are non-conducting in nature carbon coating should be done before subjecting the BMZ crystal surface to the electron beam.

The SEM study reveals that the fluence increases to 5×10^{12} ions /cm², the grain size decreases, the surface contains cauliflower like flaky or amoeba like surface morphology with an average grain size of 29.5 μ m resulting from complete destruction of the grain boundary. The collapse in the grain boundary is due to the amorphization. This can be attributed to the fact that the weak grain boundary region is susceptible for damage due to energy deposition by ions.

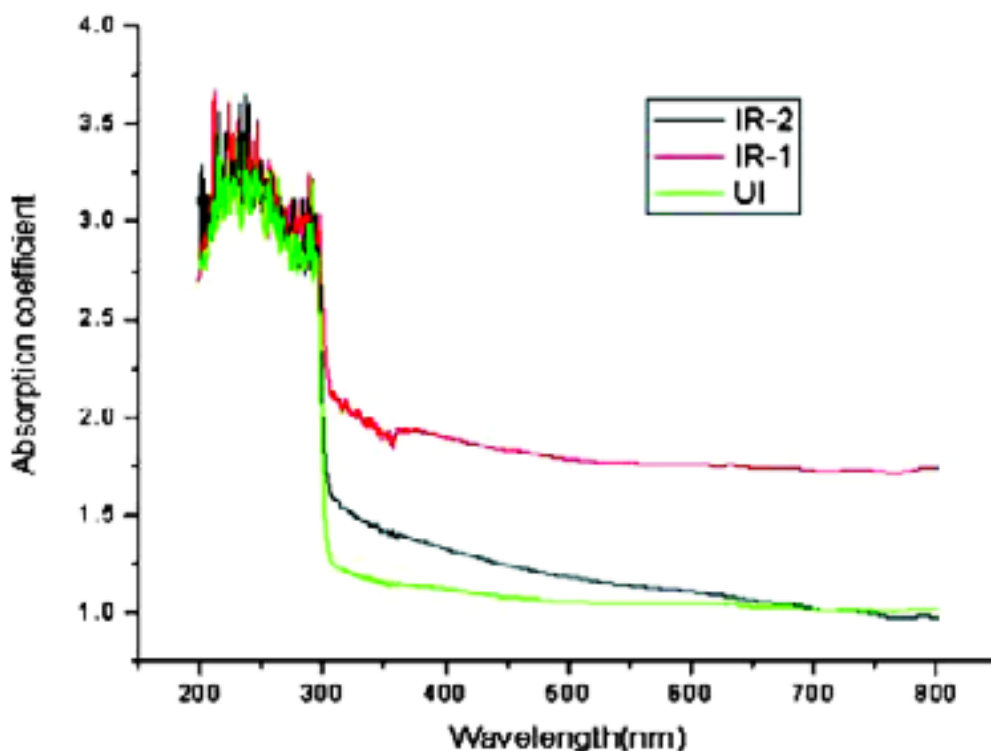


Fig. 1. Absorbance against wavelength

To summarize we have studied the effect of 50MeV Si ion irradiation on optical and structural properties of melt grown BMZ crystals. Scanning electron micrographs of irradiated BMZ crystals shows the collapse in the grain boundary due to amorphization, this can be attributed to the fact that the weak grain boundary region is susceptible for damage due to energy deposition by ions, further the results of HRXRD are in consistence with SEM analysis, evidencing destruction/collapse of the grain boundaries caused by high energy deposition by ions.

5.3 STATUS OF RADIATION BIOLOGY RESEARCH

A. Sarma

The experiments conducted in this field involved an ongoing research project on the germination properties, biochemical properties etc. of ion beam irradiated mustard seeds by users from MDU Rohtak, which utilised 50 MeV Li beam. There were no other experiments carried out as the beam line is under renovation.

5.3.1 Simulated heavy ion effect on growth and protein pattern in *Brassica juncea*

N. Lakra², S.N. Mishra² and A. Sarma¹

¹Inter-University Accelerator Centre, Post Box-10502, New Delhi 110067

²Dept of Biosciences, M.D. University, Rohtak

Introduction

In nature, the interaction of heavy ion radiations with plants takes place during the cosmic ray shower. A lot of interest has been generated in the study of response of plant under simulated condition using accelerators. Heavy ion exposures caused mutation in the organism and generally found lethal, depending on dose and exposure time. Pickert et. al.[1] demonstrated that pollen exposed to different heavy ion with different energy of U,Pb of 15 to 16 MeV/u, Ar of 14.7 MeV/u had differential response on induction of lethal mutants.

The lethality being considered due to mis or non-repair of DNA breaks could be repairable in certain conditions. It is envisaged that survival, if any, may be due to generally single point change in base pair which would depend on irradiation dose, species and its physiological state. The more damage in root than shoot with 135 MeV/u of ¹²O ion [2] and with 24 MeV ¹H in rice [3] has been demonstrated. While Schott et al. [4] observed a typical tumour at shoot meristem in cotyledons after 14-days due to exposure of ⁴⁰Ar ion (44MeV/u) but no such observation in root meristem. A Similar kind of differential response has been observed with Arabidopsis [5]. Liu et al. [6] demonstrated the production of the useful mutants like semi dwarf, early maturity and large grain size in rice. Recently, the positive growth response and biochemical changes accordingly in Indian mustard after irradiation of seeds with

${}^7\text{Li}^{3+}$ heavy ion is reported [7]. A mechanism of changing plant system exposed to HIR is still required. Therefore, in the present study the effects of 45MeV ${}^7\text{Li}^{3+}$ ion irradiation have been studied in laboratory condition to elucidate growth response and protein pattern in Indian mustard vis-à-vis to understand functional genomics.

Material & Methods

Seeds of Indian mustard (*B.juncea* cv. RH-30) were obtained from CCSHAU, Krishi Gyan Kendra , Rohtak. Similar size seeds were irradiated with different dosage [$10^7, 5 \times 10^7, 10^8$ p/cm²] of ${}^7\text{Li}$ (45MeV) using Pelletron accelerator. The plant growth was maintained up to 7 and 14-days under controlled conditions [Light 75Wm⁻² , Temp.25±2⁰C, RH 60-75]. The protein level in leaf and root tissues was measured following the method of Lowry et al [8]. The protein pattern was examined through SDS-PAGE [9].

Result and Discussions

Germination and seedling growth

Irradiations of seeds caused little decrease in germinability. The shoot and root elongation did change slightly except an increase in root length at 10^8 p/cm²

Protein profile

The protein from different developmental stages, i.e. the whole seedling of 96hr, 7th & 14th day leaf and root tissues was resolved on SDS-PAGE (12.5%). The protein banding pattern showed specific response with irradiation dosage

Whole seedling (96hr):-

After 96hr of germination few peptides of 18, 22, 23, 30,39 kDa were expressed more [band thickness] in seeds exposed to 5×10^7 and 10^8 p/cm² compared with that of control and low dose (10^7 p/cm²) exposure. However, 70, 78 & 84 kDa peptides were appeared newly at 5×10^7 and 10^8 p/cm² dosages [Fig. 1].

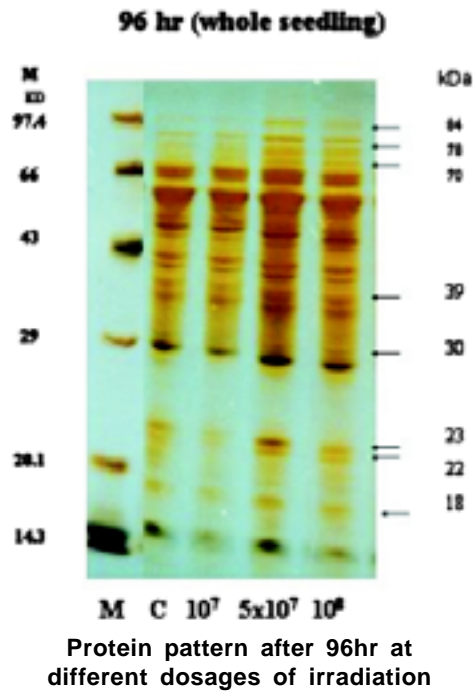
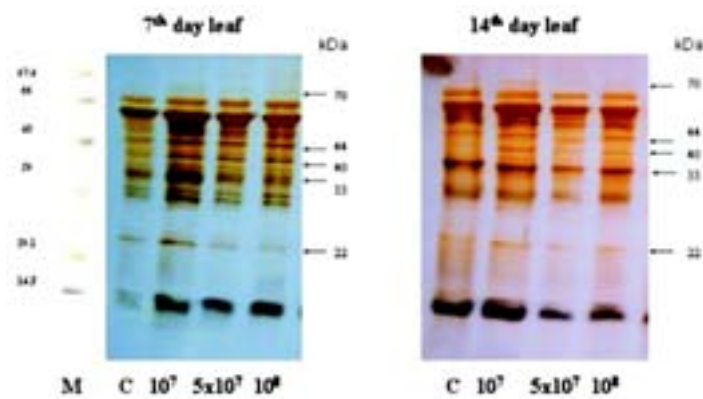


Fig. 1.

Leaf tissue

Seedlings emerging from radiation exposed seeds were allowed to grow up to 7th to 14th day in control condition. A higher accumulation of 22,33,40,44 kDa peptide was observed at low dose (10⁷p/cm²), both at 7th and 14th day of seedlings as compared to control and rest doses of irradiation. On the other hand, new peptide of 70 kDa appeared at all dosages at 7th day only while expression of this protein was more at 10⁷ and 10⁸p/cm² on 14th day of seedling leaf [Fig.2].

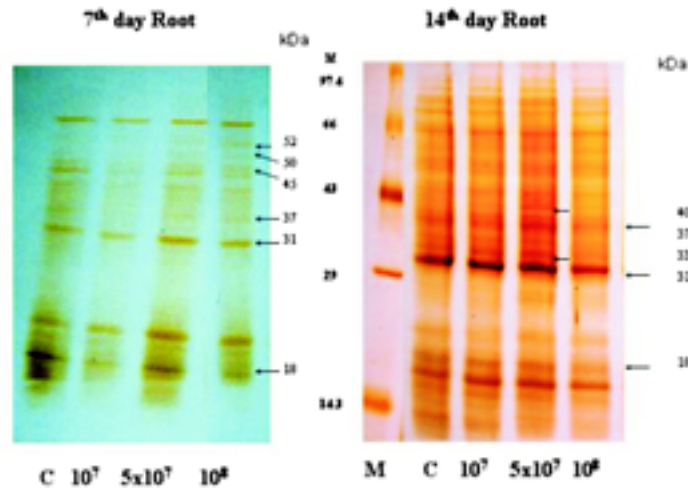


Protein pattern in leaf tissues at different developmental stages.

Fig. 2.

Root Tissue

In root tissues also, accumulation of few proteins after irradiation was observed. At dosage of 5×10^7 and 10^8p/cm^2 caused accumulation of 18, 31 & 37 kDa along with novel 50 & 52 kDa peptides in 7th day root tissues. With the advancement of the age (14th-d) accumulation of 31, 33, 37 kDa peptide were constantly observed. However, 40 kDa peptide was induced at dose 5×10^7 [Fig.3].



Protein pattern in root tissues at different developmental stages.

Fig. 3.

The characterization of these could be an interesting exploration.

Discussions

The high expression of some proteins at different stages of the seedling [96hr as in Fig.1, 2 and 3] suggests certain specific genetic modifications which could be linked with positive changes such as increase in pod no. and yield character observed in this crop [7]. The positive modifications/mutants have been demonstrated in other crop plants [6].

The future experiments are required to examine the nature of these proteins. The novel protein (70, 78 & 84 kDa) at different developmental stages suggests that specific genetic modifications responsible for developmental stages could be induced by ^7Li . The root tissues accumulation of novel protein of 50 and 52 at 7th day and 40 kDa at 14 day with specific dose of $5 \times 10^7 \text{p/cm}^2$ further indicates the tissue specific responses of heavy ion exposure. The detail study, purification and sequencing and

BLAST could provide clue for modifications and transgenic applications for improvement of growth and yield.

REFERENCES

- [1] M.Pickert,A.R.Kranz & S.Somer. Proc. IV European Symposium on Life Sciences Res. In Space. Italy.(1990) 581-582.
- [2] H. Nakai, H. Watanabe, Y. Kobayashi, T. Asai, S. Kitayama, III-4-4. RIKEN Accel Prog. Rep. 24 (1990) 91.
- [3] M. Kalimullah, J.U.Gaikwad, S. Thomas, A. Sarma, P.B. Vidyasagar. Plant Sci. 165 (2003) 447-454.
- [4] J.U. Schott, A.R. Kranz, K. Gartenbach, M. Zimmermann. The J. Photograph. Sci.41 (1993) 115-116.
- [5] A.R. Kranz, K.E. Gartenbach, V.V. Shevchenko, E. Schopper, B. Baican, J.U. Schott, R. Settz, C. Heilmann, D. Dudkin, N. Nefedov, Y. Potapov. Acta.Astronaut. 32 (1994) 761-766.
- [6] Z. Liu, Q. Qiu, W. Huang, M. Mei, J. Yang. J. Rad. Res. Radiat. Process. 9 (1991) 139-144.
- [7] S. Verma, S.N. Mishra, A. Sharma, S.B. Phogat. Brassica 6 (2004) 35-40.
- [8] O.H.Lowry, N.J.Rosenbrough,A.L.Farr & R.J.Randall. J.Biol.Chem.193 (1951) 265.
- [9] U.K. Laemmli. Nature 227 (1970) 680-685.

5.4 ATOMIC PHYSICS RESEARCH

T. Nandi

Atomic physics beam line has been tested on line up to the vacuum chamber and we are planning to carry out a test run soon for accurate measurement of the foil thickness and foil thickness dependence of the charge state fractions of the post-foil ion beam. Recently we have tested successfully the Doppler tuned spectrometer in GPSC with one spectrometer. Another spectrometer and foil translation mechanism will also be installed soon and major experiments will be performed with this facility.

Analysis of the data obtained for studying the effect of second-foil thickness on excited states produced due to ion-solid interaction in the first foil has confirmed the intra-shell transitions in He-like ions as described below. Last year we have performed an experiment for the first time to measure the role of hyperfine structure effects on x-ray production cross section in our laboratory in collaboration with Punjabi University, Patiala and found considerable effects. Further measurements to achieve higher statistics will be done this year.

Atomic and molecular physics experiments in the low energy ion beam laboratory have started good results. Position sensitive multi-hit time-of-flight measurement system is used to study the fragmentation dynamics of complete and incomplete fragmentation process as presented below.

5.4.1 Studies on ion induced molecular dissociation

Sankar De¹, P.N. Ghosh¹, Jyoti Rajput², R. Ahuja², D. Kanjilal², A. Roy² and C.P. Safvan²

¹Dept. of Physics, Univ. of Calcutta, 92, A.P.C. Road, Kolkata-700009

²Inter-University Accelerator Centre, Post Box-10502, New Delhi-110067

Studies of the dynamics of formation and subsequent dissociation of multiply charged molecules produced by collisions of neutral molecules with highly charged atomic ions have been an active field of research during the last decade [1]. In order to probe the dynamic phenomenon in ion-molecule collision, we have developed a position sensitive multi-hit time-of-flight (TOF) measurement system capable of coincident measurement of all multiple-ionization, fragmentation and capture channels [2]. Here we report the very first results of dissociation of multiply charged methanol and acetylene molecules with 1.2 MeV Ar⁸⁺ projectiles. The experiment is carried out in the atomic physics collision chamber of LEIBF. At the centre of the experimental chamber, Ar⁸⁺ projectiles produced from the ECR ion source interacts with the CH₃OH and C₂H₂ molecules effusing from a hypodermic needle. The dissociated fragments

are extracted from the interaction zone in the time-of-flight mass spectrometer (TOFMS) on application of an uniform electric field perpendicular to both ion beam and gasjet. The dissociation products are finally detected by a position-sensitive MCP detector. Ejected electrons are extracted in the opposite direction to TOFMS and detected by a channeltron which gives the trigger for multi-hit coincidence data acquisition.

From the TOF spectrum of methanol, we observed a wide range of dissociation products starting from undissociated molecular ions (CH_3OH^+) to fragments losing a hydrogen atom due to breakage of C-H and O-H bonds (CH_2OH^+ , CHOH^+ , COH^+ , CO^+). From the 2-dimensional coincidence map as shown in figure 1, we had separated out different dissociation channels between C^q+ ($q=1-3$) and O^p+ ($p=1-3$) produced from the complete rupture of C-O skeleton as well as H^+ formation pathways in coincidence with carbon and oxygen ions produced. Complete and incomplete dissociation events such as $\text{CH}_3\text{OH}^{2+} \rightarrow \text{CH}_{3-n}^+ + \text{OH}^+$ ($n=0-2$) are also observed in the coincidence map. For incomplete ones the missing fragments are either undetected neutrals or detected as a third or fourth hit in the MCP. The most striking feature in the coincidence map is the formation of H^+ , H_2^+ and H_3^+ due to breakage of the C-H bonds.

The TOF spectrum of C_2H_2 shows a wide range of dissociation products starting from undissociated molecular ions like C_2H_2^+ and doubly ionized $\text{C}_2\text{H}_2^{2+}$ to fragments losing an hydrogen atom due to breakage of C-H bonds (C_2H^+ , C_2^+). From the 2-dimensional coincidence map as shown in figure 2, we had separated out correlations between different dissociation channels corresponding to C^+ , C^{2+} and C^{3+} fragments produced from complete rupture of C-C triple bond. Detection of backward

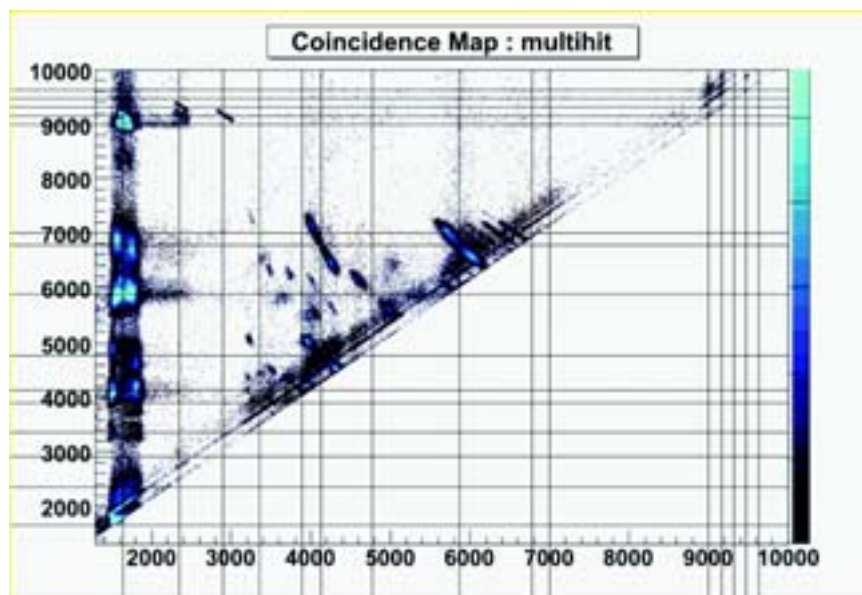


Fig. 1. : Coincidence map of dissociative products of methanol.

component of CH^+ in coincidence with its forward counterpart confirms breakage of the triple bond without breaking the single bond C-H part. Also observed is the coincidence between C^+ and CH^+ which are formed from the breakup of C_2H^{2+} . The shape of the islands gives information about the fragmentation dynamics of complete and incomplete fragmentation processes. The most interesting feature in figure 2 is the H^+ formation pathways and the “butterfly-like” structure in coincidence with C^+ , C^{2+} and C^{3+} fragments respectively. This structure confirms that the breakage of bonds of highly charged molecular ions does not always occur simultaneously but there is a tough competition from sequential manner as well.

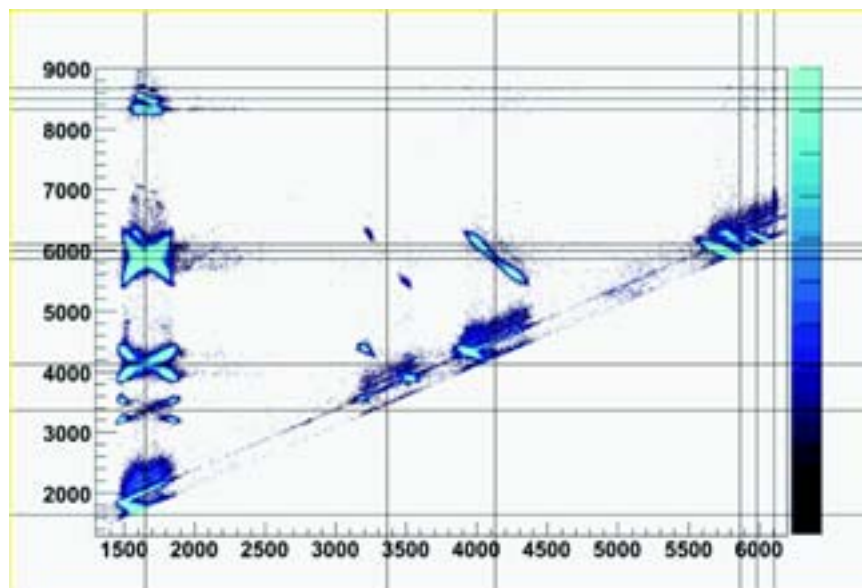


Fig. 2. Coincidence map of dissociative products of acetylene.

REFERENCES

- [1] D. Mathur, Phys. Rep., 225 (1993) 193 ; 391 (2004) 1
 [2] S. De, P. N. Ghosh, A. Roy and C. P. Safvan, Nucl. Instr. and Meth. B, 243 (2006) 435

5.4.2 Effect of foil thickness on excited states in the beam-foil interactions

T. Nandi² and Nissar Ahmad¹

¹Dept. of Physics, Aligarh Muslim University, Aligarh 202002

²Inter University Accelerator Centre, Post Box-10502, New Delhi 110067

The charge state distribution of any ion beam colliding with a solid foil varies with the thickness and the incident charge states. It is supposed to be so for the formation of excited states too. The K-x-ray fluorescence yield for H-like ions vary significantly on the charge state of the incident ions during the collision of H-

like Si beam with He gas target [1]. If the probability for excitation within an atomic shell is large, then electrons may jump back and forth rapidly between the sub-levels (2s-2p) during collisions between a target atom and a proton [2] as predicted theoretically in late seventies. However, as no experimental effort was made to verify this prediction till date, we have made an attempt to see how intra-shell transition alters the data on collisions using the beam-single-foil and beam-two-foil experiments [3].

A beam of 143 MeV Ti from Pelletron accelerator at IUAC was passed through 90 $\mu\text{g}/\text{cm}^2$ carbon foil (first foil) loaded in a dedicated experimental set up as reported in our earlier paper [4] to produce He-like Ti $1s2s\ ^3S_1$ and $1s2p\ ^3P^0_2$ states. As these excited states decay to ground states, via M1 and M2 transition lines, which are not resolved, appearing at 4.78 KeV as a composite peak. The concerned transition rates are 0.8×10^9 /sec and 3.76×10^7 /sec, respectively. The excited states are made to undergo a collision with a $4\mu\text{g}/\text{cm}^2$ thin foil (second foil) in which He-like Ti $1s2p\ ^3P^0_2$ state may convert to He-like Ti $1s2s\ ^3S_1$ state and vice versa. If the abundance of these two states is unequal, the normalized intensity would either increase or decrease. The reduced intensity on single collision with carbon foil implies that $1s2p\ ^3P^0_2$ state is more abundant than the $1s2s\ ^3S_1$ state as produced from the first foil. Further, measurements were done with two ($8\mu\text{g}/\text{cm}^2$), three ($12\mu\text{g}/\text{cm}^2$) and five ($20\mu\text{g}/\text{cm}^2$) collisions in the second foil also to show the effect of intra-shell transitions in subsequent collisions. Such effect can be revealed from the change in intensity ratios of M1 and M2 lines of He-like Ti in the 4.78 KeV peak with the thickness of the second foil. Number of collision was estimated from carbon foil thickness using the prescription given in [4]. A theoretical model describes well the data so obtained as shown in Fig. 1. Results give a direct evidence of the intra-shell

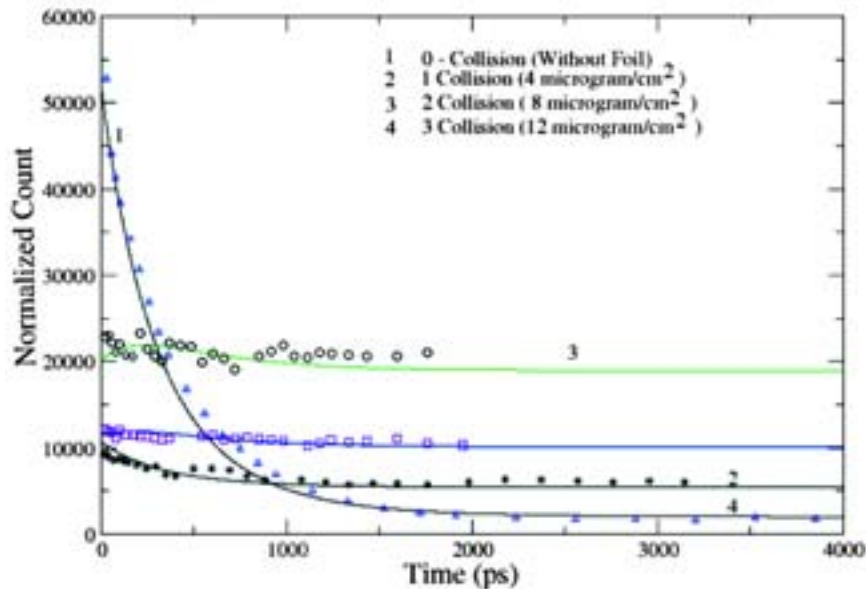


Fig. 1. Normalized counts are plotted against time for different foils at place of second foil. These data are fitted with a theoretical model as shown by solid lines.

transitions in the He-like Ti-ions. Data indicate that after few more collisions, two states will be totally indistinguishable. Accordingly a simple calculation shows that six collisions are sufficient to admix two states completely as shown in Fig 2.

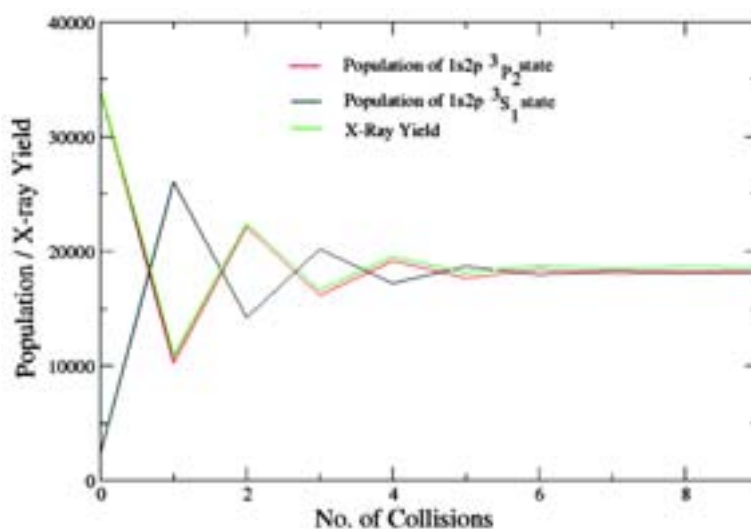


Fig. 2. Level population / x-ray yield are plotted against average number of collisions in the second foil. Both level population and x-ray yield exhibit an oscillation with the number of collisions up to 5 such collisions and oscillation disappears on further collisions.

The above said experiment gives the researchers an opportunity to make invaluable contributions on the interaction mechanism between the excited states and thin solid foils. In the present talk; novel features of the experiment, salient results, the model calculations, and the future scope will be highlighted.

REFERENCES

- [1] B. L. Doyle *et al.*, Phys. Rev. A17, 523(1978).
- [2] J. H. McGuire *et al.*, Phys. Rev. A19, 2180(1979).
- [3] T. Nandi *et al.*, J. Phys. B37, 703(2004).
- [4] T. Nandi, N Ahmad, A. A. Wani and P. Marketos, Phys. Rev. A72, 22711(2005).

5.4.3 Effect of hyperfine splitting on K X-ray production cross sections

B.P. Mohanty¹, P. Balouria², R.K. Karn³, N. Ahmad⁴, M.L. Garg⁵, D.K. Avasthi³, V.K. Mittal¹, I.M. Govil² and T. Nandi³

¹Department of Physics, Punjabi University, Patiala, 147002

²Department of Physics, Panjab University, Chandigarh, 160014

³Inter University Accelerator Centre, New Delhi, 110067

⁴Department of Physics, Aligarh Muslim University, Aligarh, 202002

⁵Department of Biophysics, Panjab Univeristy, Chandigarh, 160014

The hyperfine interaction in He-like ions induces a small admixture of $1s2p\ ^{1,3}P_1$ state to the $1s2p\ ^3P_0$ state. Consequently the forbidden E1 transitions from the $1s2p\ ^3P_0$ state to $1s^2\ ^1S_0$ ground state become allowed. Similarly, the $1s2p\ ^3P_0$ state may decay through E1 transitions in addition to the M2 decay. In light of this phenomenon it can be expected that, in case of single vacancy conditions the effect of hyperfine interaction can increase the radiative transition probability for such transitions.

Due to the hyperfine splitting of 2p levels in the atom having a K-shell vacancy the number of possible transitions from $2p_{3/2}$ level increases in comparison to that of $2p_{1/2}$ level. For example, in an isotope of Gd with non-zero nuclear spin (say ^{157}Gd , $I = 3/2$), there will be a change in total angular momentum due to hyperfine interaction. This will lead in splitting of the $2p_{3/2}$ level in to four with F ($F=I+J$) values from 0 to 3 and the $2p_{1/2}$ level in to two with F values 1 and 2 as shown in Figure 1. As evident from the figure the original single E1 transition from $2p_{3/2}$ to $1s_{1/2}$ ($K_{\square 1}$) is now replaced with a total of 8 transitions (6 E1 and 2 M2) and for $2p_{1/2}$ there are four E1 transitions. Therefore it is expected that the intensity ratio of $K_{\square 1}$ to $K_{\square 2}$ may increase for elements with a non-zero nuclear spin.

The experimental set up was installed at the beam exit port of general purpose scattering chamber (GPSC). Thin targets of Ti, Ni, Au, Ba, ^{157}Gd and ^{160}Gd on carbon or aluminium backing were mounted at an angle of 45° to the $^7\text{Li}^{3+}$ beam of energy 28 to 45.5 MeV. Two x-ray detectors positioned at $\pm 90^\circ$ were used to detect the x-rays coming from the targets. Two SSB detectors at $\pm 15.5^\circ$ were used to detect the scattered particles for beam normalisation. Typical K x-ray spectra of Gd and L x-ray spectra of Ba & Gd are shown in Figure 2. Efficiency of the x-ray detectors were evaluated using calibrated radioactive sources of ^{55}Fe , ^{57}Co , ^{152}Eu and ^{241}Am .

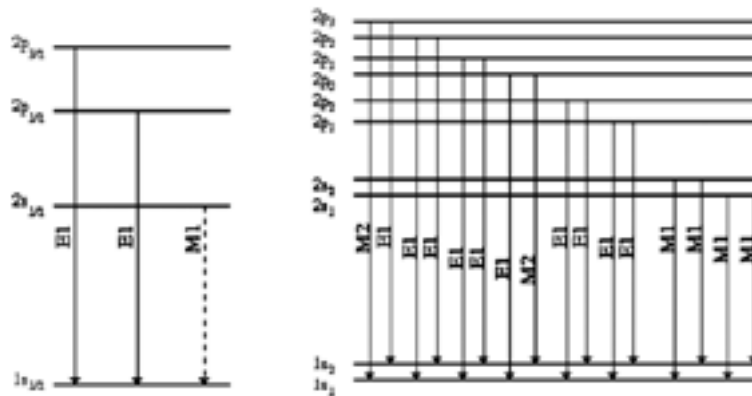


Fig. 1. Transitions from different 2p levels to 1s level with and without hyperfine splitting.

Area under the K X-ray peaks of both ^{157}Gd and ^{160}Gd were extracted using the GUPIX software package. The ratio between their intensities is given in table 1. It can be seen that there is remarkable difference in intensity ratios as compared to theoretical values for ^{157}Gd . Analysis of the data to extract the inner shell ionisation cross section is in progress.

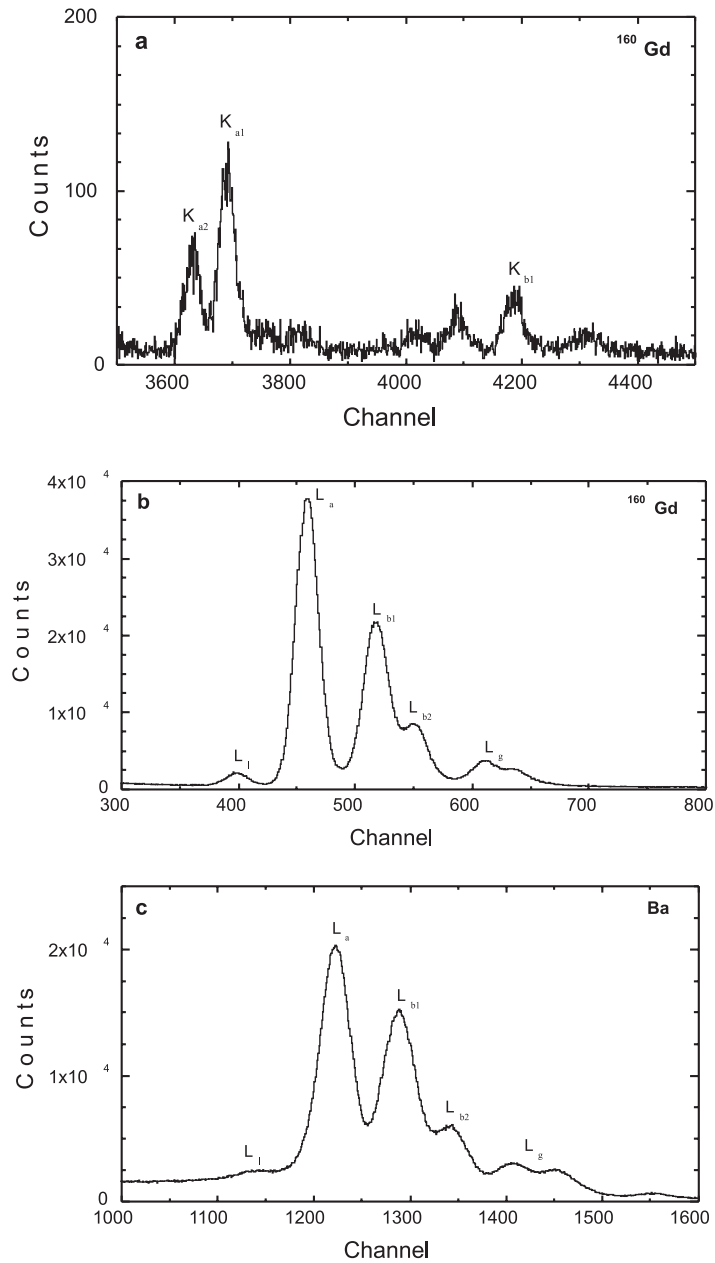


Fig. 2. (a) K x-ray spectra, (b) L x-ray spectra from ^{160}Gd at 30MeV incident energy taken with ULGe detector and (c) L X-ray spectra of Ba at 28 MeV incident energy taken with Si(Li) detector.

Table 1: Experimental and theoretical intensity ratios for different K x-ray lines of Gd.

Energy (MeV)	Target	$K_{\alpha 2}/K_{\alpha 1}$	$K_{\beta 1,3}/K_{\beta 1}$
42	^{157}Gd	47.2 %	27.0 %
	^{160}Gd	56.5 %	39.7 %
45.5	^{157}Gd	50.4 %	21.3 %
	^{160}Gd	54.4 %	35.2 %
Theoretical Intensity ratio for natural Gd		56%	30 %